# Influence of the Atrial Natriuretic Peptide on TNF-α-activated human endothelial cells: Regulation of adhesion molecule expression and cytoskeleton changes


Dissertation zur Erlangung des Doktorgrades
der Fakultät für Chemie und Pharmazie
der Ludwig-Maximilians-Universität München

vorgelegt von

**Nina Claudia Weber**

aus Köln

2002

Erklärung

Diese Dissertation wurde im Sinne von § 13 Absatz 3 bzw. 4 der Promotionsordnung vom 29. Januar 1998 von Frau Prof. Dr. Angelika. M. Vollmar betreut.

Ehrenwörtliche Versicherung

Diese Dissertation wurde selbständig ohne unerlaubte Hilfe erarbeitet.

München, im April 2002

.....
(Unterschrift des Autors)

Dissertation eingereicht am 30.04.2002

1. Gutachter: Frau Prof. Dr. A. M. Vollmar
2. Gutachter: Herr Prof. Dr. M. Biel

Tag der Bekanntgabe des Prüfungsergebnisses: 11.06.02

**Meinen Eltern und meinem Freund Christian**

# CONTENTS

# 1 INTRODUCTION

# 1.1 Background and aim of the work

The atrial natriuretic peptide, ANP, was the first described member of the natriuretic peptide family, a family of cardiovascular cyclic peptide hormones. Due to its natriuretic and diuretic properties ANP exhibits strong cardiovascular effects, such as regulation of blood pressure and plasma volume expansion (Levin et al. 1998).
ANP mediates most of its cardiovascular and renal effects through interaction with the guanylyl-cyclase-coupled natriuretic peptide receptor, NPR-A, *via* cGMP as second messenger (Levin et al. 1998). ANP also binds to the non-guanylyl-cyclase-linked natriuretic peptide "clearance" receptor (NPR-C) (Levin 1993). Besides the clearance function exerted by NPR-C, an NPR-C-mediated inhibition of adenylyl-cyclase was shown to be responsible for several *in vitro* effects of ANP.
In the last years natriuretic peptides and their receptors have been demonstrated to be expressed in diverse tissues besides the cardiovascular and renal system. In this context, ANP and its receptors were shown to be expressed in thymus (Vollmar and Schulz 1990a), as well as in macrophages (Vollmar and Schulz 1994; Vollmar and Schulz 1995; Kiemer and Vollmar 1997). ANP was therefore suggested to be a modulator of immune functions. In fact ANP was shown to attenuate the induction of inflammatory mediators, such as cyclooxygenase-2 (Kiemer et al. 2002b) and TNF-α (Kiemer et al. 2000a; Tsukagoshi et al. 2001). The latter was demonstrated in LPS-stimulated macrophages (Kiemer et al. 2000a) as well as in reperfused livers (Kiemer et al. 2000b). These observations provide novel aspects in the biological profile of NP by demonstrating a relationship of ANP to the immune system. In this context it was determined whether ANP may not only inhibit the *production* of proinflammatory factors like TNF-α, but also their *effects* on vascular cells. TNF-α represents an important proinflammatory cytokine, known to play a crucial role in the pathogenesis of several inflammatory diseases, such as atherosclerosis, septic shock or rheumatoid arthritis (De Martin et al. 2000). It is mainly produced by activated monocytes and macrophages and influences the growth and behaviour of endothelial cells, monocytes, and smooth muscle cells (Heller and Kronke 1994). Inflammatory conditions, such as atherosclerosis, or septic shock, are closely related to the increased infiltration of leukocytes into inflamed tissue (Gimbrone, Jr. et al. 1997). Central pathomechanisms of TNF-α-induced inflammatory reactions involve the induction of endothelial cell adhesion molecules and increased endothelial cell leakiness, whereby formation of intercellular gaps in vascular endothelium is regarded as one of the initial mechanisms contributing to the development of an atheromatous plaque (Raines and Ross 1995).
Aim of this work was to clarify whether ANP is able to protect human umbilical vein

endothelial cells against TNF-α-induced expression of adhesion molecules and changes in endothelial cytoskeleton.

**Concerning these two issues the following questions had to be answered:**

**1. Increased endothelial cell adhesion molecule (CAM) expression:**

a) Does ANP influence TNF-α-induced adhesion molecule expression in HUVEC?
b) Which receptor is responsible for the observed inhibitory properties of ANP on TNF-α-induced adhesion molecule expression?
c) Does ANP affect the activation of the proinflammatory transcription factor NF-κB?
d) What is the molecular mechanism of the inhibitiory action of ANP on TNF-α-induced NF-κB DNA binding activity?
e) Does ANP influence other TNF-α-activated transcription factors? Characterization of the effects of ANP on AP-1.

**2. Endothelial cytoskeleton changes:**

a) Does ANP influence TNF-α-induced permeability and cytoskeleton changes?
b) What is the molecular mechanism of the inhibitiory action of ANP on TNF-α-induced permeability and cytoskeleton changes?
    a. Does ANP inhibit stress fiber formation in endothelial cells?
    b. Does ANP affect actin polymerization?
    c. Does ANP influence p38 MAPK?
    d. What are the pathways responsible for ANP mediated p38 MAPK inhibition?
    e. Does there exist a causal relationship between p38 MAPK and the actin cytoskeleton?

**3. Does ANP influence TNF-α-induced MCP-1 expression?**

a) Does ANP influence TNF-α-induced MCP-1 expression in HUVEC?
b) Which receptor is responsible for the observed inhibitory properties of ANP on TNF-α-induced MCP-1 expression?
c) Does there exist a causal relationship between MKP-1-induced p38 MAPK inactivation and inhibition of MCP-1 expression by ANP?

# 1.2 The natriuretic peptides

## 1.2.1 History

It is now more than 20 years ago that de Bold and coworkers observed a massive natriuresis and diuresis after infusion of an atrial tissue extract into rats. This observation led to the isolation and cloning of the first member of a group of cardiovascular natriuretic peptides, the atrial natriuretic peptide, ANP (de Bold et al. 1981). Only a few years later a structure homologue of ANP was isolated from porcine brain homogenates and therefore named "brain natriuretic peptide", BNP (Sudoh et al. 1988). After BNP, a second natriuretic peptide was isolated from the porcine brain. In analogy after ANP and BNP it was called CNP, "C-type natriuretic peptide" (Sudoh et al. 1990). Besides ANP, BNP, and CNP Urodilatin has been described as another member of the natriuretic peptide family (Schulz-Knappe et al. 1988, Forssmann et al. 2001; Schermuly et al. 2001). Urodilatin was isolated from the human kidney (Schulz-Knappe et al. 1988). Together these peptides constitute the family of natriuretic peptides.

## 1.2.2 Structure of the natriuretic peptides

Human ANP is a 28 amino acid peptide, whereas BNP contains 32 amino acids and CNP only 22. All three natriuretic peptides contain a 17 amino acid ring system as structural characteristic. The disulfide linkage between the two cysteine residues was found to be essential for the pharmacological activity of the natriuretic peptides (Inagami et al. 1984). Within the cyclic structure the three peptides are highly homologous, whereby eleven amino acids are identical for all three NP. Differences in structure refer to the different numbers of amino acids at the C- and N- termini of the peptide (figure 1).

**ANP**: The 28 amino acid ANP differs only in six amino acids in the ring structure from BNP. ANP sequence is found homologous in most species. Only one amino acid is variable, which is methionin for e.g. in humans, dogs, pigs, sheep, whereas in rodents (rats, mice, rabbits) it is isoleucine.
**BNP** is only 59% sequence homologous between the different species (Rosenzweig and Seidman 1991).

**CNP** structure is mostly different from ANP and BNP, because it ends after only 22 amino acids at the C-terminus after the last cysteine in the cyclic stucture (Rosenzweig and Seidman 1991).
**Urodilatin** is a peptide which is produced by the kidney and that could be identified from human urine. The only difference to ANP are four additional amino acids at the N-terminus of the peptide (Schulz-Knappe et al. 1988).

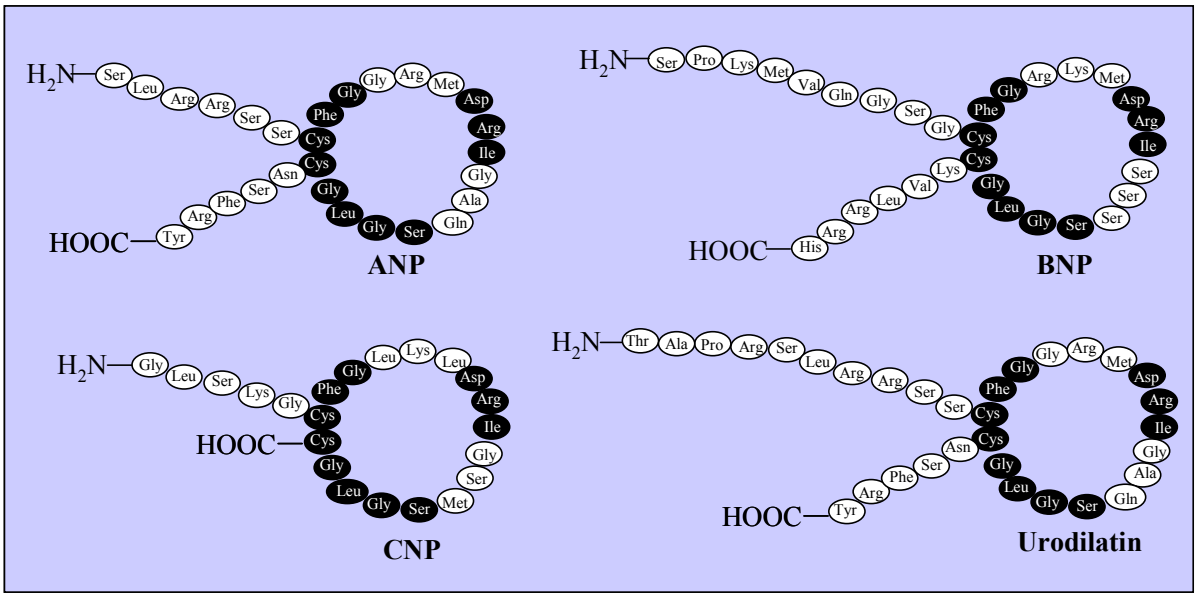


***figure 1: amino acid sequence of the natriuretic peptides ANP, BNP, CNP, and Urodilatin (common sequences are shadded black)***

## 1.2.3 Distribution of the natriuretic peptides

Highest concentrations of ANP are expressed in the left atrium, followed by the right atrium, the right ventricle, and finally the left ventricle in adult humans (Venugopal 2001). More than 1% of the atrial mRNA codes for ANP (Venugopal 2001). Besides the heart, ANP is found in lower concentrations in tissues of the lung, the brain, the kidney, the adrenals, the gastrointestinal tract, the thymus (Vollmar and Schulz 1990b), and the eye (Salzmann et al. 1998).
The second natriuretic peptide, BNP, is predominatly distributed in the ventricles of the heart, followed by the brain of human adults (Venugopal 2001). As mentioned above, CNP is predominantly found in the brain (Stingo et al. 1992a), but also in the myocardial tissue (Venugopal 2001) and it was shown to be produced in peripheral tissues and cells, such as vascular endothelial cells (Stingo et al. 1992b).

### 1.2.4 Synthesis of the natriuretic peptides

The synthesis of ANP is typical for the synthesis of peptide hormones and may serve as an example for the biological synthesis of the three natriuretic peptides. The main synthesis of ANP occurs in the heart, where ANP mRNA codes for a 152 amino acid peptide named prepro-ANP. After cleavage of the N-terminal signal peptide pro-ANP, a 126 amino acid peptide is stored in atrial granula (Rosenzweig and Seidman 1991). Certain stimuli, like dilation of the atrium, lead to the cleavage of pro-ANP into the N-terminal fragment, ANP (1-98), and the biological active ANP (99-126), hereafter named ANP (Rosenzweig and Seidman 1991). The release of ANP from atrial myocytes into the circulation is mediated by exocytosis (Dagnino et al. 1991).

### 1.2.5 The NP receptors and their signaling

After the discovery of the natriuretic peptides and their diuretic and natriuretic effects, the question came up how these effects are mediated. It was first observed that injection of ANP leads to the release of cyclic guanosine-3´,5´-monophosphate (Cantin et al. 1984). Two years later cGMP was shown to act as a second messenger for ANP mediated effects (Leitman and Murad 1986). Kuno and coworkers showed that two different ANP-binding proteins exist, and that only binding to one of those leads to the release of cGMP (Leitman et al. 1986). The non-guanylyl-cyclase-coupled NP receptor, named NPR-C was identified in 1987 by Maack and coworkers as a clearence receptor. In 1989 Schulz and coworkers demonstrated by cDNA sequencing, that there exist two guanylyl-cyclase-coupled natriuretic peptide receptors (NPR-A and NPR-B, figure 2).

The two guanylyl-cyclase-coupled NPR (size 120-140 kDa) are composed of an extracellular binding site, a single membrane-spanning region, and an intracellular tail, composed of a protein kinase like domain and a guanylyl-cyclase-like domain (figure 2). NPR-C (size 60 kDa), the most prevalent of the NPR, has a similar extracellular ligand binding site, but only a short intracellular tail of 37 amino acids (figure 2). Since the amino acid sequence homology in the extracellular binding domain is only 30-40% (Cohen et al. 1996), the three receptors show different ligand specificity. The NPR-A binds with high affinity ANP and BNP compared to CNP. Concerning the induction of cGMP release, ANP is 10-fold more potent than equimolar amounts of BNP. CNP is a specific ligand for NPR-B (Suga et al. 1992). The ligand selectivity of the clearence receptor is much lower than the specificity of

the other receptors and it binds the natriuretic peptides in the following order of affinity ANP>CNP>BNP.

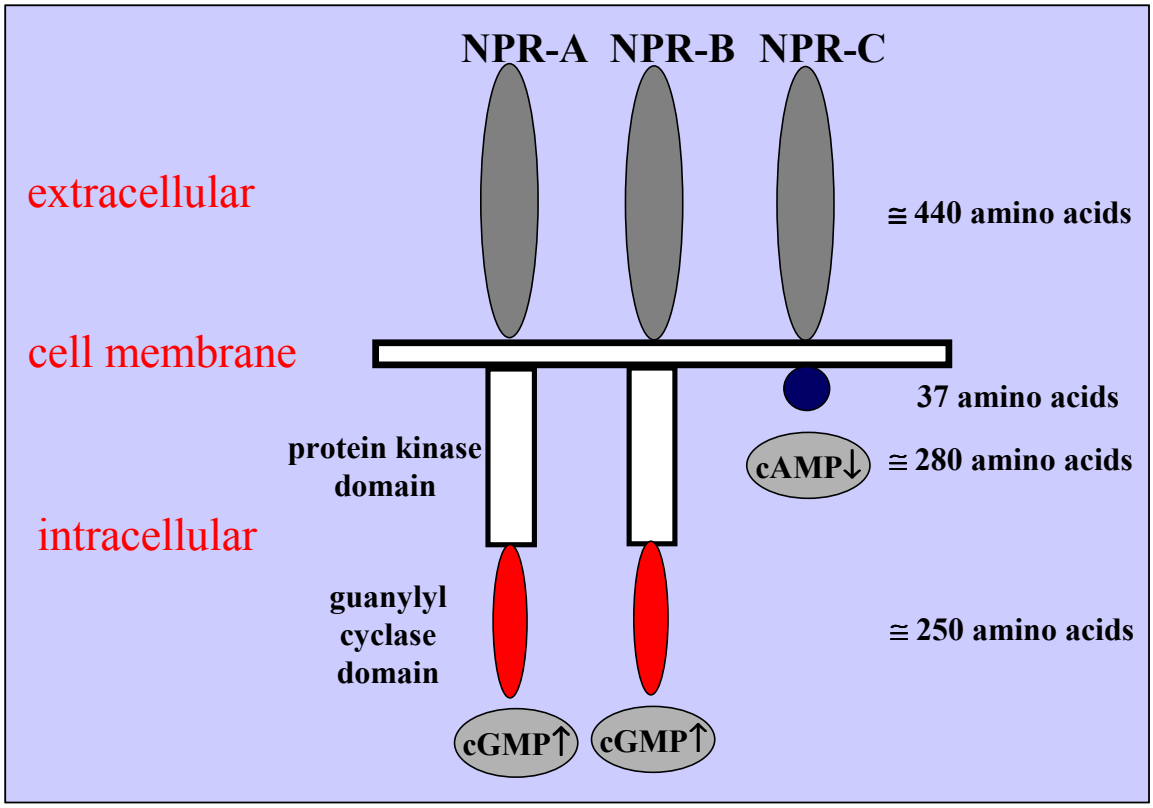


*figure 2: schematic illustration of the three natriuretic peptide receptors: NPR-A, -B, -C*

As mentioned above the two guanylyl-cyclase-coupled receptors (NPR-A and NPR-B) contain a guanylyl-cyclase (GC)-like domain as well as a kinase-like domain. It was shown that after deletion of the kinase-like domain, the GC like-domain is still active, suggesting an inhibitory action of the kinase-like domain on the GC-activity until ANP binds to the extracellular domain of the receptor (Chinkers and Garbers 1989). Ligand binding to the extracellular site of NPR-A and NPR-B allosterically regulates changes in the specific activity of the cytoplasmic domain of these receptors. Another aspect involved in activation of the GC seems to be the dimerisation of the intracellular domain of the receptor (Chinkers and Wilson 1992). Subsequently the intracellular tail of NPR-A and NPR-B catalyses the conversion of guanosine triphosphate to cyclic guanosine-3´,5´-monophosphate, which functions as a second messenger in the following signaling cascade (Leitman and Murad 1986).

The NPR-C mainly acts as a clearence receptor but several studies suggest an interaction of this receptor with two further signal transduction pathways: It was demonstrated that the NPR-C is able to inhibit adenylyl-cyclase (Savoie et al. 1995), and moreover that NPR-C specific analogues of ANP can stimulate the

phospholipase C in a process that involves G-proteins (Levin 1993). These observations may reflect a potential involvement of the NPR-C in adenylyl-cyclase-dependent and protein kinase C-mediated effects.

### 1.2.6 Antiinflammatory potential of ANP

After the discovery of natriuretic peptides, the hormones were thought to possess overall strong cardiovascular effects, such as regulation of blood pressure and plasma volume expansion (Levin et al. 1998).
Interestingly, in the last years natriuretic peptides and their receptors were found to be expressed in diverse tissues besides the cardiovascular and renal system. Vollmar and coworkers were able to show that ANP and its receptors are expressed in thymus (Vollmar and Schulz 1990a), as well as in macrophages (Vollmar and Schulz 1994; Vollmar and Schulz 1995, Kiemer and Vollmar 1997). It could be demonstrated that ANP inhibits thymocyte proliferation and thymopoesis (Vollmar et al. 1996; Vollmar 1997). Moreover, ANP seems to provide antiinflammatory action since it was shown to attenuate the induction of the inducible nitric oxide synthase (iNOS), a central proinflammatory enzyme, in an autocrine fashion (Kiemer and Vollmar 1997; Kiemer and Vollmar 1998; Kiemer and Vollmar 2001a; Kiemer and Vollmar 2001b). Additionally, ANP was found to attenuate the induction of other inflammatory mediators, such as cyclooxygenase-2 (Kiemer et al. 2002b) and TNF-α (Kiemer et al. 2000a; Tsukagoshi et al. 2001). The inhibitory action of ANP on the inflammatory mediator TNF-α could also be observed in LPS-stimulated macrophages (Kiemer et al. 2000a) as well as in reperfused livers (Kiemer et al. 2000b). Another interesting aspect to be mentioned is that ANP is able to induce the heat shock protein HSP70 in rat livers (Kiemer et al. 2002a) providing a cytoprotective potential of this natriuretic peptide.
The summary of these results of the last years demonstrate a relationship of ANP to the immune system, thereby providing novel aspects in the biological profile of NP. The present work indeed deals with the antiinflammatory and antiatherogenic potential of this cardiovascular peptide hormone.

# 1.3 Tumor necrosis factor

## 1.3.1 Overview

Tumor necrosis factor (TNF-α) is a serum glycoprotein with a molecular weight of 70 kDa. As an inducible proinflammatory cytokine TNF-α is mainly produced by activated monocytes and macrophages and influences the growth and behaviour of endothelial cells, monocytes, and smooth muscle cells (Heller and Kronke 1994). TNF-α plays a key role in mediating many inflammatory diseases such as atherosclerosis, septic shock, or rheumatoid arthritis (De Martin et al. 2000).
TNF-α enhances activation of T-cells, and induces proliferation of T-cells and B-cells. Tumor necrosis factor attracts macrophages and granulocytes to sites of inflammation. This attraction stimulates further macrophages and other immune cells to release tissue damaging, oxygen containing substances and prostaglandins to promote further inflammation.

## 1.3.2 Signal transduction by TNF-α

The intracellular pathways that are activated in response to TNF-α have been elucidated increasingly. Many of these pathways have been demonstrated to be cell type-specific. In this context the endothelium has been shown to be a major target of proinflammatory cytokines such as TNF-α.
The signaling pathway that couples TNF receptor activation to functional responses in immune defense have remained elusive. In some cells TNF-α is able to activate RAF kinase, initiating the ERK-MAPK pathway, while in other cells it activates parallel cascades, like MEK kinase, which induces p38 MAPK and JNK MAPK cell response. One of the probably most central responses upon TNF-α treatment is the binding of TNF-α to the TNFR-1 receptor of endothelial cells and subsequently the rapid translocation of the proinflammatory transcription factor NF-κB from the cytoplasm to the nucleus, where it promotes the transcription of respective genes (Karin 1999). These include the genes for adhesion molecules ICAM-1 (intercellular adhesion molecule-1), VCAM-1 (vascular cell adhesion molecule-1), E-selectin (endothelial leukocyte adhesion molecule-1) (for details see chapter 1.4.5), and chemokines like MCP-1 (monocytes chemoattractant protein-1) (see chapter 1.5).

### 1.3.3 Effects of TNF-α on endothelial cells

Effects of TNF-α on endothelial cells, which represent one potential target of this cytokine, include protein synthesis-independent changes in cell shape and motility. TNF-α increases endothelial cell leakiness. Increased vascular permeability (see chapter 1.6) is commonly attributed to the reorganization of F-actin filaments followed by contraction of cells and formation of intercellular gaps (Lum and Malik 1996). In this context formation of intercellular gaps in vascular endothelium is regarded as one of the initial conditions contributing to the development of an atheromatous plaque (Brett et al. 1989; van Hinsbergh 1997, Wojciak-Stothard et al. 1998)
Additionally TNF-α increases the expression of proteins that may subsequently regulate other cell functions such as leukocyte adhesion e.g. E-selectin, ICAM-1, VCAM-1, leukocyte activation (e.g. chemokines like IL-8 and MCP-1), and leukocyte coagulation (e.g. tissue factor and PAI-1). In health, the luminal endothelial cell surface is a relatively nonadhesive conduit for the cellular and macromolecular constituents of the blood. During inflammatory processes, like after TNF-α stimulation, various adhesive interactions between endothelial cells and the constituents of the blood are changed in order to recruit circulating leukocytes to sites of inflammation. The adhesive properties of the endothelium therefore play a central role in this pathophysiological situation.

## 1.4 Adhesion molecules

Besides transcription independent effects on endothelial cells TNF-α can modulate the adhesive properties of the endothelium by inducing the expression of cellular adhesion molecules.
Under healthy conditions, the communication between leukocytes and cells of the blood tissue barrier is well regulated in order to guarantee an efficient immune response upon invasion of pathogens. Two pathways exist which regulate this cell to cell communication system. In one case the communication is mediated by different soluble factors such as cytokines, in the other case the interaction between cells occurs *via* intimate cell-cell contact. The latter is mediated by a group of cell surface proteins, so called cell adhesion molecules (CAM). The following chapter will give an overview of these cell adhesion molecules in order to clarify the complex interactions between endothelial cells and leukocytes during inflammatory situations and diseases.

## 1.4.1 Functions of cell adhesion molecules

The recruitment of leukocytes to sites of inflammation is very critical for the inflammatory response and the repair of damaged tissue. On the one hand this recruitment of leukocytes can be very important for the defense against many pathogens, on the other hand an immoderately proceeded extravasation of leukocytes leads in consequence to inflammation. The process of leukocyte infiltration into the inflamed tissue involves several steps that are resumed in figure 3. First, the leukocytes transiently roll along the vessel wall. The rolling leukocytes then become activated by several factors released by the endothelial cell lining, such as chemokines and cytokines. Rolling of leukocytes is followed by a firm adhesion (sticking) to the vessel wall. In the last step the leukocytes transmigrate through the endothelium to sites of inflammation (diapedesis) (figure 3) (Aplin et al. 1998). These complex mechanisms are mediated by different transmembrane glycoproteins, the cell adhesion molecules (CAM). The initial rolling interactions are mediated by the selectins, while firm adhesion and diapedesis (figure 3) appear to be mediated by the interaction of integrins, present on the cell surface of leukocytes, with immunoglobulin gene superfamily members, such as ICAM-1, VCAM-1, and PECAM-1 (platelet endothelial cell adhesion molecule) expressed on endothelial cells (figure 3).

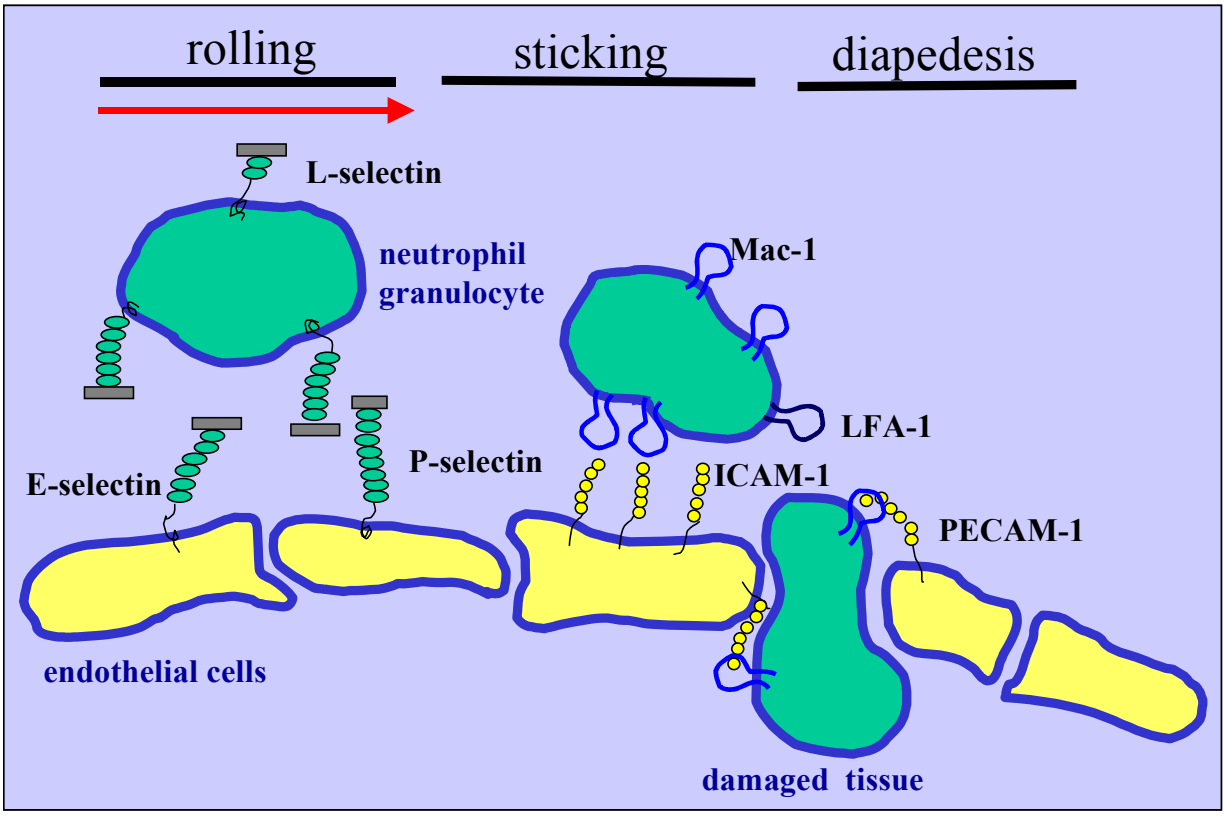


***figure 3: recruitment of leukocytes to sites of inflammation***
Mac-1= macrophage glycoprotein associated with complement receptor function; LFA-1= lymphocyte function associated molecule, ICAM-1= intercellular cell adhesion molecule-1, VCAM-1= vascular

cell adhesion molecule-1, PECAM-1= platelet endothelial cell adhesion molecule-1, E-selectin= endothelial leukocyte adhesion molecule-1, L-selectin= leukocyte adhesion molecule, P-selectin= platelet activation dependent granule-external membrane protein

Under inflammatory conditions, such as atherosclerosis, the expression of cell adhesion molecules on endothelial cells as well as on leukocytes is dynamically upregulated by different soluble chemokines (MCP-1, IL-1β) released by the endothelium. These chemokines give the driving force to the proceeding of the inflammation by forming chemokine gradients over the endothelium which are critically involved in the initial steps of leukocyte recruitment and subsequent transmigration.
In this context TNF-α can act as a proinflammatory cytokine by inducing adhesion molecule expression that bind leukocytes to endothelial cells. The regulation of CAM expression occurs at the transcriptional level and is mediated, especially for ICAM-1 and E-selectin, *via* the proinflammatory transcription factor NF-κB (Collins et al. 1995).

## 1.4.2 Classification

According to their biochemical structure the cell adhesion molecules are classified in four groups: the immunoglobulin-like adhesion molecules, the selectins, the integrins, and the cadherins. The following section will concentrate on the immunoglobulin-like cell adhesion molecules (ICAM-1 and VCAM-1) and selectins (E-selectin) because these endothelial CAM are mainly involved in mediating the recruitment of leukocytes to the inflamed tissue. Their expression can be modified by diverse stimuli produced by the inflamed tissue, like TNF-α.

## 1.4.3 Immunoglobulin-like adhesion molecules

The immunoglobulin gene superfamily is one of the biggest superfamilies of cell adhesion molecules. This family consists of a variety of different cell-surface glycoproteins which are characterized by one or more immunoglobulin homology units (figure 4A). These immunoglobulin domains are composed of 70-100 amino acid residues, which are organized into two parallel β-sheets (Aplin et al. 1998) stabilized by a disulfide binding bridge (figure 4A). More than 70 members are known, including the T-cell receptor, immunoglobulins, MHC antigens, CD2, CD3, CD4, CD8, NCAM (neutral cell adhesion molecule), ICAM-1-5, VCAM-1, and PECAM-1.

The immunoglobulin-like adhesion molecules are involved in a variety of cell functions like antigen recognition (mediated by CD4, CD8, T-cell receptor), cell adhesion (mediated by NCAM linkage to an integrine e.g. LFA, lymphocyte function associated molecule), and leukocyte diapedesis as described above (mediated by ICAM-1-3, VCAM-1, and PECAM-1) (Aplin et al. 1998; Menger and Vollmar 1996).

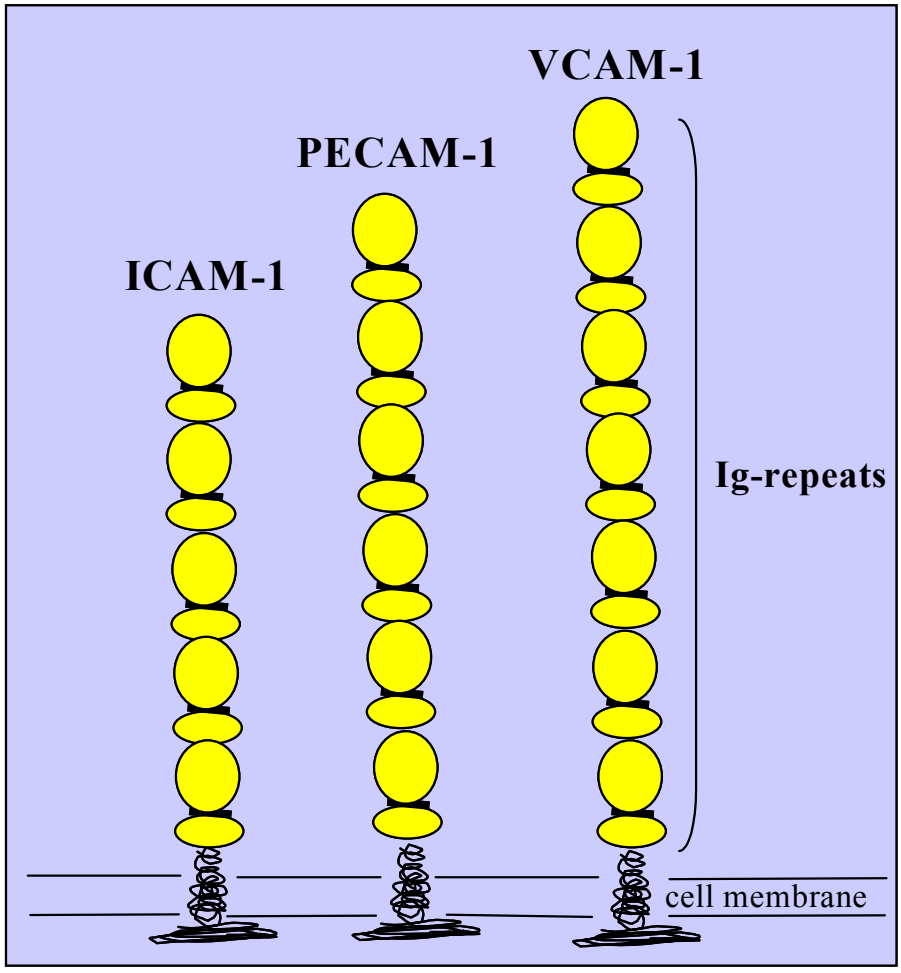


***figure 4A: schematic illustration of the structure of immunoglobulin-like adhesion molecules***

ICAM-1= intercellular adhesion molecule-1, PECAM-1= platelet endothelial cell adhesion molecule-1, VCAM-1= vascular cell adhesion molecule-1

**ICAM-1** is a transmembrane glycoprotein consisting of five immunoglobulin consensus repeats (figure 4A). Under normal conditions this CAM is present on endothelial cells only at very low levels. Upon proinflammatory stimuli (TNF-α, IFN-γ, IL-1β) it is dramatically upregulated by a *de novo* synthesis. The characteristic function of ICAM-1 is the mediation of leukocyte-endothelial interaction by binding to certain integrins like LFA-1 and MAC-1 (figure 3) (Marlin and Springer 1987, Diamond et al. 1991, Aplin et al. 1998) (see under 1.4.1.).

**ICAM-2,** containing only two extracellular immunoglobulin domains, is homologous to ICAM-1, and is constitutively expressed on endothelial cells, platelets, monocytes, and some lymphocytes (Menger and Vollmar 1996). Unlike ICAM-1, ICAM-2 is not upregulated by proinflammatory cytokines. ICAM-2 as well as ICAM-1 mediate the leukocyte-endothelial interaction by binding to certain integrins.
**VCAM-1** is described as a transmembrane protein consisting of six immunoglobulin repeats. The protein is formed after cleavage of a seven immunoglobulin VCAM-1 which is expressed on activated human endothelial cells (Hession et al. 1991). VCAM-1 is upregulated by inflammatory stimuli like TNF-α, IFN-γ and IL-1β. It is involved in the adhesion of monocytes, lymphocytes, and eosinophiles to the vascular endothelium by binding to integrins (Elices et al. 1990; Bevilacqua 1993, Berlin et al. 1995).
**PECAM-1** contains six immunoglobulin-like repeats (figure 4A) and is therefore structurally homologous to other cell adhesion molecules like the described ICAM-1-2 or VCAM-1. The expression of PECAM is constitutive and is not influenced by stimulation with TNF-α, INF-γ, or IL-1β. It is mainly expressed at intercellular junctions of endothelial cells (Albelda et al. 1991). PECAM-1 is suggested to play a key role in regulating the endothelial integrity and in consequence the transendothelial migration of leukocytes (Bevilacqua 1993).

### 1.4.4 Selectins

The selectins are the smallest of the four subclasses of adhesion molecules. They are represented by three members: E-, P-, and L-selectin (figure 4B). The selectins are composed of three different protein domains. The extracellular domain is characterized by an amino-terminal calcium dependent lectin domain (L), an epidermal growth factor-like (EGF-like) domain, and two to nine short consensus repeat units, which are highly homologous to known repeats of complement binding proteins (figure 4B) (Menger and Vollmar 1996). The transmembrane region is followed by a short cytoplasmatic tail.
The selectins are mainly involved in mediating the initial step of leukocyte infiltration in the inflamed tissue as described under 1.4.1. They mediate the transient rolling of leukocytes along the vessel wall as shown in figure 3. Different from most other cell adhesion molecules the selectins do not only bind glycoproteins, but carbohydrates, like sialyl Lewis$^x$, or structures closely related to this carbohydrate compound.

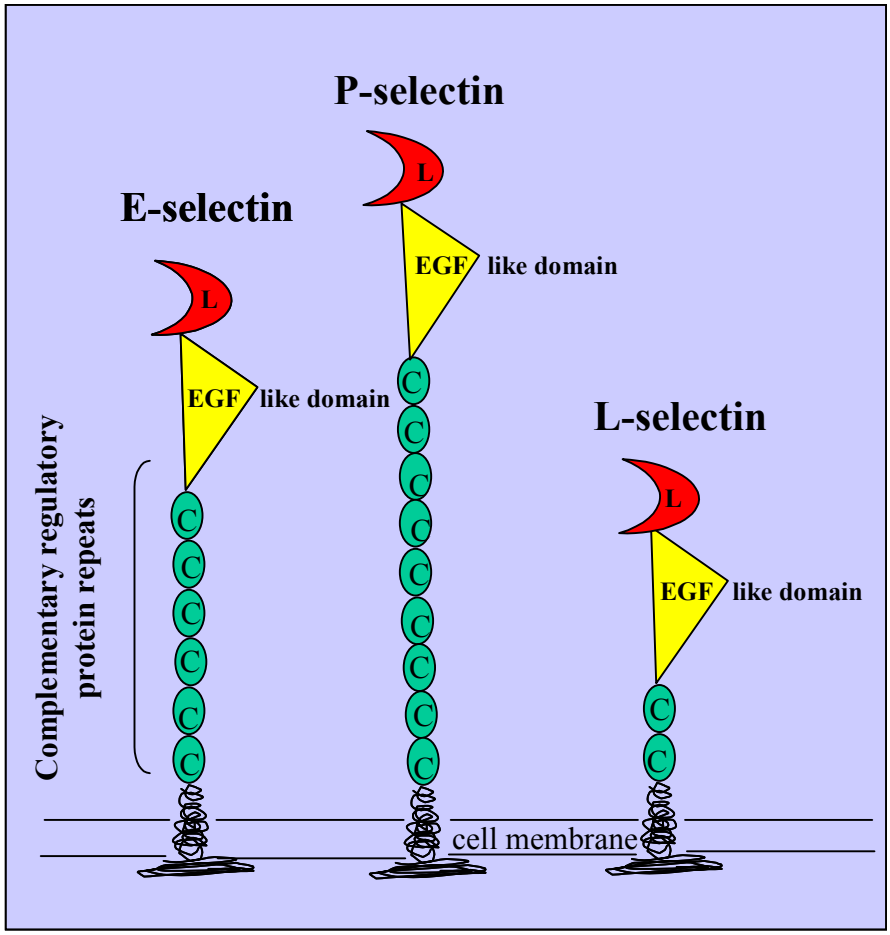


***figure 4B: schematic illustration of the structure of the selectins***

EGF= endothelial growth factor, L= lectin like domain, C= consensus repeats

**L-selectin** (CD62L) is mainly expressed by leukocytes and only consists of two consensus repeats (figure 4B). L-selectin mediates the initial binding of lymphocytes, neutrophiles, and monocytes during rolling (figure 3) (Springer 1994). Several different ligands for L-selectin have been identified, of which the following three glycosylated mucin-like proteins are the most important: CD34, MAdCAM-1, and glycosylation dependent CAM-1.

**E-selectin** (CD62E) consists of six complement regulatory protein regions (figure 4B). E-selectin is mainly expressed by the vascular endothelium and its expression is rapidly upregulated by proinflammatory compounds such as TNF-α, IFN-γ, and IL-1β (Tedder et al. 1995). E-selectin is known to bind two different carbohydrate ligands, the E-selectin-1 ligand and in some cases also the P-selectin glycoprotein ligand (PSGL)-1 (Vachino et al. 1995). E-selectin mainly functions by mediating the transient rolling of leukocytes as described under 1.4.1.

**P-selectin**, the platelet activation dependent granule-external membrane protein, (CD62P), is the biggest of the three selectins. It is charcterized by nine consensus complement regulatory protein domains (figure 4B), and is mainly expressed by platelets and the vascular endothelium (Tedder et al. 1995). Under normal conditions it is stored in Weibel-Palade bodies of endothelial cells or in the granules of platelets. Upon stimulation with certain inflammatory stimuli like thrombin, histamine, complement, and cytokines it is released within minutes to the cell surface of endothelial cells and platelets. P-selectin binds to the P-selectin glycoprotein ligand (PSGL)-1 on leukocytes (Vachino et al. 1995) and induces the leukocyte rolling under healthy and inflamed conditions.

### 1.4.5 Transcriptional regulation of CAM by nuclear factor κB (NF-κB)

The TNF-α-induced increase of CAM expression occurs at the transcriptional level and is regulated, especially for ICAM-1 and E-selectin, *via* the proinflammatory transcription factor NF-κB (Collins et al. 1995). The regulation of VCAM-1 has previously been shown to be mediated *via* pathways that include other transcription factors besides NF-κB (Lawson et al. 1999). The regulatory regions of the VCAM-1 gene are composed of multiple binding elements, which are recognized by a large number of transcription factors. The cytokine-induced transcriptional enhancer in the VCAM-1 promoter requires combinatorial interactions of NF-κB with other nuclear activators, such as stimulatory protein-1, interferon regulatory factor-1, and activator protein-1 (Neish et al. 1995a).
NF-κB was identified more than a decade ago by Sen and Baltimore as an enhancer-binding protein controlling Igκ-light chain gene expression in B-cells (Sen and Baltimore 1986). Expression of NF-κB was long time thought to be restricted to B-cells. In the following years it became evident that NF-κB is not only present in B-cells, but also in diverse other immune cells, for example T-cells with latent immunodeficiency virus (HIV) have been shown to express NF-κB (McKay and Cidlowski 1999). To date NF-κB is known as a ubiquitously expressed transcription factor that can be activated in a wide variety of cells by various stimuli, such as TNF-α, bacterial lipopolysaccharide, and IL-1 (McKay and Cidlowski 1999). NF-κB functions as a dimeric DNA-binding protein that consists of different subunits of a family of related proteins called the Rel family of transcriptional activators. The Rel family includes the mammalian proteins p65 (Rel A), Rel B, c-Rel, p50/p105, p100/p52, and the drosophila melanogaster proteins Drosal and Dif. These various

members of the Rel family are able to homodimerize or heterodimerize with different other Rel proteins. In consequence, different competent DNA-binding NF-κB factors with different sequence specificity are formed upon stimulation (McKay and Cidlowski 1999).

In unstimulated cells, the predominant form of NF-κB is present in the cytoplasm as a heterodimer of p50 and p65 subunits complexed with inhibitory IκB proteins, existing as IκB-α, IκB-β, and IκB-ε isoforms. After cell stimulation, IκBs are phosphorylated, ubiquitinylated, and degraded *via* the 26S ribosome (figure 5). In consequence the classical activated form of NF-κB, the p50/p65 heterodimer, is released and can translocate to the nucleus where it promotes the transcription of respective genes (Karin 1999) (figure 5).

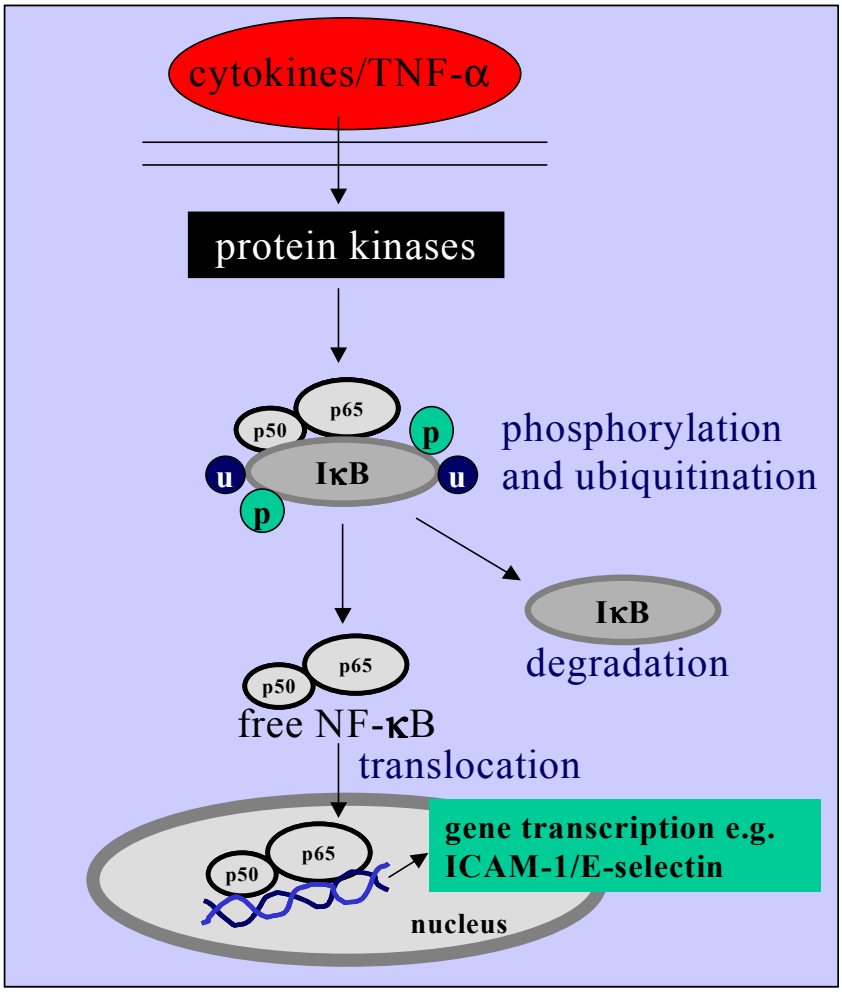


***figure 5: diagram of the signal transduction pathway of TNF-α-activated gene transcription (ICAM-1 and E-selectin)***

Several reporter gene studies using deleted or substituted NF-κB binding sites reflect the importance of this transcription factor for the expression of proinflammatory proteins, including ICAM-1, VCAM-1, E-selectin, IL-1, IL-6, IL-8, COX-2, iNOS, and IκB-α.

# 1.5 Monocyte chemoattractant protein (MCP-1)

Upon treatment of endothelial cells with proinflammatory cytokines such as TNF-α, endothelial cells express certain chemokines, that allow them to communicate with other cells (see 1.4.1). One of the most important chemokines which has been shown to be critically involved in the recruitment of leukocytes to sites of inflamed tissue, is the monocyte chemoattractant protein-1 (MCP-1) (Robinson et al. 1989). MCP-1 has been shown to be mainly regulated *via* the proinflammatory transcription factor NF-κB (Goebeler et al. 1999; Denk et al. 2001; Goebeler et al. 2001). Moreover, it has been demonstrated that the p38 MAPK and its upstream kinase MKK6 (for details see chapter 1.5.4) play a crucial role in the transcriptional regulation of this chemokine after treatment of human endothelial cells with TNF-α (Goebeler et al. 1999).
Chemokines are also termed chemotactic cytokines according to their ability to exert chemoattractive activity on monocytes and T-lymphocytes (Goebeler et al. 2001). These soluble factors represent a large family of structurally related small molecular weight proteins (8-10 kDa). According to the first four conserved cysteines the chemokines can be classified into four groups. MCP-1 is a member of the largest group of chemokines, the CC chemokines (Baggiolini 1998; Luster 1998; Wang et al. 1998). The nomenclature CC derives from the fact that the first two cysteines of the protein are adjacent. In the second subfamily of chemokines, the two first cysteines of the protein are separated by one amino acid residue (X), therefore they are termed CXC chemokines. A prominent member of this subfamily is IL-8 (Baggiolini et al. 1989). Yet only one $CX_3C$ chemokine, the fractalkine (Bazan et al. 1997), has been identified (Reape and Groot 1999). In the structure of fractalkine the first two cysteins are separated by three amino acids (X), explaining the name $CX_3C$ chemokine.
The biological activities of these chemokines are mediated by specific seven-transmembrane-domain G-protein coupled receptors, that are located on the surface of specific cells. Nine receptors for CC chemokines and five receptors for CXC chemokines have been identified and cloned (Reape and Groot 1999). It is well established that chemokine receptors accept more than one chemokine as ligand and that one chemokine can interact with several chemokine receptors (Reape and Groot 1999). It has been demonstrated that CXC chemokines mainly affect neutrophiles while CC chemokines have been shown to interact mainly with monocytes, T- and B-lymphocytes. The fact that a complex network of interactions of chemokines with different receptors and different cell types exists, reflects the crucial role of these inflammatory mediators in regulating the cellular immune response upon treatment with TNF-α or other proinflammatory stimuli. In the last years it has become evident that the expression of chemokine receptors is not restricted to leukocytes since they are

also present on endothelial cells (Gupta et al. 1998; Volin et al. 1998) and vascular smooth muscle cells (Hayes et al. 1998).
Most chemokines have a heparin-binding site which can interact with several proteoglycan receptors on cell surfaces and in the extracellular matrix (Reape and Groot 1999). This interaction has been demonstrated to be responsible for forming chemokine gradients over the endothelium which are critically involved in mediating the initial steps in leukocyte recruitment and subsequent transmigration.

# 1.6 The cytoskeleton

The eukaryotic cell can change its shape and in consequence it has the ability to move, secrete, and phagocytose. This feature of the eukaryotic cell is due to its cytoskeleton. As a very dynamical structure the cytoskeleton consists of a variety of protein filaments which are coupled to the cell membrane and the cytoplasm. By controlling cell shape, mobility, and contractility the cytoskeleton has been identified to play a crucial role in mediating the immune response. In the following chapter the three main components of the cytoskeleton and their regulation will be described.

## 1.6.1 Cytoskeleton components

The components of the endothelial cytoskeleton can be divided in three subclasses of protein filaments, whereby the different filaments consist of different protein subunits. The subclasses are intermediate filaments, microtubuli, and actin filaments which together form the dynamic framework of the cytoskeleton.

### 1.6.1.1 Microtubuli

Microtubuli filaments are the thickest of the mentioned filament subtypes. They have a diameter of 25 nm and consist of tubulin subunits. Tubulin is a cytoskeleton protein which can polymerize, resulting in a tube-like structure of filaments. Microtubuli are very prominent toward the center of the cell and much less so in the periphery (Connolly et al. 1981). Microtubuli are structure elements of the centrosomes and play a key role in giving strength to the cell, transport of cellular compounds and most notably in cell division.

#### 1.6.1.2 Intermediate filaments

The intermediate filaments represent the second subclass of protein filaments with a diameter of 10 nm. The diameter of the intermediate filaments ranks between the microtubuli and the actin filaments, and is therefore named “intermediate”. The intermediate filaments are responsible for the stabilisation and strength of the cell. They consist of long, cord like, fibrin protein subunits and can be divided into three classes according to their distribution: keratin filaments in epithelial cells, vimentin filaments in muscle and glia cells, and neuro filaments in neurones. Intermediate filaments are represented all over the cell, providing mechanical protection for the cell.

#### 1.6.1.3 Actin filaments

Actin filaments are the thinnest of the three filament subclasses with a diameter of only 6 nm. This is why they are also named microfilaments. The structure of actin filaments is typically represented by a double-stranded helical polymere composed of several monomeric actin subunits (Meijerman et al. 1997). Actin filaments are present all over the cytoplasm of the cell, but they are found in highest concentrations directly under the cytoplasmic membrane. They are organized in bundles or nets. Actin filaments are the primary structures that mainly regulate the cell shape and motility by binding certain proteins. In regard of the pivotal role of the actin filaments in several inflammatory diseases such as atherosclerosis, the following section will give detailed information about regulation and function of this special cytoskeleton component.

### 1.6.2 G-actin polymerization and stress fibers

Endothelial cells contain the contractile protein actin in two different forms: in a filamentous form, called F-actin, and in a monomeric form, called G-actin (Tobacman and Korn 1983). Actin filaments are dynamical structures, and the shift between the monomeric and the polymeric form (figure 6) of this protein plays a central role in several cell functions, especially those involving cell shape and movement. With nearly 5%, actin is the most common protein in the eukaryotic cell (Carpenter 2000), whereby about half of the actin filaments are present in F-actin form and half in G-actin form.

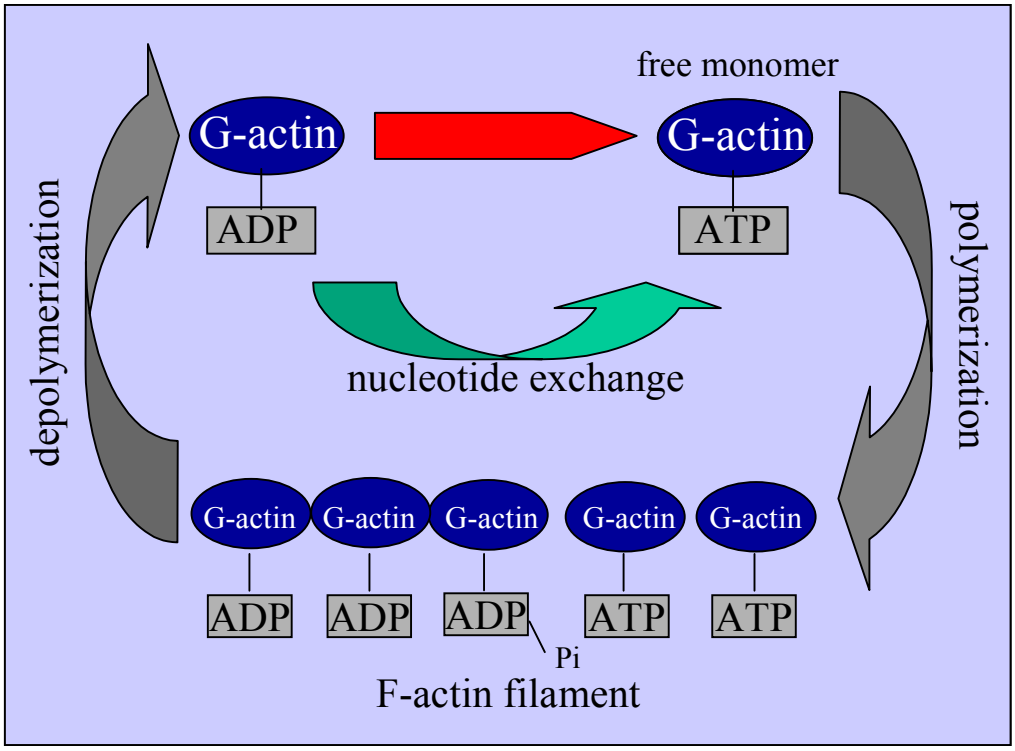


***figure 6: schematic diagram of the actin polymerization***

G-actin polymerization requires the presence of ATP, $K^+$ and $Ca^{2+}$. The formation of F-actin filaments is limited by the rate of conversion of actin monomers into dimers and trimers (Carpenter 2000). Upon the time point of binding an actin trimer the polymerization is speeded up. Subsequently, the polymerization is regulated by the concentration of free G-actin monomers. In the next step actin binds ATP, and the monomer is incorporated into the polymer (figure 6). Short time after the association of the monomeric G-actin to the polymer F-actin strand, ATP is hydrolysed into ADP. This hydrolysis leads to the stabilization of the filament. Actin filaments contain two different ends, a faster growing plus end, also named "barbed" end, and a slower growing minus end, also named "pointed" end.

The growth of F-actin filaments is determined by factors that regulate the breakdown of the filament by depolymerization. According to the polarity of F-actin filament ends, they are able to bind to several different modulating proteins. These actin binding proteins determine the superstructure of actin filaments.

There is a variety of actin binding proteins, among which **α-Actinin** plays a crucial role in regulating the tertiary structure of F-actin filaments. α-Actinin is involved in the formation of actin bundles like those found in microvilli and especially in the so called stress fibers (Carpenter 2000). F-actin stress fibers additionally contain filamin, topomyosin and myosin in periodical order. Due to their association with myosin they provide contractile properties (Sanger et al. 1980). Formation of stress fibers leads to

increased adherence of the cell since stress fibers associate with the so called adhesive matrix contacts (focal adhesions) (Reinhard et al. 1995).
F-actin stress fibers possess a dynamic, flexible structure which allows the cells to respond to stimuli such as TNF-α, by cell movement, cell division, and changes in cell shape.
Another actin binding protein is **Thymosin**. It plays a key role in regulating actin polymerization by binding monomeric G-actin, and therefore creating a kind of deposit for further polymerization. **Gelsolin** functions by cleaving F-actin filaments and masking the "capping end" of the separated pieces. Gelsolin therefore mediates the disrupture of actin filaments and acts as a so called "capping protein". On the other hand **Profilin** is an actin binding protein that is able to increase the polymerization rate by catalyzing the ADP/ATP exchange. A further actin binding protein that functions as a capping protein, is the **small heat shock protein (HSP27)**. HSP27 has been shown to interact with the actin cytoskeleton.

### 1.6.3 Heat shock protein 27

The small heat shock protein HSP27 is a member of the multigene family of heat shock proteins comprising proteins with a molecular size between ten and 150 kDa. Heat shock proteins are found to be expressed in all major tissues (Benjamin and McMillan 1998). The name heat shock proteins derives from the early observation that heat stress (5°C over normal growth temperature) rapidly induces the expression of these proteins (Tissieres et al. 1974). Further research showed that HSPs could also be induced by various other stress factors than heat, including e.g. heavy metals, amino acid analogues, inflammation, and oxidative/ischemic stress. Consequently, the term "heat shock family of stress proteins" is preferred to characterize this protein family. Heat shock proteins mainly function as so called "molecular chaperones" by facilitating the refolding of partially denatured proteins into active conformations. Therefore, they play a crucial role in protein biosynthesis (Georgopoulos and Welch 1993).
After its discovery as an inhibitor of actin polymerization (Miron et al. 1991), HSP27 was found to regulate the dynamic actin network of cells in many tissues. Diverse physiological stimuli, such as oxidative stress, cytokines, and growth factors dramatically increase the phosphorylation of HSP27. The Ser 15, Ser 78, and Ser 83 residues have been shown to be involved in this stress-induced phosphorylation (Gaestel et al. 1991; Landry et al. 1992). The phosphorylation of HSP27 is catalyzed

by a member of the family of mitogen activated protein kinases (MAPK), the p38 MAPK (Kyriakis and Avruch 1996).
It has been demonstrated in diverse tissues that in response to stress factors, such as mentioned above, the p38 MAPK is rapidly stimulated, resulting in an increased activity of the mitogen activated kinase activated protein kinase-2 (MAPKAPK-2) and subsequently in the phosphorylation of HSP27 (Gaestel et al. 1991; Landry et al. 1992). HSP27 therefore represents a downstream target of the p38 mitogen activated protein kinase (MAPK) (for review see (Obata et al. 2000)). As mentioned under 1.5.2, the function of HSP27 in regulating the actin cytoskeleton depends on the phosphorylation state and the secondary structure (formation of monomers or oligomers) of this protein (Lavoie et al. 1993). Unphosphorylated HSP27 inhibits the actin polymerization by depolarization of the actin filaments. This depolarization is mediated by the binding of monomers or small oligomers of HSP27 to the barbed end of the filament (Benndorf et al. 1994). In consequence, G-actin monomers are no longer able to be incorporated into the filament and the F-actin polymerization is inhibited. After phosphorylation by the mentioned MAPKAPK-2, HSP27 dissociates from the filament and the polymerization can continue (Benndorf et al. 1994). Besides this inhibitory property of HSP27 on the actin polymerization process, Miron and coworkers were able to show that HSP27 modulates existing actin filament structures by depolymerization (Miron et al. 1991).
From the described actin binding proteins, especially heat shock protein HSP27 has been closely associated with the regulation of the tertiary structures of actin filaments such as stress fibers (Landry and Huot 1995).

### 1.6.4 p38 mitogen activated protein kinase

As described above, the activation of the p38 MAPK cascade is involved in activating HSP27 *via* phosphorylation of the mitogen activated kinase activated protein kinase-2 (MAPKAPK-2) (Gaestel et al. 1991; Landry et al. 1992).
Besides its role in activating HSP27 the p38 MAPK is involved in multiple other cellular responses which include the mitogen activated protein kinases (MAPK) signaling pathway. For example this pathway plays a key role in the recruitment of leukocytes to sites of inflammation and the release of certain chemokines, such as monocyte chemoattractant protein-1 (MCP-1) (see chapter 1.5).
Therefore, the following chapter will give a short resume of the MAPK cascade with concentration on the p38 MAPK since this MAPK was investigated in the present work.

*Via* the MAPK signaling pathway the cell is able to transduce extracellular signals to intracellular response. To date, more than twelve MAPK have been identified and cloned. These twelve kinases can be divided into three subclasses, the stress-activated protein kinases/c-Jun N-terminal kinases (JNK/SAPK), the extracellular responsive kinases or extracellular regulated protein kinases (ERK), and the p38 MAPK (figure 7). The group of the p38 MAPK can be divided in several isoforms, which are classified due to their ability to respond to different stimuli. In endothelial cells mainly p38α, β, and γ are expressed, whereby p38δ is not found in these cells (Hale et al. 1999).

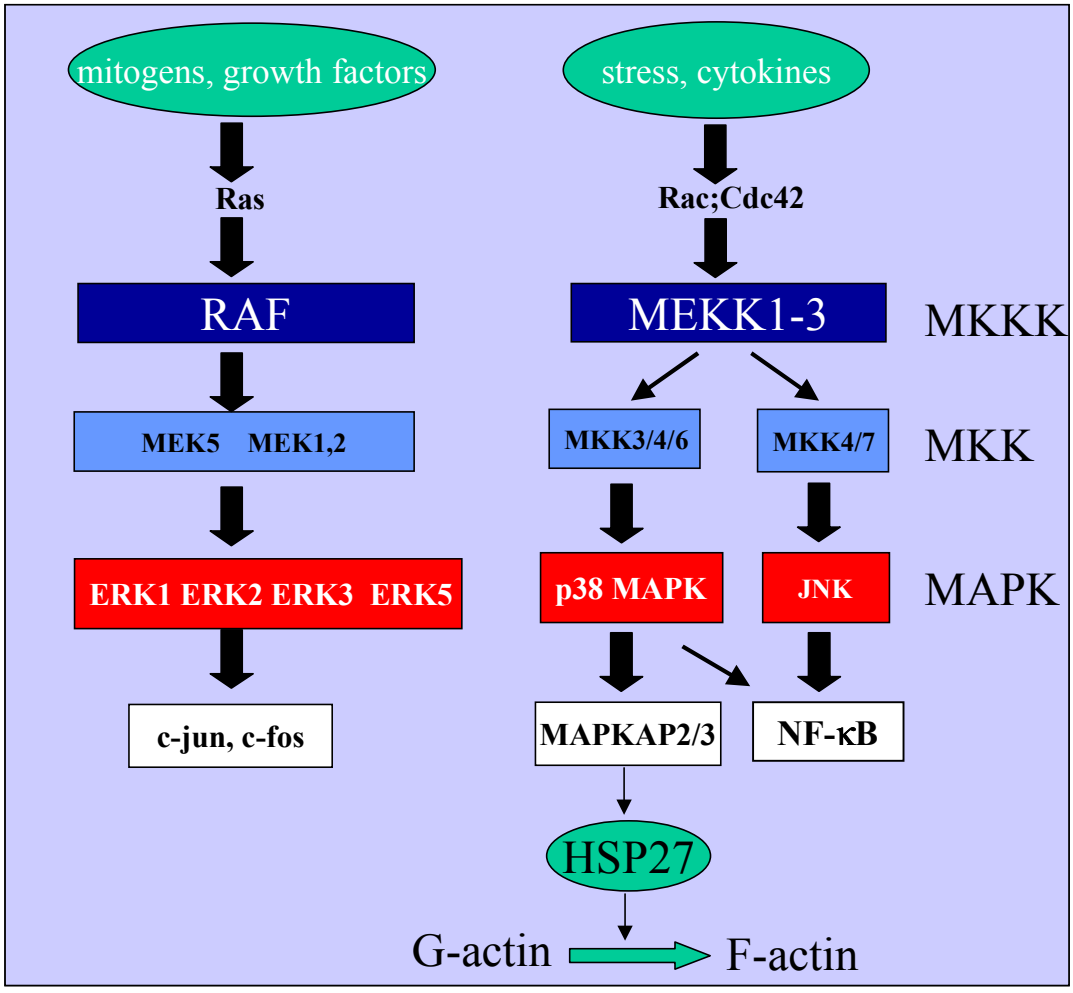


***figure 7: schematic diagram of the MAPK cascade***

A common feature of all known MAPK is the phosphorylation at both threonine and tyrosine residues by a dual specific upstream MAPK kinase (MKK). The MKK itself is phosphorylated by an upstream MKK-kinase, also called MKKK (Herlaar and Brown 1999). Once activated, the different MAPK can phosphorylate and therefore

activate several more kinases. In a final step, the activated MAPK, like p38, is able to acivate proteins, such as transcription factors or as described here, HSP27. The p38 MAPK is mainly activated by extracellular stress factors, like UV-light, osmotic shock (Herlaar and Brown 1999), and cytokines such as TNF-α. The p38 MAPK is activated by the upstream kinases MKK3 or 6, which are themselves a downstream targets of Rac and Cdc42 (Yuasa et al. 1998) (figure 7). Upon activation, p38 leads to phosphorylation of MAPKAP-2 followed by activation of HSP27. Therefore, p38 MAPK is critically involved in the regulation and modulation of the actin cytoskeleton.

### 1.6.5 MAPK phosphatase-1

Besides the regulation of p38 phosphorylation by its upstream kinases MKK3 and 6, (see chapter 1.6.4), MAPK in mammalian cells are regulated by a family of dual-specific MAPK phosphatases (MKP), which target the two critical phosphorylation sites (tyrosine and threonine) of MAPK. The first member of this expanding group of dual-specific phosphatases was isolated from the vaccinia virus in 1992 (Guan et al. 1992), called VH1. Soon a mammalian homologue was isolated and cloned, termed VHR (Ishibashi et al. 1992). The 20 kDa VHR was followed by a number of further proteins, which were termed MKP (MAP kinases phosphatases), existing as MKP-1-5, MKP-X, B23, Pac-1, and M3/6 (Saxena and Mustelin 2000). These nine members of the MKP family share a common structure, comprising a catalytic domain with amino acid homology to VH1, and an amino-terminal noncatalytic domain with two short regions of sequence homology to the cdc25 phosphatase (Keyse and Ginsburg 1993; Keyse 1995). The MKP have been shown to provide a high specificity in dephosphorylating and therefore deactivating the main subtypes of the MAPK family (Alessi et al. 1993; Sun et al. 1993; Ward et al. 1994). MKP differ in their expression pattern in various cell types. Moreover, the expression of MKP upon various stimuli, such as heat shock, stress stimuli, and oxidative stress follow different kinetics (Saxena and Mustelin 2000). MKP-1/2, Pac-1, and B23 are predominantly expressed in the nucleus, and are induced by either growth factor or stress (Keyse 2000). M3/6, MKP-3/4/5, and MKP-X however are predominatly localized in the cytosol of mammalian cells (Keyse 2000). From the known MKP, MKP-1 (CL100) has been shown to be specifically responsible for the dephosphorylation of p38 (Chen et al. 2001), which could neither be shown for MKP-2 (Chu et al. 1996) nor MKP-3 (Nichols et al. 2000).

### 1.6.6 Endothelial permeability

Due to the pivotal function of the endothelium to create a semi-permeable barrier between the blood and the interstitial space of all organs, and the fact that it is characterized by a large surface area, the endothelium represents a target for many inflammatory stimuli released during several inflammatory diseases (Brett et al. 1989; van Hinsbergh 1997; Wojciak-Stothard et al. 1998).
Inflammatory stimuli, such as TNF-α, thrombin, or histamin are able to increase the endothelial permeability by formation of intercellular gaps in the vascular endothelium. The resulting increased vascular permeability is commonly attributed to the reorganization of F-actin filaments into stress fibers, followed by contraction of cells (Lum and Malik 1996), increased macromolecule permeability, and edema formation in the inflamed tissue.

# 2 MATERIALS AND METHODS

## 2.1 Materials

Rat ANP 99-126 ("ANP") and CNP were purchased from Calbiochem (Schwalbach, Germany), 8-Br-cGMP was from Sigma (Taufkirchen, Germany). cANF was purchased from Saxon Biochemicals (Hannover, Germany). HS-142-1 was a gift from Dr. Matsuda, Pharmaceutical Research Institute, Kyowa Hakko Kogyo Co., LTD, Shizuoka, Japan. Antiserum against the "von Willebrand-factor" was from Serotec LTD (Wiesbaden, Germany). GSNO (S-Nitroso-L-glutathione) and L-NNA ($N^G$-Nitro-L –arginine) were from Alexis Biochemicals (Grünberg, Germany). Cell culture medium (M199) and penicillin/ streptomycine were from PAN (Aidenbach, Germany). Fetal calf serum was from Biochrom (Berlin, Germany), Endothelial Cell Growth Medium (ECGM®) from Promocell (Heidelberg, Germany). The enhanced chemoluminescence protein detection kit was purchased from NEN (Cologne, Germany); Complete® was obtained from Roche (Mannheim, Germany). anti-p50, anti-p65 (antibodies for Western blot and TransCruz® antibodies for supershift assays), anti-IκB-α, -β, and -ε antibodies, anti-MKP-1 and anti-HSP27 antibodies were purchased from Santa Cruz (Heidelberg, Germany), anti-phospho-IκB antibody, anti-phospho-p38, anti-phospho-HSP27, and anti-phospho MKK3/6 polyclonal rabbit anti-human antibodies were from Cell Signaling (Frankfurt/M, Germany), anti-p65 from Stressgen (San Diego, USA), peroxidase-conjugated goat anti-rabbit and donkey anti-goat antibodies were from Jackson Immunolab (Dianova, Hamburg, Germany), and anti-p38 antibody from Calbiochem (Schwalbach, Germany). Rhodamin-conjugated phalloidin was from Molecular probes-Mobitec (Göttingen, Germay). FITC-labeled antibodies against ICAM-1, VCAM-1, and E-selectin were from Biosource (Nivelles, Belgium), and FITC-labeled anti-rabbit antibody was from Dianova (Hamburg, Germany). The primer for RT-PCR for E-selectin, ICAM-1, and VCAM-1 were from Biosource Nivelles, Belgium), primer for MKP-1, MCP-1, IκB-α, GAPDH, decoy and scrambled oligonucleotides were from MWG-biotech AG (Ebersberg, Germany). All other materials were purchased from Sigma (Taufkirchen, Germany) or Merck-Eurolab (Munich, Germany).

Note: The experiments were performed with rat ANP 99-126, not human ANP, because first observations concerning ANP effects on TNF-α-induced cell changes were made after treatment with rat ANP. Moreover, as mentioned in the introduction, human ANP and rat ANP differ only in one amino acid. In case of human ANP it is methionine and in case of rat ANP it is isoleucine.

# 2.2 Cell culture

**Solutions:**

| **PBS:** | | **PBS $^{+}$:** | |
|---|---|---|---|
| $Na_2HPO_4$ | 1.48 g (8.0 mmol/L) | NaCl | 8.00 g |
| $KH_2PO_4$ | 0.43 g (1.5 mmol/L) | KCl | 0.20 g |
| NaCl | 7.20 g (160 mmol/L) | $Na_2HPO_4$ | 1.15 g |
| $H_2O$ | ad 1000 ml | $KH_2PO_4$ | 0.20 g |
| | | $MgCl_2$ x 6 $H_2O$ | 0.10 g |
| | | $CaCl_2$ | 0.10 g |
| | | $H_2O$ | ad 1000 ml |

| **Trypsin/EDTA:** | |
|---|---|
| Trypsin (diluted 1:250 in PBS) | 0.05 g |
| EDTA (Sigma) | 0.20 g |
| PBS | ad 100 ml |

## 2.2.1 Cell isolation

Human umbilical vein endothelial cells (HUVEC) were prepared by digestion of umbilical veins with 0.1 g/L of collagenase A (Roche, Mannheim, Germany) and were either grown in endothelial cell growth medium (ECGM, Promocell, Heidelberg, Germany) or in M199 (PAN, Aidenbach, Germany) supplemented with 20% heat-inactivated FCS, 1x endothelial cell growth supplement (Sigma, Taufkirchen, Germany), and penicillin (100 U/ml)/streptomycine (100 ng/ml). In order to compensate inter-individual differences, cells of at least two umbilical cords were combined for each cell preparation.

## 2.2.2 Passaging of HUVEC

For passaging of HUVEC medium was removed and the cells were washed three times with ice-cold $PBS^{+}$. Afterwards HUVEC where incubated with 2 ml trypsin/EDTA solution for 2 min at 37°C. The cells where gradually detached and the digestion of trypsin was stopped with M199 containing 10% FCS. After centrifugation at 218 x *g*,

4°C for 10 min the supernatant was discarded and the pellet was resuspended in M199 supplemented with 20% heat-inactivated FCS, 1x endothelial cell growth supplement (Sigma, Taufkirchen, Germany), and penicillin (100 U/ml)/streptomycine (100 ng/ml). HUVEC were subcultured 1:3 in culture flasks or plates and grown until confluence. Experiments were performed with cells of passage number three or four grown until confluence in 6-, 12-, or 24-well plates (Peske, Aindling-Pichl, Germany). HUVEC were found > 95% pure as judged by FACS analysis (FACScan, Becton Dickenson, Heidelberg, Germany), using an antiserum against the "von Willebrand-factor" (Serotec LTD, Wiesbaden, Germany).

### 2.2.3 Freezing, storage, and thawing of HUVEC

For long time storage confluent HUVEC monolayers were trypsinized and the detached cells were centrifuged at 218 x *g* for 10 min, 4°C. The pellet was resuspended in 1.5 ml freezing medium [M199 supplemented with 20% heat-inactivated FCS, 1x endothelial cell growth supplement (Sigma, Taufkirchen, Germany)], containing 10% [v/v] DMSO. Cells in cryovials were gradually frozen at –20°C for one day, overnight at -80°C and than stored at -196°C in liquid nitrogen. For thawing, cells were rapidly warmed at 37°C and for removing DMSO centrifuged at 218 x *g* for 10 min, 4°C in M199 containing 10% FCS. The supernatant was discarded and the pellet was resuspended in culturing medium. Cells were subcultured into culture plates and cultivated until confluence.

## 2.3 Flow cytometric analysis of cell adhesion molecules

**Solutions:**

**FACS-buffer:**

| | |
|---|---|
| NaCl | 8.12 g |
| $KH_2PO_4$ | 0.26 g |
| $Na_2HPO_4$ | 2.35 g |
| KCl | 0.28 g |
| $Na_2EDTA$ | 0.36 g |
| LiCl | 0.43 g |

Na-azide 0.20 g
$H_2O$ ad 1000 ml pH 7.37

PBS/PBS$^+$
Trypsin/EDTA see under 2.2

**Used antibodies:**

Sheep anti-human "von Willebrand Factor": FITC (Serotec)
Mouse anti-human Vascular Cell Adhesion Molecule-1 (VCAM-1) (Biosource)
Anti-ELAM-1, FITC/mouse anti human CD62 E (Calbiochem)
Mouse anti-human Intercellular Adhesion Molecule-1/FITC (ICAM-1) (Biosource)

**Experimental procedure:**

HUVEC (24 well plates, 200 µl) were grown until confluence and were left either untreated or treated with TNF-α (10 ng/ml, Sigma, Taufkirchen, Germany). The effect of the following substances on the surface expression of cell adhesion molecules was determined: ANP ($10^{-8}$-$10^{-6}$ mol/L), CNP ($10^{-8}$-$10^{-6}$ mol/L), cANF ($10^{-6}$ mol/L), 8-Br-cGMP ($10^{-3}$ and $10^{-4}$ mol/L), and HS-142-1 (10 µg/ml). Substances were added to the cells 30 min before TNF-α. After 5 h (E-selectin) or 6 h (ICAM-1, VCAM-1), surface expression of adhesion molecules was measured by flow cytometry using FITC-labeled antibodies against ICAM-1, VCAM-1, and E-selectin (Biosource, Nivelles, Belgium). Briefly, cells were washed with ice-cold PBS three times and trypsinized. After scraping the cells with a rubber policeman and transferring them into FACS tubes the digestion was stopped by addition of M199 containing 10% FCS. After centrifugation (218 x *g*, 4°C, 15 min), the cell pellet was washed with ice-cold PBS three times. Cells were incubated with 1% bovine serum albumine (BSA) for 30 min at room temperature. After 30 min of incubation with the respective antibody the cells were again washed with PBS and resuspended in a volume of 300 µl PBS for flow cytometric analysis. For the adjustment of instrument settings control cells were prepared by performing the procedure as described above but by omitting the addition of the antibody. In each experiment the mean fluorescence of TNF-α treated cells was set as 100% and all other treatment conditions were compared to this group. At least three different sets of experiments with cells from different isolations were performed in triplicates.

# 2.4 Electrophoretic mobility shift assay

## 2.4.1 Isolation of nuclear and cytosolic protein

**Solutions:**

| **Buffer A:** | | **Buffer B:** | |
|---|---|---|---|
| HEPES pH 7.9 (Sigma) | 10 mmol/L | HEPES pH 7.9 | 20 mmol/L |
| KCl (Merck) | 10 mmol/L | NaCl (Roth) | 0.4 mol/L |
| EDTA (Sigma) | 0.1 mmol/L | EDTA | 1.0 mmol/L |
| EGTA (Sigma) | 0.1 mmol/L | EGTA | 1.0 mmol/L |
| $H_2O$ | ad 50 ml | Glycerol (100%) | 25% |
| | | $H_2O$ | ad 50 ml |

DTT 1.0 mmol/L (fresh)
PMSF 0.5 mmol/L (fresh)
**DTT stock solution:** 1 ml of a 1 mol/L solution was aliquoted and stored at -20° C
**PMSF stock solution:** 1 ml of a 50 nmol/L solution in isopropanol was aliquoted and stored at -20° C

**Experimental procedure:**

HUVEC were cultured in 6-well plates until confluence and were either left untreated or stimulated with TNF-α (10 ng/ml) for 1 h in the presence or absence of ANP ($10^{-7}$-$10^{-6}$ mol/L), CNP ($10^{-8}$-$10^{-6}$ mol/L), or 8-Br-cGMP ($10^{-3}$ mol/L), which were added to the cells 30 min before TNF-α. Nuclear and cytosolic extracts were prepared as described in (Schreiber et al. 1989). Briefly, HUVEC were washed with PBS, scraped, and resuspended in 400 µl of hypotonic buffer A. Cells were allowed to swell on ice for 15 min. Nonidet P-40 (10%, 25 µl) was added followed by 10 sec of vigorous vortexing and centrifugation at 12,000 x *g* for 30 sec. The supernatant (containing the cytosolic protein) was removed and frozen at -20 °C for Western blot analysis. The nuclear pellet was extracted with 50 µl of hypertonic buffer B by shaking at 4°C for 15 min. The extract was centrifuged at 12,000 x *g* and the supernatant was frozen at -85°C. Protein concentrations were determined by the method of Lowry (Lowry OH 1951).

## 2.4.2 Radioactive labeling of oligonucleotides

**Solutions:**

**5 x binding buffer:**

| | |
|---|---|
| Glycerol | 20% (v/v) |
| $MgCl_2$ | 5.0 mmol/L |
| EDTA | 2.5 mmol/L |
| NaCL | 250.0 mmol/L |
| Tris-HCl (Roth) pH 7,5 | 50 mmol/L |
| $H_2O$ | ad 50 ml |

**DTT:** final concentration 2.5 mM added directly

**Loading buffer:**

| | |
|---|---|
| Tris-HCl (Roth) pH 7,5 | 250 mmol/L |
| Bromphenolblue (Sigma) | 0.2% (m/v) |
| Glycerol | 40% (v/v) |

**10 x TBE buffer:**

| | |
|---|---|
| Tris-Base (Roth) | 900 mmol/L |
| Boric acid | 25 mmol/L |
| $H_2O$ | ad 1000 ml |

**PAGE-non denaturing 4.5% Gel:**

| | | |
|---|---|---|
| 10 x TBE | 1 ml | |
| Acrylamide-bis 30 % (Roth) | 3 ml | |
| Glycerol (100%) | 500 µl | |
| $H_2O$ | 15.5 ml | |
| TEMED (N,N,N´,N´-tetramethylethylendiamine) | | 10 µl |
| APS (Ammonium persulfate) 10% (m/v) | | 150 µl |

**Experimental procedure:**

A 22-mer double-stranded oligonucleotide probe containing a consensus binding-sequence for NF-κB (5'-AGT TGA GGG GAC TTT CCC AGG C-3', Promega, Mannheim, Germany), AP-1 (5`-CGC TTG ATG AGT CAG CCG GAA-3`), AP-2 (5`-GAT CGA ACT GAC CGC CCG CGG CCC GT-3`) or Sp-1 (5'-ATT CGA TCG

GGG CGG GGC GAG C-3', Promega, Mannheim, Germany) was 5' end-labeled with [$\gamma^{32}$P]-ATP (10 µCi) using T4 polynucleotide kinase.

## 2.4.3 Binding reaction and electrophoretic separation

Equal amounts of nuclear protein (10 - 20 µg) were incubated (20 min, RT) in a 15 µl reaction volume containing 10 mmol/L Tris-HCl pH 7.5, 5 x $10^4$ cpm radiolabeled oligonucleotide probe, 2 µg poly (dIdC), 4% glycerol, 1 mmol/L $MgCl_2$, 0.5 mmol/L EDTA, 50 mmol/L NaCl, and 0.5 mmol/L DTT. Nucleoprotein-oligonucleotide complexes were resolved by electrophoresis (4.5% non-denaturing polyacrylamide gel, 100 V) and bands were visualized by phosphorimaging (Packard, Meriden, USA). Specificity of the DNA-protein complex was confirmed by competition with a 100-fold excess of unlabeled NF-κB, SP-1, and AP-2 (5'-GAT CGA ACT GAC CGC CCG CGG CCC GT-3') binding sequences, respectively.

## 2.4.4 Supershift assay

**Solutions (see 2.4.3 electrophoretic mobility shift assay)**

**Used antibodies:**

| | |
|---|---|
| Anti-p65 NF-κB | (Santa Cruz, Heidelberg, Germany) |
| Anti-p50 NF-κB | (Santa Cruz) |
| Anti-c-jun | (Santa Cruz) |
| Anti-c-fos | (Santa Cruz) |

**Experimental procedure:**

For supershift analysis, 1 µg of antibodies against p50 , p65, c-jun, or c-fos was added to the reaction mixtures 10 min before the addition of radiolabeled probe.

### 2.4.5 Decoy experiment

For Decoy experiments HUVEC were transiently transfected with decoy (5`-CGC TGG ATG AGT CAG CCG GAA-3`) or scrambled (5`-CAG GAG AGT ATC CTG CGA TGC ATC TGC T-3`) oligonucleotides (0,04 µg/well) using an Effectene™ transfection kit (Quiagen, Hilden Germany). After 4 hours and addition of fresh medium, cells were treated for EMSA.

## 2.5 Western blot analysis

**Solutions:**

**RIPA buffer (lysis buffer):**

| | |
|---|---|
| NaCl | 150 mmol/L |
| Tris-HCl | 50 mmol/L |
| Nonidet P40 | 1.00% (v/v) |
| Deoxycholat | 0.25% (v/v) |
| SDS | 0.10% (m/v) |
| $H_2O$ | ad 1000 ml |

\+ DTT final concentration 1 mmol/L added freshly before use
\+ PMSF final concentration 1 mmol/L added freshly before use
\+ Complete®(Protease inhibitor) 25x stock solution added freshly before use

for detection of phospho-MAPK:

| | |
|---|---|
| NaF | final concentration 50 mmol/L and |
| $Na_3VO_4$ | final concentration 50 mmol/L were added in order to inhibit phosphatases |

**SDS Sample buffer (5 x)** was stored at -20°C and added freshly before use

| | |
|---|---|
| Tris-HCl (pH 6.8) | 3.125 mol/L |
| Glycerol | 5% (v/v) |
| SDS (ICN biomedicals) | 20% (m/v) |
| DTT | 16% (m/v) |
| Pyronin Y (Sigma) | 5% (m/v) |
| $H_2O$ | ad 1000 µl |

**Resolving gel 10% :**

| | |
|---|---|
| Acrylamide 30%-Bisacrylamide 0.8% solution (Roth) | 5.0 ml |
| Tris-base pH 8.8 (Roth) final concentration | 1.5 mol/L |
| 10% SDS | 0.15 ml |
| $H_2O$ | ad 6.10 ml |

The solution was degassed 10 min before addition of:
15 µl TEMED (cross linker) and
75 µl APS (radical starter)
to ensure anaerobic conditions.

**Stacking gel 10%:**

| | |
|---|---|
| Acrylamide 30%-Bisacrylamide 0.8% solution (Roth) | 1.70 ml |
| Tris-base pH 6.8 (Roth) final concentration | 1.25 mol/L |
| 10% SDS | 0.10 ml |
| $H_2O$ | 7.00 ml |

The solution was degassed 10 min before addition of:
+ 20 µl TEMED (cross linker)
+ 100 µl APS (radical starter)

**Electrophoresis buffer:**

| | |
|---|---|
| Tris-base | 3 g |
| Glycin | 14.4 g |
| SDS | 1.0 g |
| $H_2O$ | ad 1000 ml |

**Anode buffer I pH 10.4:**
Tris-base 15 g
+ 100 ml Methanol
+ 400 ml $H_2O$ dest.

**Anode buffer II pH 10.4:**
Tris-base 1.5 g
+ 100 ml Methanol
+ 400 ml $H_2O$ dest.

**Cathode buffer pH 7.6:**
ε-Amino-n-caproic acid 2.6 g
+ 100 ml Methanol

+ 400 ml $H_2O$ dest.

**Tris buffered saline solution containing Tween pH 8.0 (TBS-T):**

| | |
|---|---|
| Tris-base | 3.0 g |
| NaCl | 11.1 g |
| Tween 20 | 1 ml |
| $H_2O$ | ad 1000 ml |

**Primary antibodies:**

| | |
|---|---|
| Phospho-HSP27 (Ser 32) Antibody | Cell signaling |
| Phospho-p38 MAP Kinase Antibody | Cell signaling |
| Anti-p38/HOG1 | Calbiochem |
| MKP-1 (V-15) sc1199 Antibody | Santa Cruz |
| Phospho-IκB (Ser 32) Antibody | Cell signaling |
| I-κB -α, -β, -ε, Antibody | Santa Cruz |
| NF-κB p65 (C-20)-G sc-372-G (goat) | Santa Cruz |
| NF-κB p50 (C-20)-G sc-1192-G (goat) | Santa Cruz |
| anti-Sp1 | Santa Cruz |
| anti-actin | Chemicon international |
| anti-α-tubulin | Sigma |

**Secondary antibodies:**

| | |
|---|---|
| Peroxidase-conjugated donkey anti goat IgG | Jackson I. research |
| Peroxidase-conjugated goat anti rabbit IgG | Jackson I. research |

**Experimental procedure:**

For detecting proteins in whole cell lysates HUVEC were cultured in 12-well plates until confluence and were either left untreated or stimulated with TNF-α (10 ng/ml) in the presence or absence of ANP ($10^{-6}$ mol/L), which was added to the cells 30 min before TNF-α incubation. Briefly, cells were washed with ice-cold PBS and lysed in RIPA buffer which was supplemented with a protease inhibitor cocktail (Complete®), 1 mmol/L DTT, and 1 mmol/L PMSF. For determination of phospho-IκB, phospho-HSP27, and phospho-p38, 50 mmol/L NaF and 50 mmol/L sodium vanadate were additionally added. In some cases Western blots were performed after pretreating the cells with actinomycin D (2 µmol/L for 30 min). For investigating proteins in cytosolic or nuclear fractions, the isolation of cell fractions was performed as described under 2.4.1. Cells were homogenized and centrifuged at 12,000 x *g* for 10 min at 4°C. After determination of protein concentrations in the supernatant by the

method of Lowry (Lowry OH 1951), sample buffer was added to the probes. The samples were heated at 95°C and loaded onto an SDS/PAGE gel (10%) for protein separation, electroblotted, and the respective proteins were detected using the mentioned antibodies. An enhanced chemoluminescence protein detection kit (NEN, Cologne, Germany) and a Kodak Image station (Kodak digital science, Stuttgart, Germany) were used for visualization of the bands.

## 2.6 Enzyme-linked immunosorbent assay (ELISA)

For ELISA HUVEC were grown until confluence in 24-well plates. Cells were left either untreated or treated with TNF-α (10 ng/ml). The effect of the following substances on the expression of TNF-α-induced MCP-1 was determined: ANP ($10^{-11}$-$10^{-6}$ mol/L), cANF ($10^{-8}$-$10^{-6}$ mol/L), 8-Br-cGMP ($10^{-10}$-$10^{-3}$ mol/L), CNP ($10^{-11}$-$10^{-6}$ mol/L), GSNO (S-Nitroso-L-glutathione 125 and 500 µmol/L) and L-NNA ($N^G$-Nitro-L –arginine, 125 and 500 µmol/L). Substances were added to the cells 30 min before TNF-α. After 6 h the supernatants (200 µl) were transferred into a 96-well microtiter plate and the measurement of surface expression of human MCP-1 was determined by an ELISA based on commercial antibody pairs (R&D, Wiesbaden, Germany). Binding of biotinylated antibody was quantified using streptavidin-peroxidase (Jackson Immuno Research, West Grove, PA, USA) and the substrate TMB (3,3',5,5'-tetramethylbenzidine, Sigma). Recombinant MCP-1 (R&D) served as standard.

## 2.7 Antisense assay

**Experimental procedure:**

For antisense experiments, HUVEC were cultured in 12-well plates until confluence. Phosphorothioate oligonucleotides (modifications are shown by small letters in the oligonucleotide sequence) were used in a final concentration of 0.03 µg/well for each transfection reaction. The used oligonucleotides for MKP-1 were: antisense, 5`-cc-CACTTCCATGACCA-tgg-3´; sense, 5`-cc-ATGGTCATGGAAGT-ggg-3`. The cells were transfected using an Effectene™ transfection kit (Qiagen, Hilden, Germany). The mentioned amount of antisense or sense DNA was diluted in water and after addition of an appropriate amount of Enhancer, Effectene reagent was added and the mixture was incubated for 10 min at RT to allow Effectene-reagent-DNA complex formation. During this incubation time HUVEC medium was removed from the monolayers and

fresh M199, supplemented with 20% heat-inactivated FCS, 1x endothelial cell growth supplement, and penicillin (100 U/ml)/streptomycine (100 ng/ml), was added. The transfection complex was added to the cells for an incubation of 3 h. Subsequently medium containing transfection complex was removed and fresh medium was added. Cells were either left untreated or stimulated with TNF-α (10 ng/ml) in the presence or absence of ANP ($10^{-6}$ mol/L), which was added to the cells 30 min before TNF-α incubation. The stimulation time was 30 and 60 min for MKP-1, 15 min for phospho-p38 detection by Western blot, and 6 h for detection of human MCP-1 protein by ELISA. Western blot and ELISA were performed as described under 2.6.

## 2.8 Detection of mRNA

**Used primer:**

| | **sense primer** | **antisense primer** |
|---|---|---|
| **ICAM-1** | 5`-TAT-GGC-AAC-GAC-TCC-TTC-T-3` | 5`-CAT-TCA-GCG-TCA-CCT-TGG-3` |
| **VCAM-1** | 5`-ATG-ACA-TGC-TTG-AGC-CAG-G-3` | 5`-GTG-TCT-CCT-TCT-TTG-ACA-CT-3` |
| **E-Selectin** | 5`-CTC-TGA-CAG-AAG-AAG-CCA-A-3` | 5`-ACT-TGA-GTC-CAG-TGA-AGC-CA-3` |
| **IκB-α** | 5`-CGG-AAT-TCC-AGG-CGG-CCG-AGC-GCC-CC-3´ | 5`-GGG-GTA-CCT-CAT-AAC-GTC-AGA-CGC-TG-3` |
| **MKP-1** | 5`-GCT-GTG-CAG-CAA-CAG-TC-3` | 5`-TAC-CTT-ATG-AGG-ACT-AAT-CG-3` |
| **MCP-1** | 5`-GAT-GCA-ATC-AAT-GCC-CCA-GT-3` | 5`-TTG-CTT-GTC-CAG-GTG-GTC-CAT-3` |
| **GAPDH** | 5`-TCA-CTC-AAG-ATT-GTC-AGC-AA-3` | 5`-AGA-TCC-ACG-ACG-GAC-ACA-TT-3` |

**Conditions:**

| | **denaturing** | **annealing** | **extension** | **cycles** |
|---|---|---|---|---|
| **ICAM-1** | 94°C for 1 min | 55°C for 1 min | 72°C for 1 min | **30** |
| **VCAM-1** | 94°C for 1 min | 55°C for 1 min | 72°C for 1 min | **30** |
| **E-Selectin** | 94°C for 1 min | 55°C for 1 min | 72°C for 1 min | **30** |
| **IκB-α** | 94°C for 1 min | 55°C for 2 min | 72°C for 2 min | **35** |
| **MKP-1** | 95°C for 1 min | 57°C for 2 min | 72°C for 1 min | **35** |
| **MCP-1** | 94°C for 50 sec | 55°C for 1 min | 72°C for 1 min | **28** |
| **GAPDH** | 93°C for 24 sec | 55°C for 30 sec | 73°C for 1 min | **30** |

HUVEC were treated with ANP ($10^{-8}$-$10^{-6}$ mol/L) or TNF-α (10 ng/ml) alone or in combination for 10 min up to 8 h. RNA was prepared using RNeasy® RNA isolation

kit (Qiagen, Hilden, Germany). Reverse transcription was performed using a reverse transcription system kit (Promega, Mannheim, Germany). RT-PCR experiments were performed with primers for ICAM-1, VCAM-1, E-Selectin, IκB-α, MKP-1, iNOS, MCP-1, and GAPDH (see above). PCR was followed by gel electrophoresis, ethidium bromide staining, and densitometric analysis (Kodak Image station, Kodak digital science, Stuttgart, Germany).

## 2.9 Microscopic investigations

**Solutions:**

3.7% (v/v) paraformaldehyde (Sigma)
$PBS^+$ see 2.2 Cell Culture
Triton X-100 0.1% (v/v) (Sigma)
BSA-bovine serum albumin (Sigma) 1% in PBS

### 2.9.1 Immunocytochemistry

**Used antibodies:**

Anti-ELAM-1, FITC/mouse anti-human CD62 E (Calbiochem)
Mouse anti-human Intercellular Adhesion Molecule-1/FITC (Biosource)
Rabbit polyclonal anti-p65 antibody (Stressgen, San Diego, USA)

**Experimental procedure:**

HUVEC were cultured in 24-well plates until confluence and either left untreated or stimulated with TNF-α (10 ng/ml) for 1 h (p65), 5 h (E-selectin), or 6 h (ICAM-1) in the presence or absence of ANP ($10^{-6}$ mol/L, which was added to the cells 30 min before TNF-α). Cells were washed with $PBS^+$ three times and fixed with 3.7% paraformaldehyde for 10 min at RT (20°C).
After fixation the cells were washed, incubated with a 1% solution of BSA (30 min, RT), followed by antibody binding for 30 min at 4°C in the darkness. Visualization of adhesion molecules was performed with a Zeiss Axiovert 25 microscope (Zeiss, Munich, Germany, 400-fold magnification, 450 nm emission wavelength).

For p65 staining the cells were washed twice with $PBS^+$ after fixation and permeabilized for 10 min with 0.2% Triton X-100. The cells were washed again and incubated with a 1% solution of BSA (30 min, RT), followed by staining with an anti-p65 antibody for 1 h at 4°C and a secondary FITC-labeled anti-rabbit antibody. After washing the cells p65, ICAM-1, and E-Selectin were visualized in a Zeiss Axiovert 25 microscope (Zeiss, Munich, Germany) at 450 nm emission wavelength with a 400-fold magnification.

## 2.9.2 Morphological investigations

HUVEC (24-well plates) were either left untreated or stimulated with TNF-α (10 ng/ml) in the presence or absence of ANP ($10^{-6}$ mol/L), which was added to the cells 30 min before TNF-α. After 1 or 24 h cells were washed with $PBS^+$ three times and stained with Haemacolor® (Merck, Munich, Germany) as indicated by the manufacturer. Cells were photographed with a Zeiss Axioskop MC 80 DX microscope (Zeiss, Munich, Germany) with a 200- or 400-fold magnification.

## 2.9.3 Actin staining

HUVEC (24-well plates) were either left untreated or stimulated with TNF-α (10 ng/ml) for 30 min in the presence or absence of ANP ($10^{-6}$ mol/L) or the p38 MAPK inhibitor SB203580 (5 or 10 µmol/L, Calbiochem, Schwalbach, Germany). ANP and SB203580 were added to the cells 30 min before TNF-α. Cells were washed with $PBS^+$ three times and fixed with 3.7% paraformaldehyde for 10 min (RT). After washing twice, cells were permeabilized for 5 min with 0.1% Triton X-100 (RT) and washed again. Cells were incubated with a 1% solution of BSA (30 min, RT), and stained with rhodamine-phalloidine (0.16 mol/L) for 20 min at 4°C in the darkness. After washing, stained F-actin was visualized using a Zeiss Axiovert 25 microscope (Zeiss, Munich, Germany) with a 200- or 400-fold magnification (excitation: 554 nm; emission: 573 nm).

## 2.10 Quantification of F-actin

**Solutions:**

3.7 % (v/v) paraformaldehyde
$PBS^+$ see 2.2 Cell culture
Triton X-100 0.1% (Sigma)
BSA bovine serum albumin 1% in PBS
**Experimental procedure:**

HUVEC were cultured in 24-well plates and were left either untreated or treated with TNF-α (10 ng/ml). The effect of ANP ($10^{-10}$-$10^{-6}$ mol/L), SB203580 ($10^{-5}$ mol/L), and 8-Br-cGMP ($10^{-3}$ and $10^{-4}$ mol/L) alone or in combination with TNF-α on F-actin formation was determined. Substances were added to the cells 30 min before TNF-α. F-actin staining was performed as described above. Bound dye was extracted from the cells with 1.5 ml of methanol (1 h, 4°C, in the dark). Fluorescence of the methanolic dye solution was measured in a Shimadzu spectrofluorophotometer RF 1501 (Shimadzu Duisburg, Germany) (excitation: 554 nm; emission: 573 nm). The mean fluorescence of TNF-α-treated cells was set as 100% and all other treatment conditions were compared to this group.

## 2.11 Permeability assay

HUVEC were cultured in 12-well transwell clear plates (0.4 µm pore size, Costar Cambridge) in a volume of 500 µl (upper compartment). Cells were either left untreated or stimulated with TNF-α (25 ng/ml) with or without ANP ($10^{-6}$ mol/L) or SB203580 (1 µg/ml), added to the cells 30 min before TNF-α. After 24 h, 100 µl of fluoresceine-isothiocyanate-labeled BSA (FITC-BSA, 10 mg/ml, Sigma, Taufkirchen, Germany) was given to the cells. Cell culture medium from the lower compartment (1,500 µl) was removed after 60 min. FITC-BSA was quantified in a Shimadzu spectrofluorophotometer RF 1501 (Shimadzu Duisburg, Germany) at a wavelength of 538 nm (excitation 485 nm). BSA flux is expressed as ratio between fluorescence intensities in the lower compartment (after 60 min) and the upper compartment (0 min).

## 2.12 MTT cytotoxicity assay

**Solutions:**

5 mg/ml MTT [3-(4,5-dimethylthiazol-2-yl)2,5-diphenylthetrazolium bromide] (Sigma, Taufkirchen, Germany) in PBS, sterile.

**Experimental Procedure:**

For MTT assay HUVEC were seeded into 96-well plates and cultured until confluence. The culturing medium was discarded and cells were incubated for at least 6 h with all substances, in the highest concentrations used, in 50 µl M199 containing 10% FCS. Afterwards 5 µl MTT reagent was added for an overnight incubation at 37°C. The next day 250 µl DMSO was added to the supernantant for 3 h. Absorbtion was measured in an SLT Spectra ELISA reader (SLT Labinstruments, Crailsheim, Germany) at 570 nm.

The results of the MTT cytotoxicity assay demonstrated that none of the used substances had any cytotoxic effect on HUVEC (data not shown).

## 2.13 Statistical analysis

All experiments were done from cells of at least three different cell preparations. Each experiment was performed at least in triplicates. Data are expressed as mean ± S.E.M. Values with $p \leq 0.05$ were considered statistically different compared to 100% or 1-fold (TNF-α treated cells) (one sample t-test). Statistical analysis was performed with Graph Pad Prism (version 3.02).

# 3 RESULTS

# 3.1 Adhesion molecules

## 3.1.1 ANP inhibits TNF-α-induced expression of adhesion molecules

In order to determine the influence of ANP on the TNF-α-induced expression of the three adhesion molecules ICAM-1, VCAM-1, and E-selectin, the mRNA expression and cell surface protein levels were determined by RT-PCR, flow cytometry and immunocytochemistry.

### 3.1.1.1 mRNA expression of adhesion molecules

TNF-α treatment (10 ng/ml) of cells significantly induced CAM mRNA in HUVEC (figure 8). ANP dose-dependently ($10^{-8}$-$10^{-6}$ mol/L) reduced the TNF-α-induced mRNA expression of E-selectin and ICAM-1, whereas it did not affect VCAM-1 gene expression (figure 8).

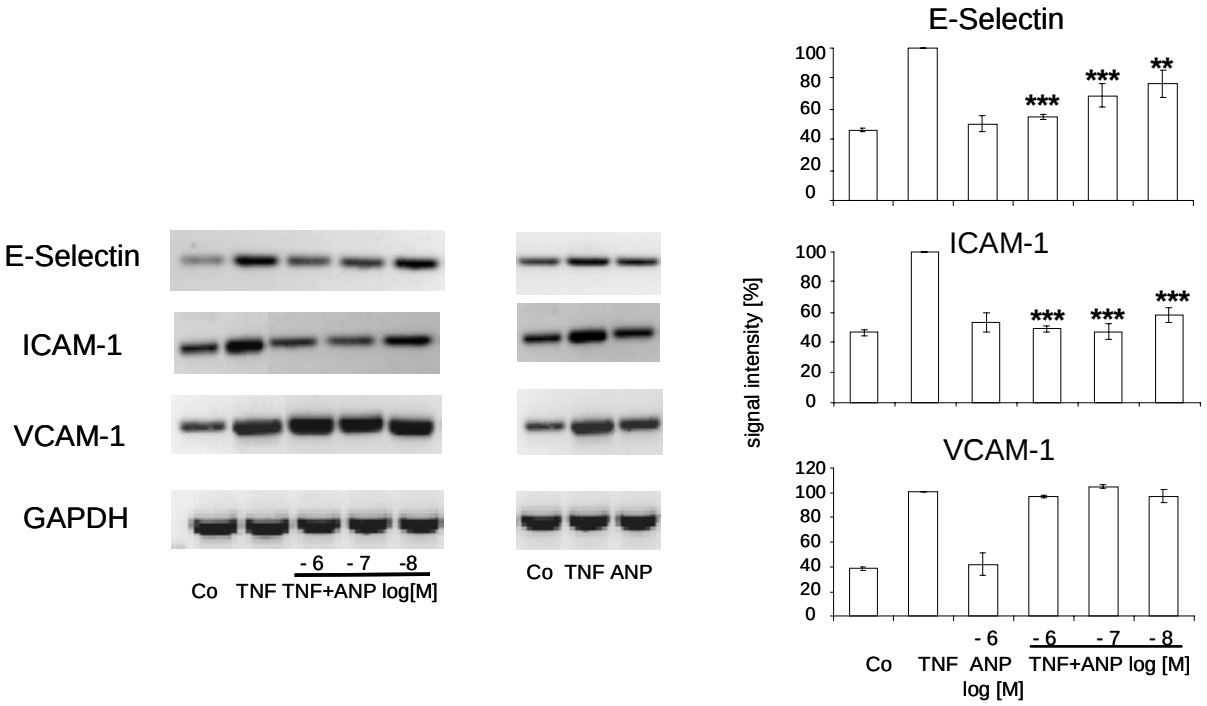


***figure 8: Dose-dependent inhibition of E-selectin and ICAM mRNA expression by ANP.***
HUVEC were cultured in either medium alone (Co), or in medium containing TNF-α (10 ng/ml) with or without pretreatment (30 min) of the cells with various concentrations of ANP ($10^{-8}$-$10^{-6}$ mol/L). RT-PCR was performed as described under "Materials and methods". Data show representative gels out of three independent experiments performed, each. Histograms show densitometric evaluation of

signal intensities normalized on GAPDH and are expressed as percentage of values for TNF-α treatment only. Data show mean ± S.E.M. of three independent experiments from different cell preparations. *** $p<0.001$ and ** $p<0.01$ represent significant differences compared to the values seen in TNF-α-activated cells.

### 3.1.1.2 Expression of surface protein

After showing the inhibitory action of ANP on the TNF-α-induced mRNA expression of ICAM-1 and E-selectin but not VCAM-1, the expression of surface protein of the three adhesion molecules was investigated by flow cytometry (figure 9) and immunocytochemistry (figure 10).

ANP pretreatment dose-dependently reduced E-selectin and ICAM-1 surface protein, but did not affect levels of VCAM-1 (figure 9). Interestingly, ANP ($10^{-6}$ mol/L) alone slightly but significantly elevated basal ICAM-1 expression.

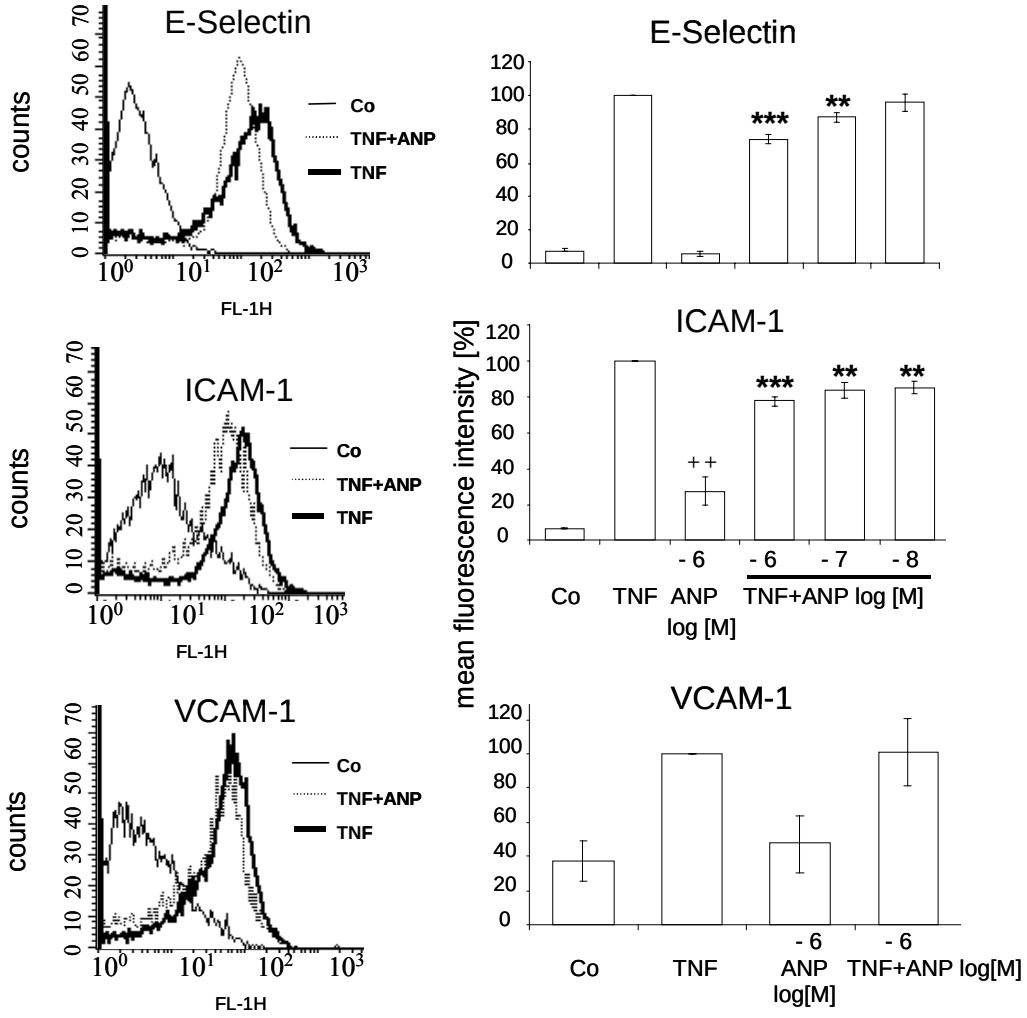


*figure 9: Flow cytometry analysis of ICAM-1, VCAM-1 and E-selectin surface protein*

E-selectin, ICAM-1, and VCAM-1 expression was detected by the corresponding FITC-labeled antibodies in untreated, TNF-α-treated, and TNF-α + ANP ($10^{-8}$-$10^{-6}$ mol/L) treated cells, whereby ANP was added 30 min before TNF-α. Data in the left panels show representative histogram out of 6 independent experiments. Demonstrating numbers of cells *vs.* fluorescence intensity at 520 nm. Data in the right panel show mean fluorescence ± S.E.M. of three independent experiments from different cell preparations. *** $p<0.001$ and ** $p<0.01$ represent significant differences compared to the values seen in TNF-α-activated cells, whereby TNF-α was set as 100%. $^{++}$ $p<0.01$ represents significant differences compared to the values seen in control cells.

The results of immunofluorescence staining for E-selectin and ICAM-1 are shown in figure 10. Increased staining of E-selectin and ICAM-1 was seen in TNF-α-treated cells, which was reduced in cells pretreated with ANP ($10^{-6}$ mol/L).

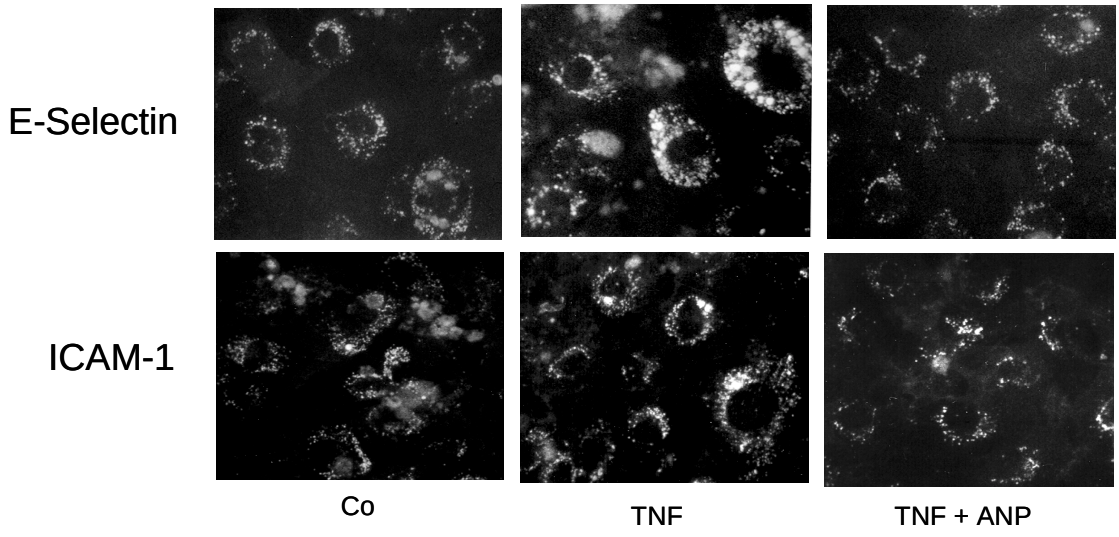


***figure 10: Immunofluorescence staining of ICAM-1 and E-selectin surface protein***
After treatment with TNF-α in the presence or absence of ANP ($10^{-6}$ mol/L, 30 min pretreatment), monolayers were washed and stained for CAM as described under "Materials and methods". The pictures show a representative photograph out of three independent experiments (original magnification 400-fold).

## 3.1.2 Receptor specificity of the ANP effect on CAM

For clarifying the receptor specificity of the inhibitory effect of ANP on CAM expression, the following substances were tested for their influence on the TNF-α-induced expression of adhesion molecules: the specific NPR-C ligand cANF, an antagonist of the guanylyl-cyclase-coupled NPR-A, HS-142-1 (Morishita et al. 1991), and the cell-permeable analogue of cGMP, 8-Br-cGMP. Experiments with the mentioned substances were performed with TNF-α-treated cells by flow cytometry.

The specific NPR-C ligand cANF did neither affect basal nor TNF-α-induced expression of CAM as shown in figure 11.

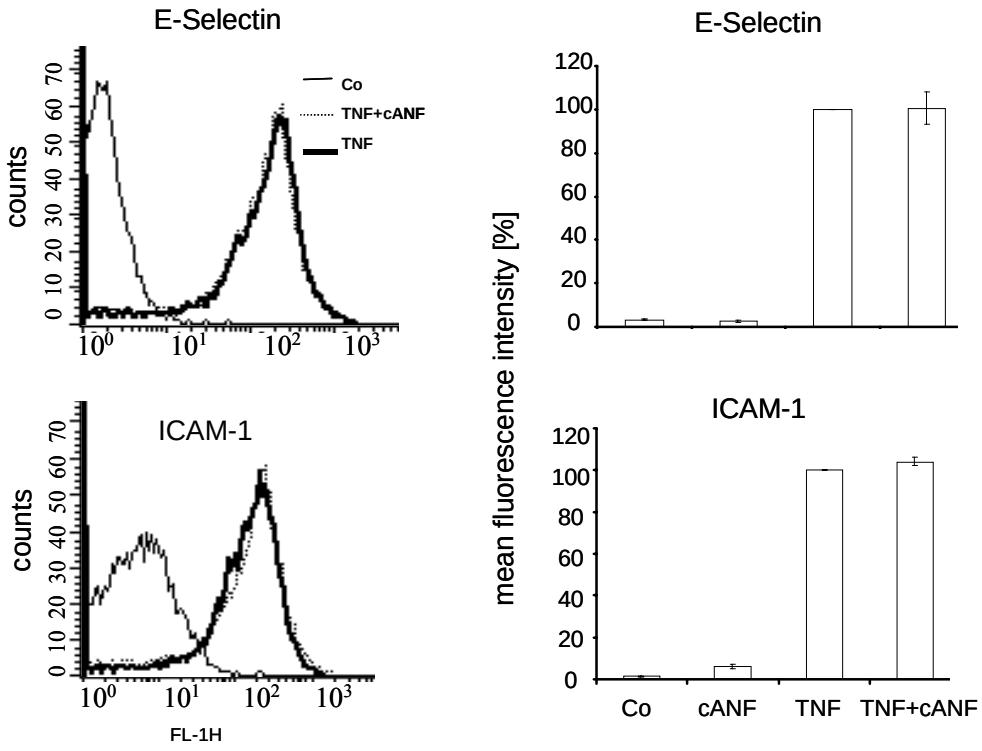


***figure 11: Effect of the NPR-C specific ligand cANF on CAM expression***

CAM expression of control cells (Co) or of cells treated with TNF-α (10 ng/ml), was determined by flow cytometry as described under "Materials and methods". The effect of cANF ($10^{-6}$ mol/L) on the expression of E-selectin and ICAM-1 was determined for cANF added to the cells 30 min before TNF-α, or for cANF given to the cells alone for 6 hours. Data in the left panel show representative histogram out of 6 independent experiments. Demonstrating numbers of cells *vs.* fluorescence intensity at 520 nm. Data in the right panel show mean fluorescence ± S.E.M. of three independent experiments from different cell preparations, whereby TNF-α was set as 100%.

The antagonist of the guanylyl-cyclase-coupled NPR-A, HS-142-1, abrogated the effect of ANP on both TNF-α-induced expression of E-selectin as well as on ICAM-1, whereas HS-142-1 alone had no effect on basal CAM expression (figure 12). The cell-permeable analogue of cGMP, 8-Br-cGMP, significantly reduced TNF-α-induced CAM expression in a dose-dependent manner (figure 12).

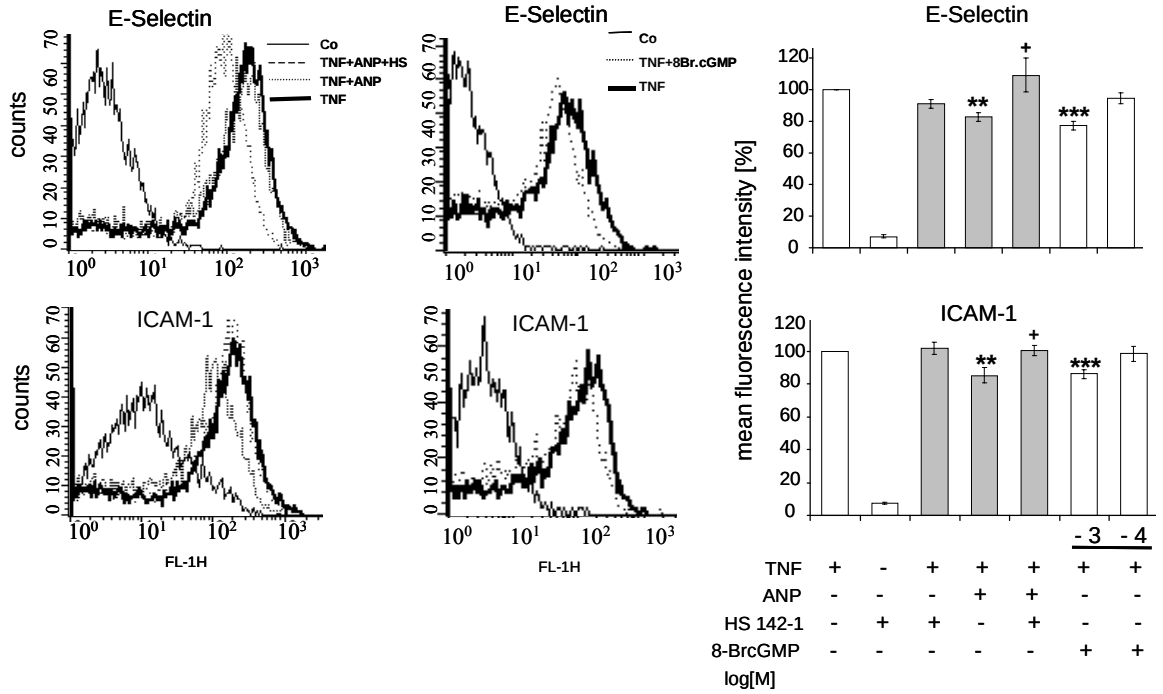


***figure 12: Effect of HS-142-1 and 8-Br-cGMP on TNF-α-induced CAM expression***

The A receptor antagonist HS-142-1 (HS 10 μg/ml) was given to the cells alone or in combination with TNF-α, in the presence or absence of ANP ($10^{-6}$ mol/L). Furthermore, the effect of 8-Br-cGMP ($10^{-3}$ - $10^{-4}$ mol/L) on TNF-α-induced CAM expression was determined by addition of 8-Br-cGMP 30 min before TNF-α. Results are shown as histograms (dose 8-Br-cGMP $10^{-3}$ mol/L, left panel) showing numbers of cells *vs.* fluorescence intensity at 520 nm. Data in the right panel show mean ± S.E.M. of three independent experiments form different cell preparations. *** $p<0.001$ and ** $p<0.01$ represent significant differences compared to the values seen in TNF-α-activated cells, whereby TNF-α was set 100%. $^{+}$ $p<0.01$ represents significant differences compared to the values seen in TNF-α + ANP activated cells.

These results suggest that the inhibition of CAM surface expression by ANP was mediated *via* the guanylyl-cyclase-coupled NPR-A, and therefore by cGMP as second messenger.

After demonstrating, that the NPR-A receptor is involved in mediating the inhibitory action of ANP on TNF-α-induced expression of E-selectin and ICAM-1, it was investigated whether the other guanylyl-cyclase-coupled receptor, NPR-B, is also able to mediate this inhibitory property of ANP. Therefore the effect of the specific NPR-B ligand, CNP, on cell surface expression of CAM was tested. CNP also significantly

inhibited the TNF-α-induced expression of both E-selectin and ICAM-1 (figure 13). CNP alone did not affect basal CAM expression.

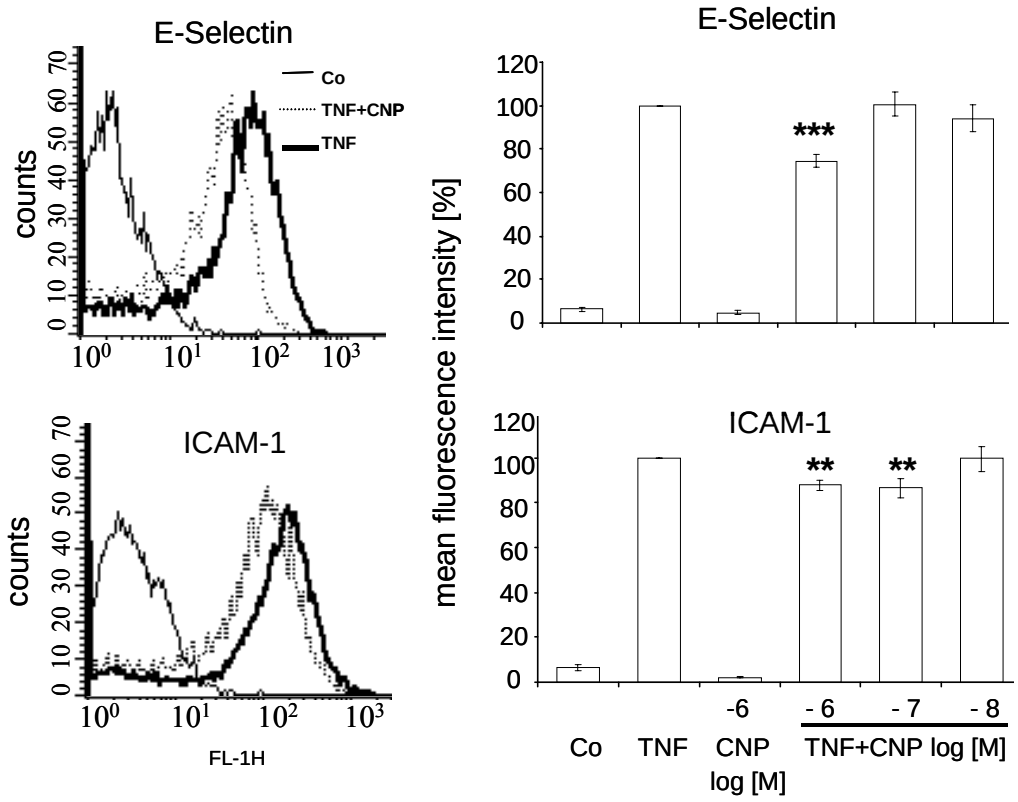


***figure 13: Effect of the NPR-B specific ligand CNP on CAM expression***
CNP ($10^{-8}$-$10^{-6}$ mol/L) was added to the cells in combination with TNF-α (30 min pretreatment) and flow cytometry was performed as described under "Materials and methods". Data in the left panel show representative histograms (dose CNP $10^{-6}$ mol/L) demonstrating numbers of cells *vs.* fluorescence intensity at 520 nm. Data in the right panel show mean fluorescence ± S.E.M. of three independent experiments from different cell preparations. *** $p<0.001$ and ** $p<0.01$ represent significant differences compared to the values seen in TNF-α-activated cells, whereby TNF-α was set as 100%.

Due to the fact, that the specific NPR-B receptor ligand, CNP, did also significantly reduce the surface expression of the two CAM, the other guanylyl-cyclase-coupled receptor, NPR-B, seems to be able to mediate the inhibitory action of ANP on TNF-α-induced up-regulation of CAM, too.

### 3.1.3 Inhibition of TNF-α-induced activation of NF-κB by ANP

TNF-α mainly induces adhesion molecule expression by activating DNA binding activity of the proinflammatory transcription factor NF-κB (Collins et al. 1995).

Especially the regulation of ICAM-1 and E-selectin is known to be mediated at a transcriptional level *via* activation of this transcription factor (Karin 1999). As demonstrated above, ANP reduces TNF-α-induced CAM expression on a transcriptional level as shown by RT-PCR of CAM. Therefore the following experiment aimed to elucidate if ANP mediates its inhibitory action on TNF-α-induced adhesion molecule expression *via* the transcription factor NF-κB. Electrophoretic mobility shift assays for NF-κB were performed as follows.

### 3.1.3.1 Characterization of TNF-α-induced NF-κB activation

**NF-κB activation after TNF-α treatment**

First a time- and concentration-course (figure 14 and 15) for TNF-α-induced NF-κB activation was performed to establish the experimental procedure for further electrophoretic mobility shift assays.

As shown in figure 14, TNF-α-activated NF-κB DNA binding activity was maximal at 60 min.

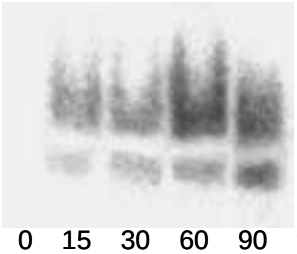


***figure 14: Time course TNF-α***
Cells were either left untreated (Co) or treated with TNF-α (10 ng/ml) for 15 min up to 90 min. Results show one representative EMSA out of three independent experiments.

The concentration for TNF-α of 10 ng/ml, was shown to be most suitable to stimulate NF-κB DNA binding activity (figure 15).

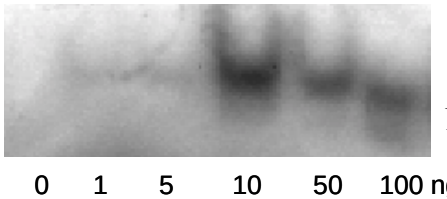


***figure 15: Concentration course TNF-α***
Cells were treated with TNF-α in different concentrations (1-100 ng/ml) for 1 h. Results show one representative EMSA out of three independent experiments.

**Supershift analysis of NF-κB**

In the following experiment the composition of the two NF-κB bands was investigated by supershift analysis. The faster migrating band represents a homodimer of two p50 subunits, whereas the slower migrating band is a p50/p65 heterodimer. This was shown due to the fact that the faster migrating band was supershifted only by an anti-p50 antibody, whereas the slower migrating band was supershifted by both an anti-50 as well as by an anti-p65 antibody. Excess of unlabeled NF-κB or AP-2 binding sequence to binding reactions of TNF-α-treated cells served as specificity control of EMSA (figure 16).

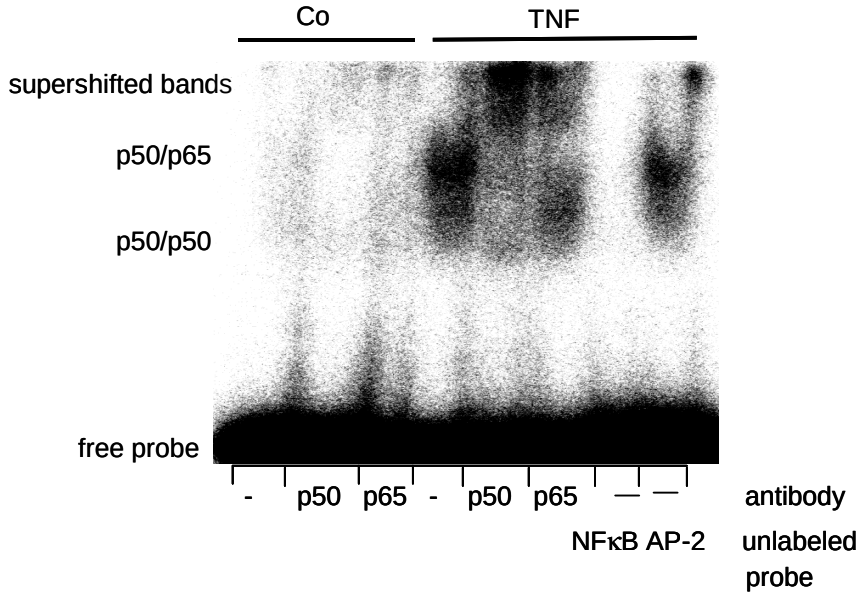


***figure 16: Supershift analysis of NF-κB***
Supershift experiments employing specific antibodies against the NF-κB subunits p50 and p65 were performed in untreated or TNF-α-activated HUVEC (10 ng/ml, 1 h). Specificity of the binding reaction was assessed by using an excess of unlabeled NF-κB or AP-2 binding sequence to binding reactions of TNF-α-treated cells. One representative out of two independent experiments from different cell preparations with similar results is shown.

### 3.1.3.2 Effect of ANP on TNF-α-induced activation of NF-κB

In order to investigate whether ANP affects NF-κB, the transcription factor mainly responsible for the induction of CAM, the effect of ANP on TNF-α-induced DNA binding activity of NF-κB was investigated by EMSA.

Treatment of HUVEC with TNF-α (10 ng/ml) resulted in a marked activation of NF-κB DNA binding activity after 1 h of stimulation, as assessed by EMSA (figure 17).

Cotreatment of the cells with TNF-α and ANP ($10^{-8}$-$10^{-6}$ mol/L) significantly reduced NF-κB binding activity (figure 17). ANP alone ($10^{-6}$ mol/L) significantly increased basal NF-κB activity (figure 17).

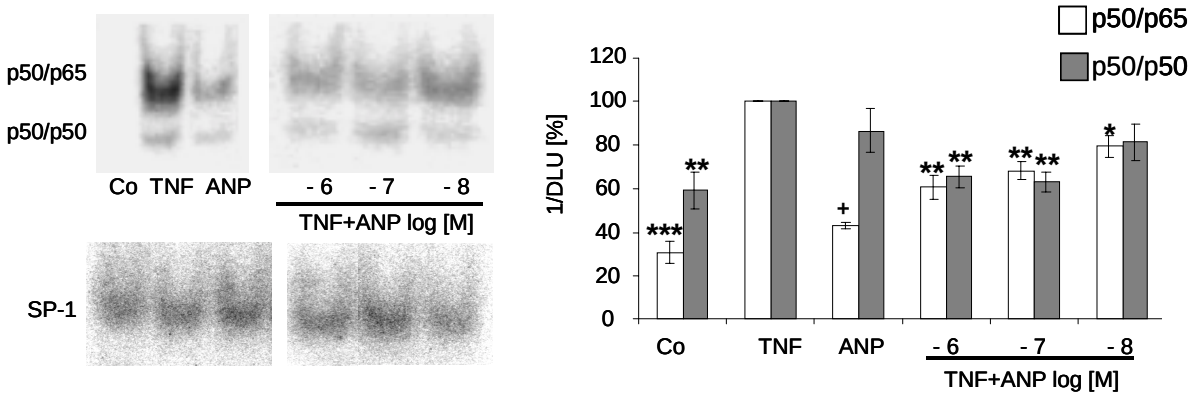


***figure 17: Effect of ANP on TNF-α-induced activation of NF-κB***

Cells were either left untreated (Co) or treated with TNF-α (10 ng/ml) for 1 h. ANP was added to the cells alone ($10^{-6}$ mol/L for 1 h) or 30 min before ($10^{-8}$-$10^{-6}$ mol/L) TNF-α. After 1 h NF-κB EMSA was performed as described under "Materials and methods". Using SP-1 probes served as a loading control (left panel). Data in the left panel represent one representative out of five independent experiments from different cell preparations with similar results. Data in the right panel show phosphorimaging analysis of EMSA experiments and are expressed as percentage of values for TNF-α treatment only. Data represent means ± S.E.M. out of three independent experiments from different cell preparations with *** $p<0.001$, ** $p<0.01$, * $p<0.05$ significantly different compared to the values seen in TNF-α-activated cells and $^{+}$ $p<0.05$ significantly different compared to untreated controls, whereby TNF-α was set as 100%.

### 3.1.3.3 Effect of 8-Br-cGMP on TNF-α-induced activation of NF-κB

In order to determine whether the inhibitory effect of ANP on NF-κB is mediated by cGMP, the cell-permeable cGMP analogue, 8-Br-cGMP, was used in the same experimental setting as for ANP.

Cotreatment of the cells with TNF-α and 8-Br-cGMP ($10^{-4}$-$10^{-3}$ mol/L) significantly reduced NF-κB DNA binding activity (figure 18), suggesting a participation of the guanylyl-cyclase-coupled NPR-A receptor in signal transduction by ANP.

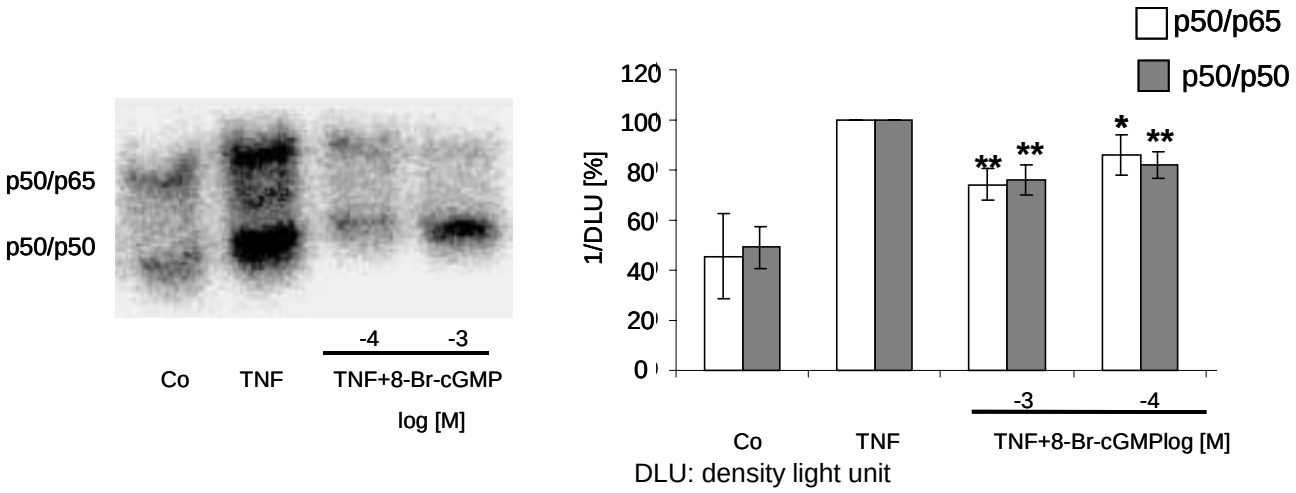


***figure 18: Effect of 8-Br-cGMP on TNF-α-induced activation of NF-κB***
Cells were either left untreated (Co) or treated with TNF-α (10 ng/ml) in the presence or absence of 8-Br-cGMP ($10^{-4}$ and $10^{-3}$ mol/L), which was added to the cells 30 min before TNF-α. Data represent one representative out of three independent experiments from different cell preparations with similar results (left panel). Data in the right panel show phosphorimaging analysis of EMSA experiments and are expressed as percentage of values for TNF-α treatment only. Data represent means ± S.E.M. out of three independent experiments from different cell preparations with ** $p<0.01$, * $p<0.05$ significantly different compared to the values seen in TNF-α-activated cells.

### 3.1.3.4 Effect of CNP on TNF-α-induced activation of NF-κB

As shown under 3.1.3.3 the guanylyl-cyclase-coupled NPR-A receptor is able to mediate the inhibition of ANP on TNF-α-induced NF-κB activation. In order to demonstrate whether the other guanylyl-cyclase-coupled receptor, NPR-B, is also involved in mediating the inhibitory property of ANP on TNF-α-induced NF-κB up-regulation, the effect of the specific NPR-B ligand, CNP was also tested in EMSA of NF-κB.

CNP alone had no effect on NF-κB activity, whereas CNP dose-dependently ($10^{-8}$–$10^{-6}$ mol/L) inhibited TNF-α-induced activation of NF-κB (figure 19). Therefore the guanylyl-cyclase-coupled NPR-B receptor also mediates the inhibitory property of ANP on TNF-α-induced NF-κB up-regulation.

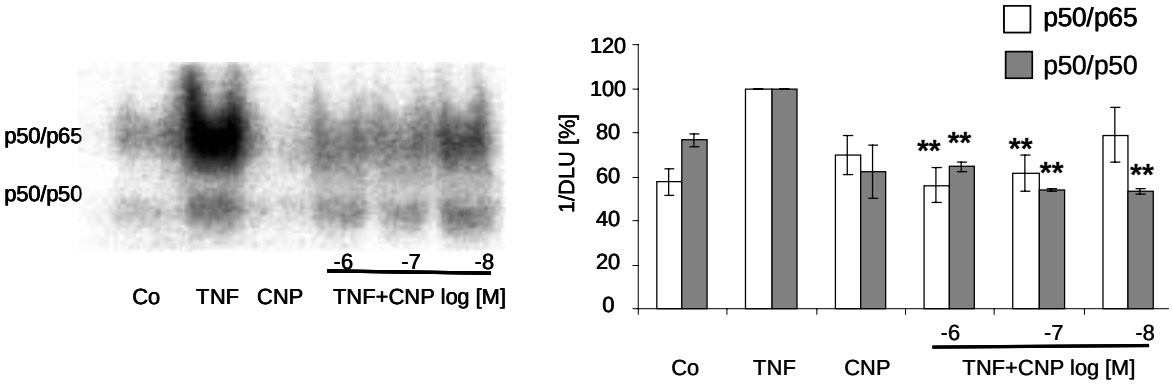


***figure 19: Effect of CNP on TNF-α-induced activation of NF-κB***

Cells were either left untreated (Co) or treated with TNF-α (10 ng/ml) alone for 1 h or with TNF-α after 30 min pretreatment with CNP ($10^{-8}$-$10^{-6}$mol/L). Data show one representative out of three independent experiments from different cell preparations (left panel). Data in the right panel show phosphorimaging analysis of EMSA experiments and are expressed as percentage of values for TNF-α treatment only. Data represent means ± S.E.M. out of three independent experiments from different cell preparations with ** $p<0.01$ significantly different compared to the values seen in TNF-α-activated cells.

## 3.1.4 ANP treatment attenuates TNF-α-induced nuclear translocation of NF-κB subunits.

As described above, TNF-α induces adhesion molecule expression *via* the proinflammatory transcription factor NF-κB. In unstimulated cells, the predominant form of NF-κB is present in the cytoplasm as a heterodimer of p50 and p65 subunits complexed with inhibitory IκB proteins. Upon stimulation IκB is phosphorylated and degraded, releasing NF-κB and thus allowing its translocation to the nucleus where it promotes the transcription of respective genes (Karin 1999). The next question we asked was how ANP is able to mediate reduced NF-κB DNA binding activity. One possibility is through inhibition of the translocation of NF-κB into the nucleus. Therefore in the following experiments especially the translocation of NF-κB (p65 subunit) was assessed by immunocytochemistry and Western blot analysis of both, the nuclear and the cytosolic fraction of HUVEC.

### 3.1.4.1 Immunocytochemistry of p65

In order to investigate whether the reduced NF-κB DNA binding activity in ANP-treated cells shown by EMSA experiments is associated with a decreased translocation of NF-κB, immunocytochemistry of the p65 subunit was performed. Staining of the p65 subunit in indeed showed that ANP abrogated the TNF-α-induced translocation of NF-κB into the nucleus (figure 20): TNF-α-treated cells showed a distinct fluorescence of the nucleus, indicating p65 localization, compared to cytosolic staining of untreated cells. Pretreatment with ANP resulted in a reduced number of cells with translocated p65 (figure 20).

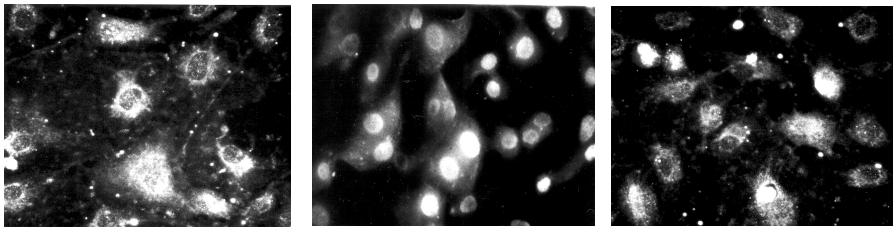


***figure 20: ANP attenuates translocation of the p65 subunit of NF-κB***

HUVEC were cultured in either medium alone (Co) or in medium containing TNF-α (10 ng/ml) in the presence or absence of ANP ($10^{-6}$ mol/L, 30 min pretreatment) for 1 h. Cells were permeabilized and stained with FITC-labeled antibody as described under "Materials and methods". The pictures show representative photographs out of three independent experiments from different cell preparations (original magnification 200-fold).

### 3.1.4.2 Influence of ANP on nuclear translocation of p50 and p65

The results presented above were confirmed by Western blots performed with nuclear and cytosolic extracts of cells treated either with TNF-α alone or with TNF-α after pretreamtent with ANP ($10^{-8}$-$10^{-6}$ mol/L).
ANP significantly inhibited the TNF-α-induced translocation of p65 and p50 into the nucleus (figure 21). Probing the blots with SP-1 and G-actin antibodies served as loading controls. ANP treatment alone ($10^{-6}$ mol/L) significantly increased p65 nuclear translocation (figure 21).

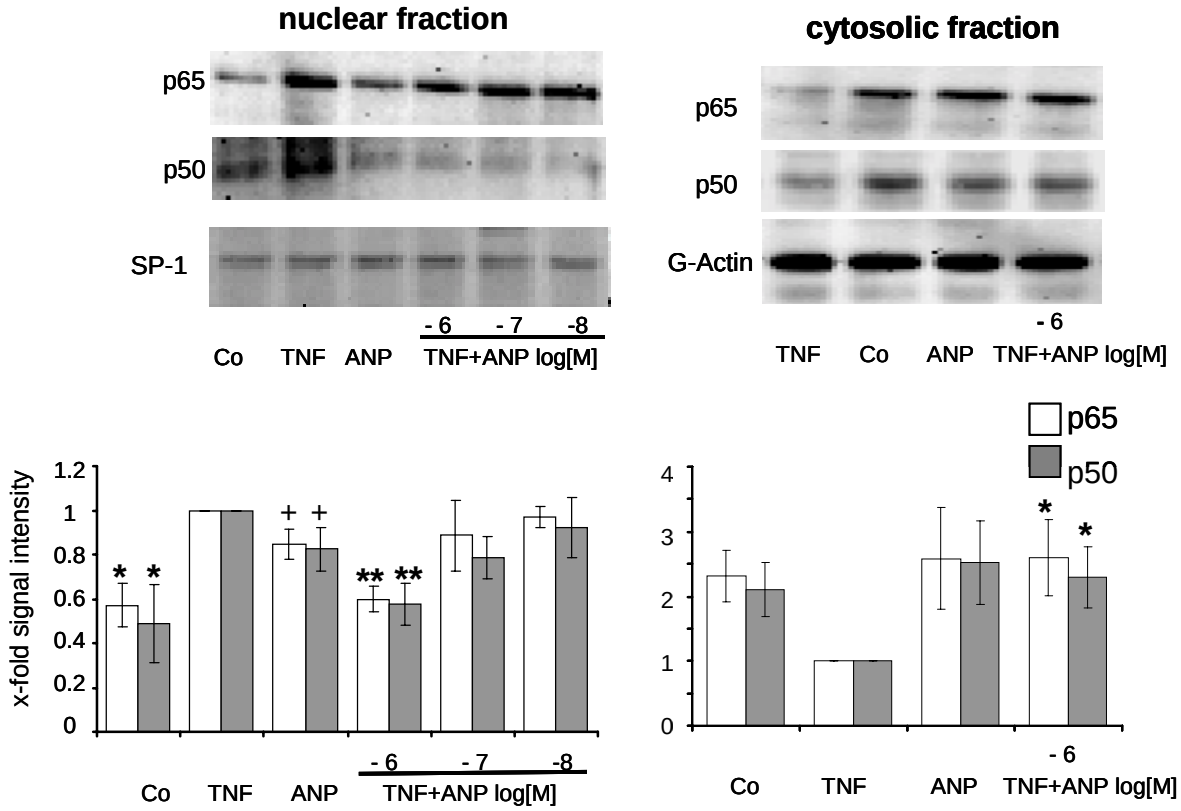


***figure 21: ANP effects on cytosolic and nuclear levels of p50 and p65***
Cells were either left untreated (Co) or treated with TNF-α (10 ng/ml) for 1 h. ANP was added to the cells alone ($10^{-6}$ mol/L for 1 h) or in combination ($10^{-8}$-$10^{-6}$ mol/L) with TNF-α (30 min pretreatment). Western blots of cytosolic and nuclear fractions were performed as described under "Materials and methods" with antibodies against p50 and p65. Data in the upper panel show one representative out of three independent Western blot experiments from different cell preparations with similar results in each case. Histograms in the lower panels show densitometric evaluation of Western blots and are expressed as x-fold of values for TNF-α treatment only. Data represent means ± S.E.M. out of three independent experiments from different cell preparations with ** $p<0.01$, * $p<0.05$ significantly different compared to the values seen in TNF-α-activated cells and $^{+}$ $p<0.05$ significantly different compared to untreated controls.

## 3.1.5 Influence of ANP on IκB isoforms

A crucial step in the activation of NF-κB by TNF-α is the rapid phosphorylation and degradation of the cytoplasmic inhibitor protein IκB, existing as IκB-α, -β, and -ε isoform. Because it could be demonstrated that ANP reduces the nuclear translocation of p65 subunit (see 3.1.4), it was now investigated whether ANP is able to influence the TNF-α-induced phosphorylation and degradation of IκB-α. For detection of the phosphorylated IκB-α an antibody specifically detecting phosphorylated IκB-α was used in Western blot analysis. Besides the effect of ANP on IκB-α phosphorylation its effect on degradation of all three isoforms induced by TNF-α was determined using specific antibodies detecting IκB-α, IκB-β, and IκB-ε isoforms.

### 3.1.5.1 Influence of ANP on IκB-α phosphorylation

A marked increase of phosphorylated inhibitor protein (IκB) was detected subsequently to TNF-α treatment (figure 22). Cotreatment of the cells with TNF-α and ANP, however, did not have any influence on the phosphorylation degree of IκB-α compared to TNF-α treatment only.

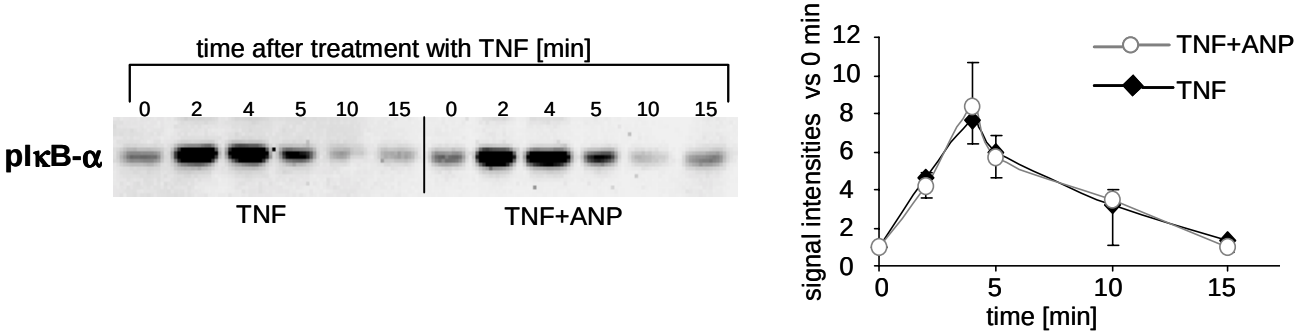


***figure 22: Effect of ANP on TNF-α-induced IκB-α phosphorylation***
HUVEC were treated with TNF-α (10 ng/ml) in the presence or absence of ANP ($10^{-6}$ mol/L; 30 min before TNF-α) for the indicated times. Data in the left panel show one representative out of three independent Western blots from different cell preparations. Graph shows densitometric evaluation of Western blots whereby data are expressed as x-fold of values for TNF-α treatment only.

### 3.1.5.2 Influence of ANP on degradation of IκB isoforms

As described under 3.1.5.1 no effect of ANP on TNF-α-induced phosphorylation of IκB was detectable. In the next step it was investigated by Western blot, whether ANP affects TNF-α-induced degradation of the three isoforms of IκB. Time-course experiments were performed using antibodies detecting IκB-α, IκB-β, and IκB-ε. Probing the blots with α-tubulin antibodies served as loading control (figure 23).

Pretreatment of the cells with ANP ($10^{-6}$ mol/L) did not attenuate the TNF-α-induced degradation rate of IκB-α and IκB-β, whereas it delayed the degradation of IκB-ε. Interestingly, resynthesis of IκB-α after degradation was significantly elevated in ANP-pretreated cells (figure 23).

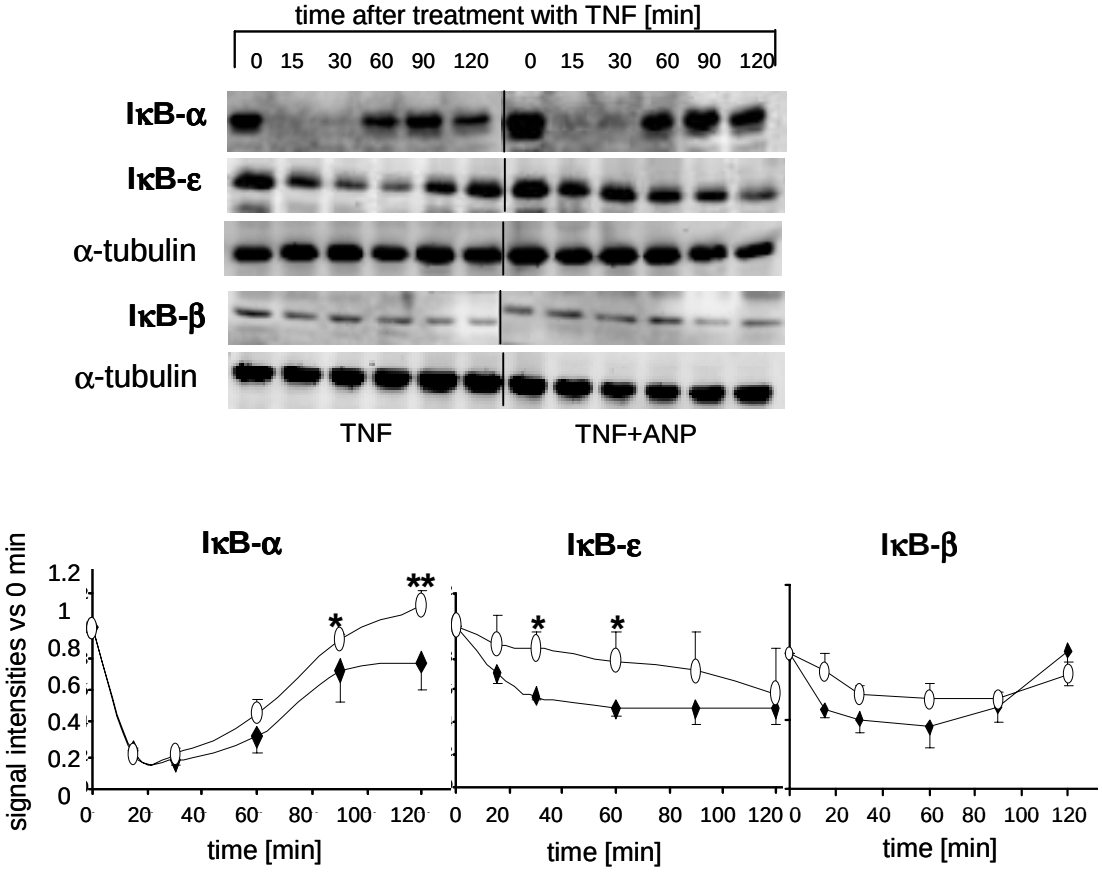


***figure 23: Effects of ANP on degradation of IκB isoforms***

HUVEC were treated with TNF-α (10 ng/ml) alone or in combination with ANP ($10^{-6}$ mol/L, 30 min pretreatment) for the indicated times. The upper panel shows representative blots out of three independent experiments from different cell preparations, each. Densitometric evaluation of Western blots is shown in the lower graphs whereby data are expressed as x-fold of values for TNF-α. Data represent means ± S.E.M. out of five independent experiments from different cell preparations with ** $p<0.01$, * $p<0.05$ significantly different compared to the values seen in TNF-α-activated cells.

### 3.1.5.3 Influence of ANP on expression of IκB-α, - β, and -ε isoforms

The observed increased resynthesis of IκB-α after ANP treatment led to the suggestion that ANP may be able to induce the expression of IκB isoforms. Further Western blot experiments with ANP-treated cells were performed in order to confirm this hypothesis.

As seen in figure 24, HUVEC stimulated with ANP showed significantly increased expression of IκB-α and IκB-ε. This inducing effect of ANP could not be observed for the IκB-β isoform.

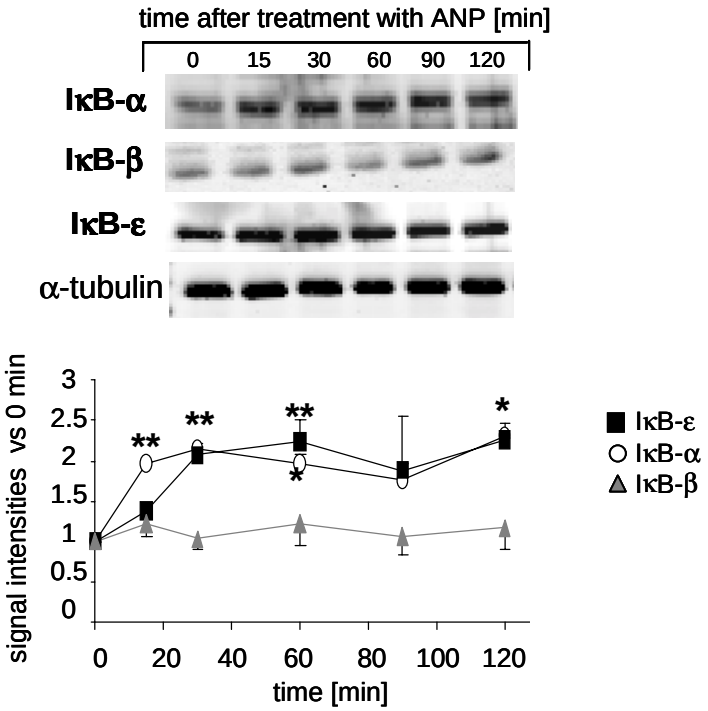


***figure 24: ANP induces expression of IκB-α and -ε***

Cells were treated with ANP ($10^{-6}$ mol/L) for the indicated times. Western blots using antibodies against IκB-α, -β, -ε, and α-tubulin were performed as described under "Materials and methods". Data in the upper panel show one representative out of four independent experiments from different cell preparations. Graph shows densitometric evaluation of Western blots whereby data are expressed as x-fold of values for IκB-α signal intensities at time point 0 min. Data represent means ± S.E.M. out of four independent experiments from different cell preparations with ** $p<0.01$, * $p<0.05$ significantly different compared to the values seen in control cells.

## 3.1.6 Transcriptional induction of IκB-α by ANP

As shown by Western blot ANP is able to induce IκB-α. In order to demonstrate whether the IκB induction is mediated on the transcriptional level, IκB-α levels were determined after pretreating cells with actinomycin D, a known inhibitor of transcription.

### 3.1.6.1 IκB-α expression in the presence of actinomycin D

ANP elevated IκB-α levels only in the absence of actinomycin D (figure 25). This indicates that in case of inhibiting the transcription by actinomycin D, ANP is no longer able to induce IκB-α protein expression. Thus ANP acts on a transcriptional level to increase IκB-α protein.

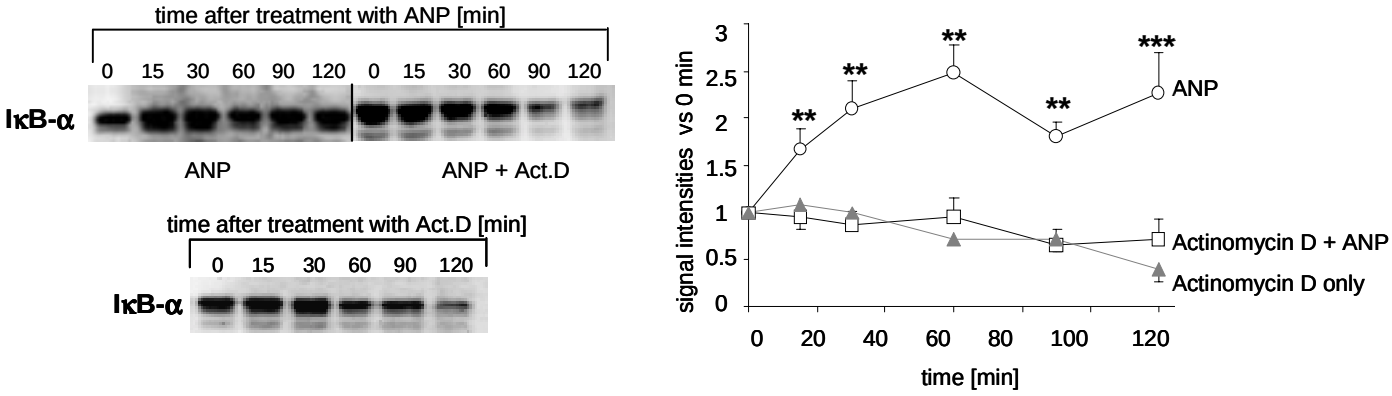


***figure 25: Effect of ANP on IκB-α induction in the presence of actinomycin D.***
HUVEC were treated with ANP ($10^{-6}$ mol/L) or actinomycin D (2 µmol/L) for the indicated times or with ANP after pretreatment (30 min) of the cells with actinomycin D. Data in the left panel show one representative out of four independent experiments from different cell preparations. Graph shows densitometric evaluation of Western blots whereby data are expressed as x-fold of values for IκB-α signal intensities at time point 0 min of the respective blot. Data represent means ± S.E.M. out of four independent experiments from different cell preparations. *** $p<0.001$, ** $p<0.01$ significantly different compared to the values at 0 min.

### 3.1.6.2 Influence of ANP on IκB-α mRNA expression

In the following experiments the observations described under 3.1.6.1 were confirmed by investigating the mRNA levels of HUVEC after treatment with ANP (figure 26).

As shown in figure 26, treatment of the cells with ANP ($10^{-6}$ mol/L) showed after 10 min slightly and after 20 min significantly elevated IκB-α mRNA levels.

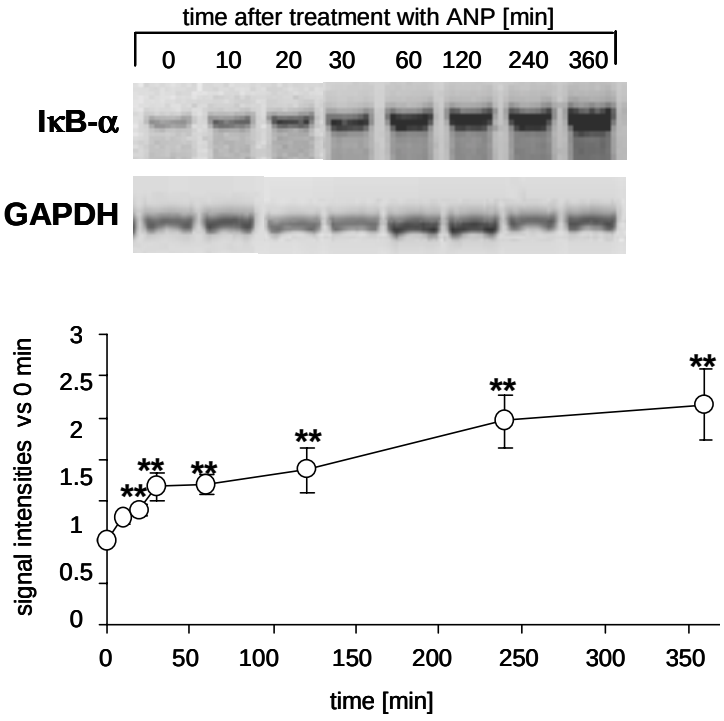


***figure 26: Effect of ANP on IκB-α mRNA expression***
HUVEC were treated with ANP ($10^{-6}$ mol/L) for the indicated times. RNA was isolated and IκB-α and GAPDH mRNA was estimated by RT-PCR. Data show one representative out of three independent experiments from different cell preparations. Densitometric evaluation of ethidium bromide stained gels is shown whereby data are expressed as x-fold of values of cells at time point 0 min normalized for GAPDH. ** $p<0.01$ significantly different compared to the values seen at 0 min.

## 3.1.7 Influence of ANP on the activator protein 1 (AP-1)

Another transcription factor activated by TNF-α is the activator protein-1. In order to determine whether the inhibitory action of ANP is specific for TNF-α-induced NF-κB activity, the effect of ANP on AP-1 activity and TNF-α-induced AP-1 activity was examinated.
[In another study performed by Nicole Bildner, a coworker in the group of Prof. Vollmar, this issue is worked out in context of HO-1 induction by ANP *via* upregulation of AP-1. With reference to the work of Nicole Bildner the following results are given in a short version.]

### 3.1.7.1 Characterization of TNF-α-induced AP-1 activity

#### AP-1 activation after TNF-α treatment

First a time- and concentration-course (figure 27 and 28) for TNF-α-induced AP-1 activation was performed to establish the experimental procedure for further electrophoretic mobility shift assays.

As shown in figure 27, TNF-α-induced AP-1 DNA binding activity was detectable after 30 up to 60 min.

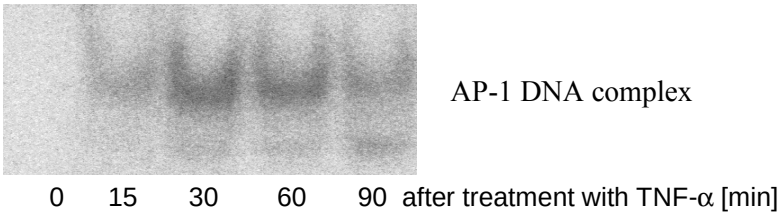


***figure 27: Time course TNF-α***
Cells were either left untreated (Co) or treated with TNF-α (10 ng/ml) for 15 min up to 90 min. Results show one representative EMSA out of three independent experiments.

A suitable concentration for stimulation of AP-1 DNA binding activity was 10 ng/ml TNF-α as shown by the following EMSA (figure 28).

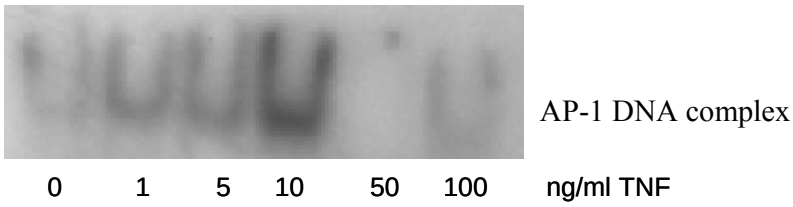


***figure 28: Concentration course TNF-α***
Cells were treated with TNF-α in different concentrations (1-100 ng/ml) for 1 h. Results show one representative EMSA out of three independent experiments.

#### Supershift analysis of AP-1

In the next experiment the composition of AP-1 was investigated by supershift analysis. It was demonstrated that the AP-1 complex is composed of c-jun and c-fos subunits, because after addition of an anti-c-jun as well as an anti-c-fos antibody the signal intensity of the AP-1 band decreased (figure 29).

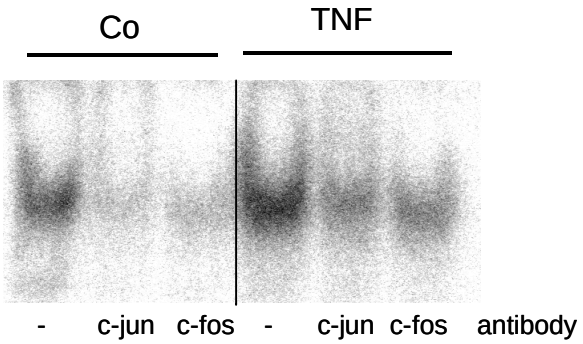


***figure 29: Supershift analysis of AP-1***
Supershift experiments employing specific antibodies against the AP-1 subunits c-jun and c-fos were performed in untreated or TNF-α-activated HUVEC (10 ng/ml, 1 h). One representative out of three independent experiments from different cell preparations with similar results is shown.

### 3.1.7.2 Effect of ANP on TNF-α-induced activation of AP-1

To investigate whether ANP affects TNF-α-induced DNA binding activity of AP-1 electrophoretic mobility shift assay was performed .

Treatment of HUVEC with TNF-α (10 ng/ml) resulted in a marked activation of AP-1 DNA binding activity after 1 h of stimulation, as assessed by electrophoretic mobility shift assay (figure 30). ANP alone ($10^{-6}$ mol/L) significantly increased basal AP-1 activity (figure 30). Interestingly cotreatment of the cells with TNF-α and ANP ($10^{-8}$-$10^{-6}$ mol/L) had no effect on AP-1 DNA binding activity (figure 30).

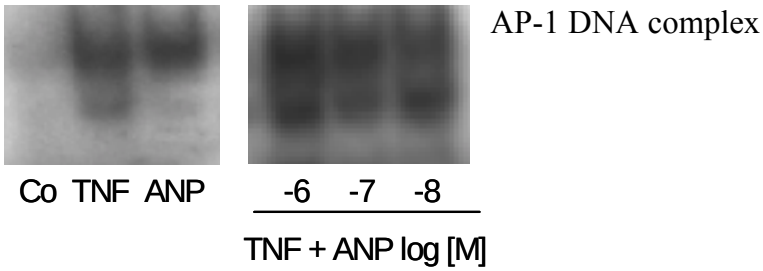


***figure 30: Effect of ANP on TNF-α-induced AP-1 activity***
Cells were either left untreated (Co) or treated with TNF-α (10 ng/ml) for one hour. ANP was added to the cells alone ($10^{-6}$ mol/L for 1 h) or 30 min before ($10^{-8}$-$10^{-6}$ mol/L) TNF-α (1 h). EMSA was performed as described under "Materials and methods". Data represent one representative out of three independent experiments from different cell preparations with similar results.

### 3.1.7.3 Effect of ANP on AP-1 activity

Due to the observed induction of basal AP-1 in figure 30 the following EMSA aimed to determine the influence of ANP alone on transcriptional activity of AP-1. Therefore a time (figure 31) and concentration (figure 32) course for ANP was performed.

The time course shown in figure 31 demonstrated that the stimulation of AP-1 DNA binding activity was maximal after 15 and 90 min of treatment with ANP suggesting a biphasic time course for ANP-induced AP-1 activity.

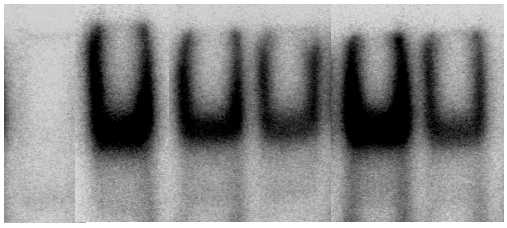


***figure 31: Time course ANP***
Cells were either left untreated (Co) or treated with ANP ($10^{-6}$ mol/L) for 15 min up to 120 min. EMSA was performed as described under "Materials and methods". Results show one representative EMSA out of three independent experiments.

The results in figure 32 show that ANP is dose-dependently ($10^{-7}$-$10^{-6}$ mol/L) able to induce the DNA binding activity of AP-1.

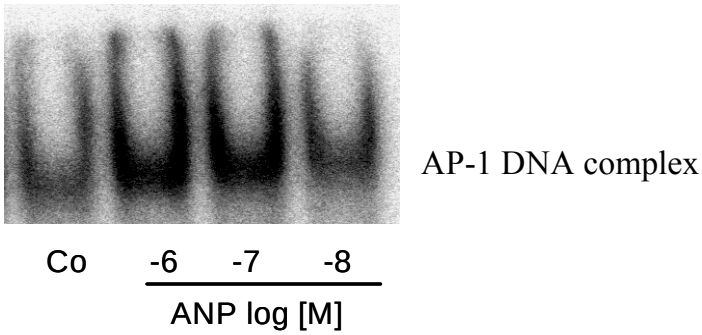


***figure 32: Concentration course ANP***
Cells were treated with ANP in different concentrations ($10^{-8}$-$10^{-6}$ mol/L) for 1 h. Results show one representative EMSA out of three independent experiments.

### 3.1.7.4 Blocking of AP-1 by oligonucleotide decoys

In order to show a causal relationship between HO-1 induction, observed by Nicole Bildner, and the induction of AP-1 detected by EMSA, the DNA protein binding was

blocked by the use of AP-1 oligonucleotide decoys and subsequently Western blot for HO-1 (Nicole Bildner) and EMSA for AP-1 was performed. HUVEC were transfected with decoys using an Effectene™ transfection kit (Qiagen) and EMSA was performed as usual.

The results given in figure 33 demonstrate that it was possible to block AP-1 DNA binding activity by specific AP-1 decoys. The transfection with scrambled decoys did not result in decreased DNA binding activity of AP-1 and served as control of specificity.

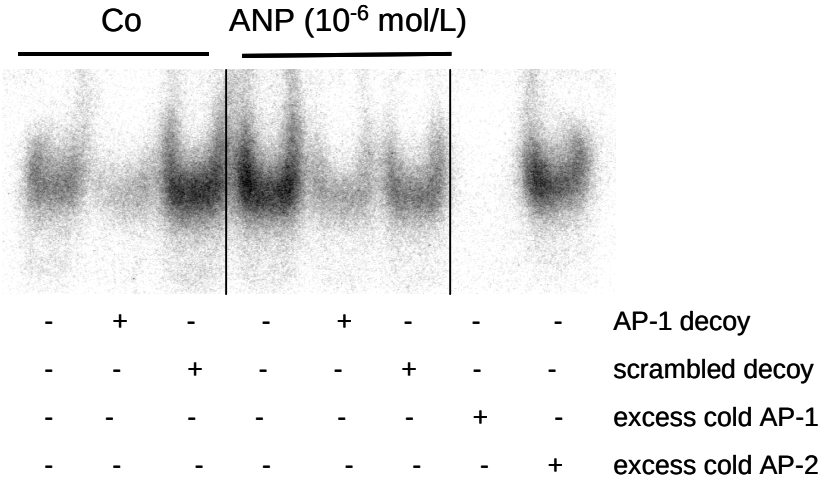


***figure 33: Blocking of AP-1 by oligonucleotide decoys***
Cells were either left untreated (Co) or treated with ANP ($10^{-8}$-$10^{-7}$ mol/L) for 1 h after a 4 h transfection of cells with AP-1 decoy or scrambled decoy. EMSA was performed as described under "Materials and methods". Specificity of the binding reaction was assessed by using an excess of unlabeled AP-1 or AP-2 DNA oligonucleotides to binding reactions of TNF-α-treated cells. Data represent one representative out of three independent experiments from different cell preparations with similar results.

### 3.1.7.5 Inhibition of AP-1 DNA binding activity by U0126

Another possibility to demonstrate the causal link between HO-1 induction and the observed AP-1 induction by ANP is to inhibit the activity of AP-1 by the use of U0126, a specific inhibitor of AP-1 activity. After incubation of cells with U0126 for 30 min EMSA was performed as usual.

Figure 34 shows that it was possible to inhibit the DNA binding activity of AP-1, because the ANP induced AP-1 activation was no longer detectable after treatment of the cells with U0126 (figure 34).

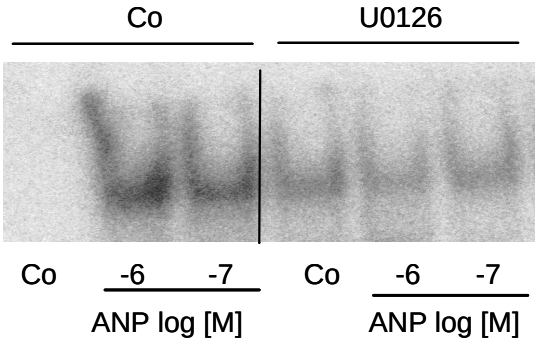


***figure 34: Inhibition of AP-1 DNA binding activity by U0126***

After preincubation of cells with U0126 for 30 min cells were either left untreated (Co) or treated with ANP ($10^{-7}$-$10^{-6}$ mol/L) for 1 h. EMSA was performed as described under "Materials and methods". Data represent one representative out of three independent experiments from different cell preparations with similar results.

# 3.2 Cytoskeleton

## 3.2.1 Inhibitory properties of ANP on TNF-α-induced permeability in HUVEC

Besides the observation that ANP is able to reduce TNF-α-induced E-selectin and ICAM-1 expression, effects of ANP on TNF-α-induced cytoskeleton changes were investigated in the following experiments. TNF-α exerts several effects that facilitate the formation of an atheromatous plaque. For example it increases endothelial cell gap formation. As a result of TNF-α-induced cell damage an increased vascular permeability is commonly attributed to the reorganization of F-actin filaments followed by contraction of cells and formation of intercellular gaps (Brett et al. 1989; Lum and Malik 1996; van Hinsbergh 1997; Wojciak-Stothard et al. 1998).

In order to test the effects of ANP on this TNF-α-mediated permeability- and cytoskeleton-changes, the subsequent experiments were performed.

Endothelial permeability was assessed by a FITC-albumin permeability assay as described under "Materials and methods". Treatment of HUVEC with TNF-α led to an increase in endothelial permeability as indicated by an increased FITC-albumin flux through endothelial monolayers (figure 35 A+B). ANP significantly abrogated the TNF-α-induced increase in permeability, whereas ANP alone showed no effect on albumin flux (figure 35 A+B). In order to stress the observed effects of ANP data were recalculated by substraction of permeability of control cells and in figure 35 panel B percentage of TNF-α-induced permeability is shown, whereby TNF-α was set 100%.

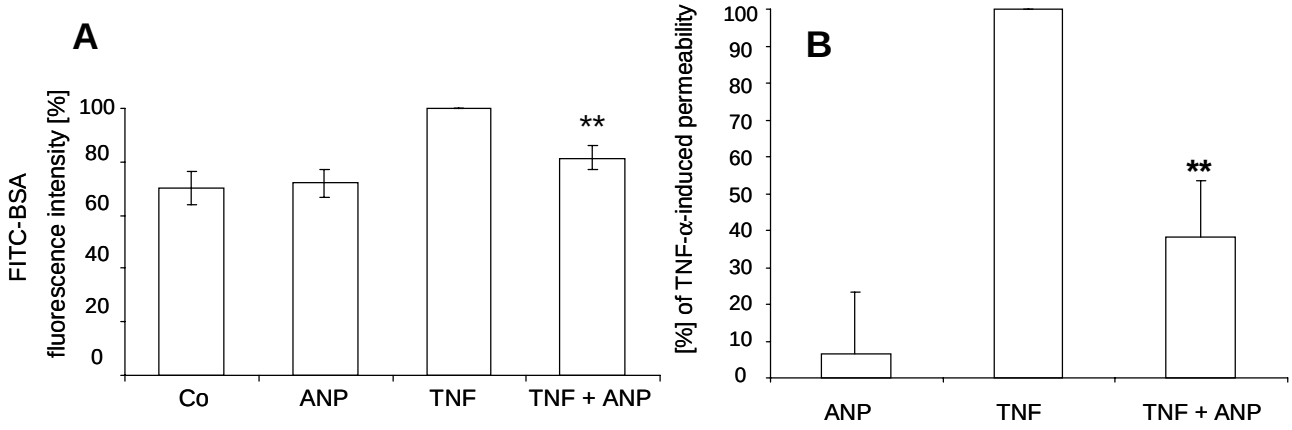


***figure 35: ANP inhibits TNF-α induced increase in HUVEC permeability***
Panel A: HUVEC in transwell chambers were either left untreated or treated with TNF-α (25 ng/ml) alone or in combination with ANP ($10^{-6}$ mol/L) for 24 h whereby ANP was added to the cells 30 min

before TNF-α. Permeability of FITC-labeled BSA was determined as described in "Materials and methods" and albumin flux of TNF-α treated cells were referred to as 100%. Panel B: Data show percentage of TNF-α-induced permeability after substraction of permeability of control cells and TNF-α was set as 100%, treatment of cells see panel A. Data show mean ± S.E.M. of three different experiments (different cell preparations) prepared in triplicates or quadruplets. **p<0.01 represents significant difference from values in TNF-α-activated cells.

## 3.2.2 Influence of ANP on TNF-α-induced morphological changes and stress fiber formation

In the subsequent morphological investigations the influence of ANP ($10^{-6}$ mol/L) on TNF-α-induced cytoskeleton changes was examined either after Haemacolor® staining (figure 36) or after intracellular staining of F-actin stress fiber bundles with a specific F-actin binding rhodamine phalloidin dye (figure 37).

### 3.2.2.1 Morphological investigations

As demonstrated in figure 36, untreated HUVEC were well spread and showed a typical "cobblestone" morphology. After treatment of the cells with TNF-α, cells started to retract, elongate, and form intercellular gaps. ANP almost completely abrogated these changes in HUVEC morphology (figure 36).

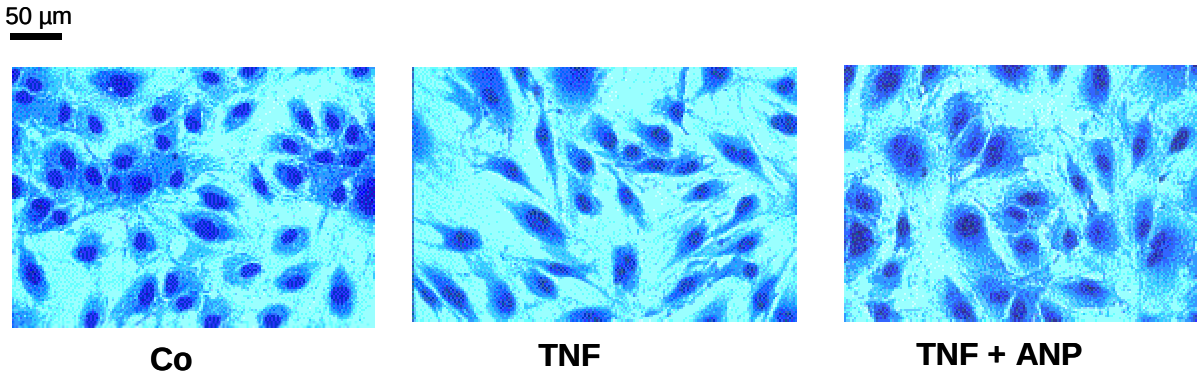


***figure 36: Effect of ANP on TNF-α induced morphological changes***
Confluent HUVEC monolayers were cultured in either medium alone (Co) or in medium containing TNF-α (10 ng/ml) in the presence or absence of ANP ($10^{-6}$ mol/L) for 1 h (pretreatment with ANP for 30 min). Cells were stained as described in "Materials and methods". The pictures show representative photographs out of four independent experiments from different cell preparations (original magnification 200-fold).

### 3.2.2.2 Stress fiber formation

The results of the intracellular staining for F-actin are shown in figure 37. After permeabilisation of HUVEC with Triton X-100, the intracellular cytoskeleton component F-actin was stained with rhodamin phalloidin, a specific antibody detecting only polymerized actin.

In untreated, confluent HUVEC monolayers F-actin was concentrated in fine F-actin filaments transversing the cells. As shown in figure 37, TNF-α induced changes in F-actin organization whereby the cells showed an increase and thickening of actin bundles and the formation of stress fibers. Intercellular gaps and cell retraction were indicated by large unstained areas of the image. Cotreatment of the cells with ANP inhibited TNF-α-induced alterations in actin distribution (figure 37).

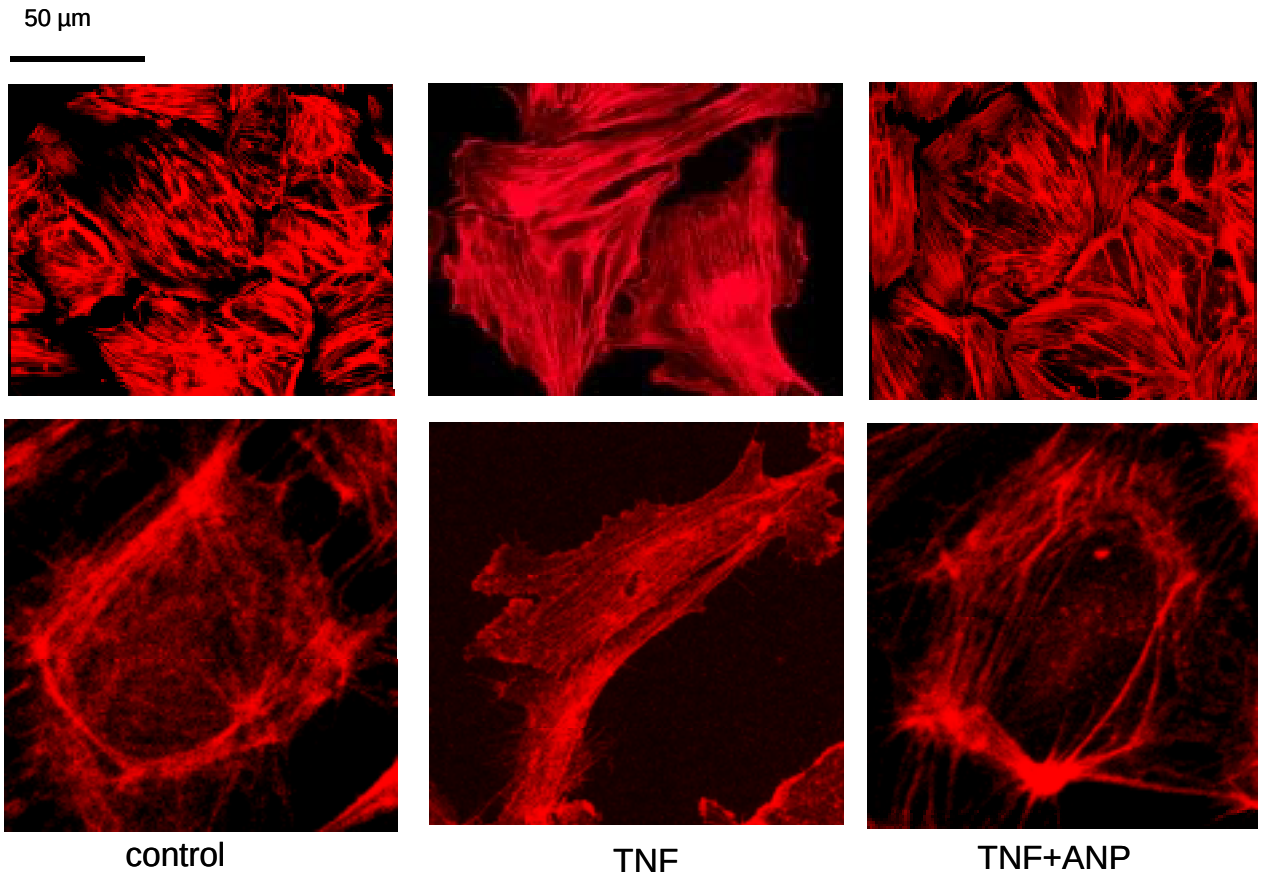


***figure 37: ANP attenuated TNF-α-induced stress fiber formation in HUVEC***
HUVEC were either untreated (Co) or activated with TNF-α (10 ng/ml) with or without ANP ($10^{-6}$ mol/L) for 30 min. Data show one representative out of three independent experiments from different cell preparations (original magnification 400-fold). The lower panel shows a detailed confocal microscopic picture of one untreated, TNF treated or TNF and ANP treated cell.

### 3.2.2.3 Investigations on F-actin content

For quantification of the given results, HUVEC were again stained for F-actin and the intracellular F-actin content was determined by methanolic extraction and quantification of bound rhodamin phalloidin in a fluorescence spectral photometer. In order to investigate the receptor specificity of the observed ANP effect the cell permeable analogue of cGMP, 8-Br-cGMP was used in the same experimental settings.

TNF-α led to a strong increase of cellular F-actin content. Treatment of the cells with ANP ($10^{-8}$-$10^{-6}$ mol/L) significantly inhibited TNF-α-induced actin polymerization. ANP in a concentration of $10^{-6}$ mol/L alone did not significantly affect F-actin content (figure 38).

The second messenger analogue 8-Br-cGMP mimicked the effect of ANP on the TNF-α-induced increase in F-actin content (figure 38).

In order to determine whether ANP-induced changes in F-actin content were related to different expression of actin upon treatment with ANP, whole actin content was determined by performing Western blots of G-actin. The amount of actin was not different in cells treated with TNF-α + ANP compared to cells treated with TNF-α (figure 38, insert Western blot).

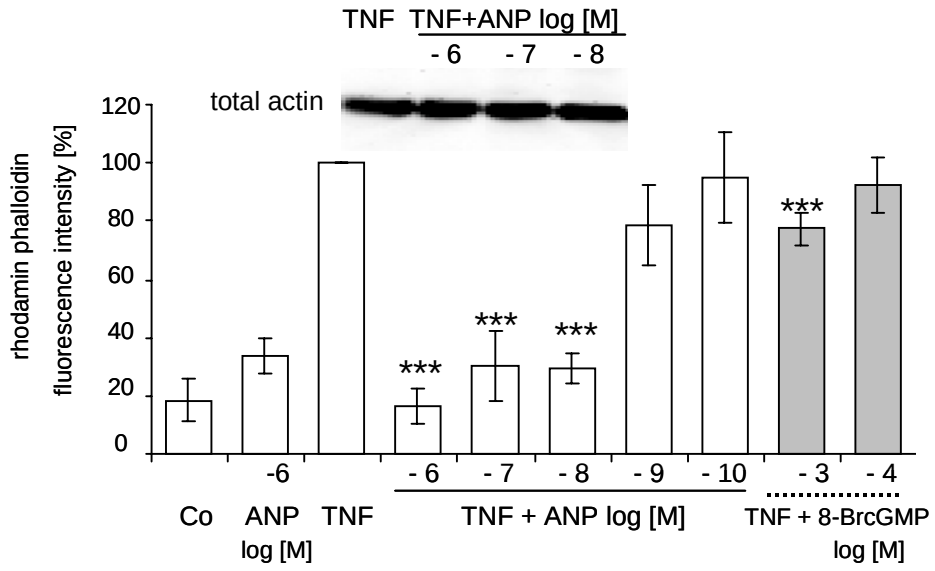


***figure 38: Effect of ANP and 8-Br-cGMP on F-actin polymerization.***
Cells were either left untreated (Co) or treated with TNF-α (10 ng/ml) for 1 h. ANP ($10^{-10}$-$10^{-6}$ mol/L) or 8-Br-cGMP ($10^{-3}$ and $10^{-4}$ mol/L) was added to the cells alone or 30 min before TNF-α. Data are

expressed as percentage of mean fluorescence with 100% representing values for TNF-α treatment only. Data show mean ± S.E.M. of three to five independent experiments from different cell preparations, each performed in triplicates. *** $p<0.001$ and ** $p<0.01$ represent significant differences compared to the values seen in TNF-α-activated cells. The inserted Western blot shows total actin of cells treated with TNF-α (10 ng/ml) for 1 h with or without 30 min ANP pretreatment ($10^{-8}$-$10^{-6}$ mol/L).

### 3.2.3 Molecular mechanism involved in the inhibitory action of ANP on TNF-α-induced cytoskeleton changes

The TNF-α-induced reorganization of F-actin and therefore the formation of stress fibers, is associated with the polymerization of G-actin into F-actin fibers (Wojciak-Stothard et al. 1998). Phosphorylation of the heat shock protein HSP27 has previously been shown to regulate actin polymerization (Landry and Huot 1995) and to contribute to stress fiber formation in endothelial cells (Huot et al. 1997). The next investigations therefore aimed to determine the influence of ANP on TNF-α-induced phosphorylation of HSP27 and to examine whether ANP influences actin polymerization *via* this pathway.
The phosphorylation of HSP27 was examined by Western blot using a specific anti phospho HSP27 antibody (figure 39).

#### 3.2.3.1 Inhibition of HSP27 phosphorylation by ANP

Treatment of the cells with TNF-α (0-120 min) led to a marked phosphorylation of HSP27 (figure 39, upper Western blot), whereas ANP significantly inhibited TNF-α-induced phosphorylation of HSP27. Changes in phosphorylation of HSP27 were not due to different amounts of HSP27 as shown by Western blot using an antibody against HSP27 (figure 39, lower Western blot).

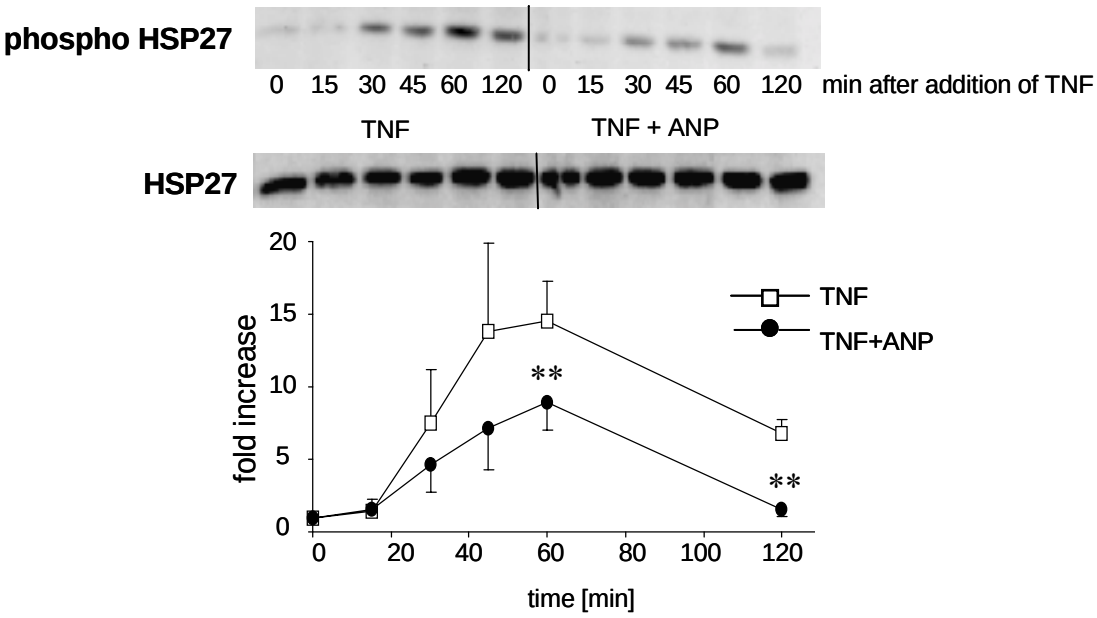


***figure 39: Influence of ANP on TNF-α-induced phosphorylation of HSP27***
HUVEC were treated with TNF-α (10 ng/ml) alone or in combination with ANP ($10^{-6}$ mol/L) for the indicated times. HSP27 served as loading controle and is shown in the lower Western blot. One representative out of three independent experiments from different cell preparations is shown, each. The lower panel shows densitometric evaluation of three experiments expressed as x-fold increase *vs.* 0 min. ** $p<0.01$ represent significant differences compared to TNF-α treatment alone.

### 3.2.3.2 Involvement of p38 MAPK in cytoskeleton changes

HSP27 is phosphorylated by the mitogen activated protein kinase activated protein kinase-2 (MAPKAPK-2) (Obata et al. 2000) and therefore represents a downstream target of the p38 mitogen activated protein kinase (MAPK). The role of p38 MAPK for actin polymerization has been shown in oxidant-stress induced stress fiber formation (Huot et al. 1997). In order to investigate a potential role for p38 MAPK in the described signal transduction pathway, the effect of a specific p38 MAPK inhibitor, SB203580, on TNF-α-induced cytoskeleton changes was tested in the following experiments.

TNF-α-induced formation of stress fibers was abrogated by SB203580 as shown by actin staining (figure 40).

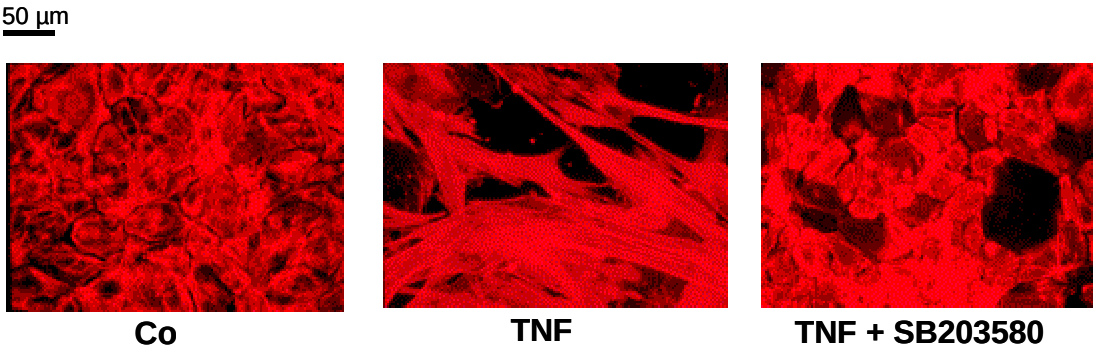


***figure 40: Effect of specific p38 inhibitor SB203580 on stress fiber formation***
Cells were either left untreated (Co) or treated with TNF-α (10 ng/ml) in the presence or absence of SB203580 ($5x10^{-6}$ mol/L) for 30 min. Cells were permeabilized and stained with rhodamine-phalloidin. Data show one representative out of four independent experiments from different cell preparations (original magnification 200-fold).

As demonstrated in figure 41, SB203580 alone did not affect basal F-actin content, whereas it significantly reduced TNF-α-induced F-actin formation.

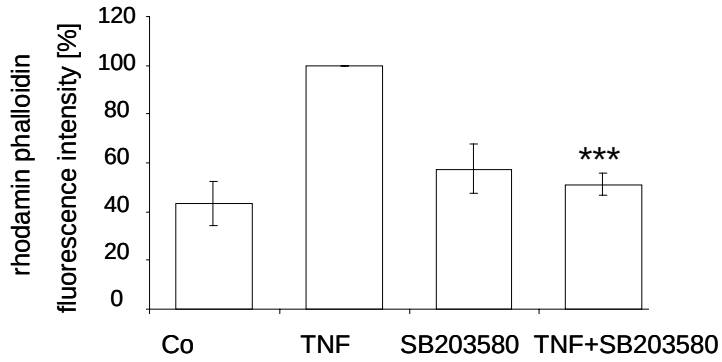


***figure 41: Effect of specific p38 inhibitor SB203580 on F-actin content***
HUVEC were cultured in either medium alone (Co), in medium with SB203580 ($10^{-5}$ mol/L), or in medium containing TNF-α (10 ng/ml) in the presence or absence of SB203580 ($10^{-5}$ mol/L). F-actin was quantified by fluorescence photometry. Values for TNF-α treatment only were referred to as 100%. Data show mean ± S.E.M. of four independent experiments from different cell preparations, each performed in triplicates. *** $p<0.001$ represent significant differences compared to the values seen in TNF-α-activated cells.

### 3.2.3.3 Involvement of p38 MAPK in TNF-α-induced permeability

As shown under 3.2.3.2 the p38 MAPK is involved in the signal transduction of TNF-α-induced cytoskeleton changes as demonstrated by the use of the specific p38 MAPK inhibitor SB203580. Besides this result it was investigated whether the p38 MAPK is additionally participating in the TNF-α-induced permeability signal transduction. Therefore the specific p38 MAPK inhibitor SB203580 was used in the same experimental settings as described under 3.2.1 for ANP to determine the effect of SB203580 on TNF-α-induced endothelial permeability (figure 42 A+B).

SB203580 alone did not affect endothelial permeability. But SB203580 abrogated TNF-α-induced elevated BSA flux (figure 42 A+B). In order to stress the observed effects of SB203580 data were recalculated by substraction of permeability of control cells and in figure 42 panel B percentage of TNF-α-induced permeability is shown, whereby TNF-α was set as 100%.

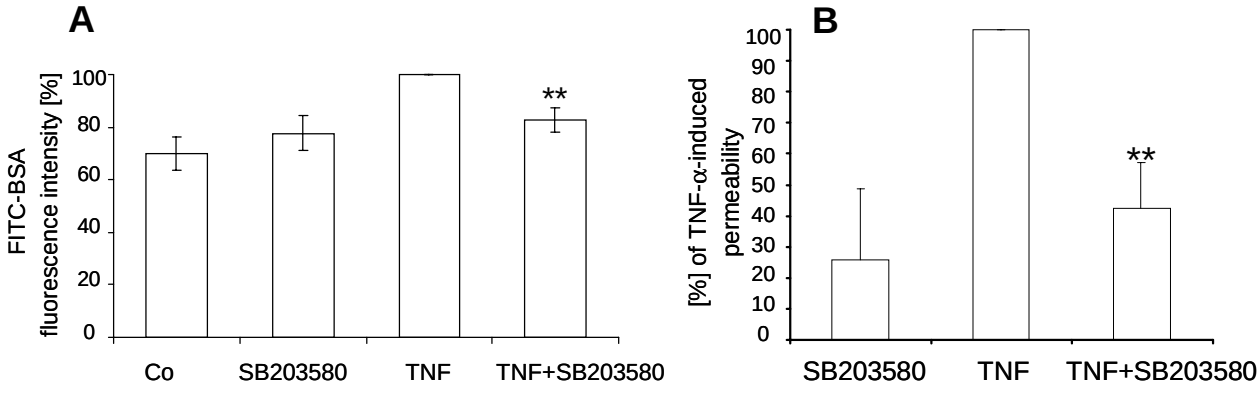


***figure 42: Effect of specific p38 inhibitor SB203580 on permeability***

Panel A: HUVEC in transwell chambers were either left untreated or treated with TNF-α (25 ng/ml) alone or in combination with SB203580 ($5x10^{-6}$ mol/L for 24 h). Permeability of FITC-labeled BSA was determined as described in "Materials and methods" and albumin flux of TNF-α treated cells were referred to as 100%. Panel B: Data show percentage of TNF-α-induced permeability after substraction of permeability of control cells and TNF-α was set as 100%, treatment of cells see panel A. Data show mean ± S.E.M. of three different experiments (different cell preparations) prepared in triplicates or quadruplets. ** $p<0.01$ represents significant difference from values in TNF-α-activated cells.

### 3.2.3.4 Inhibition of TNF-α-induced phosphorylation of p38 MAPK by ANP

These results suggest the participation of p38 MAPK in the signal transduction of ANP mediated reduction of TNF-α-induced changes in permeability and cytoskeleton. Due to the causal role of TNF-α-induced p38 MAPK activation for actin polymerization, an effect of ANP on p38 MAPK was investigated. MAPK activation was measured by immunoblotting with epitope-specific anti-phosphotyrosine-antibodies to determine MAPK phosphorylation (figure 43).

ANP significantly reduced TNF-α-mediated activation of p38 MAPK as shown by Western blot (figure 43, upper Western blot). ANP did not affect the amount of total p38 MAPK (figure 43, lower Western blot).

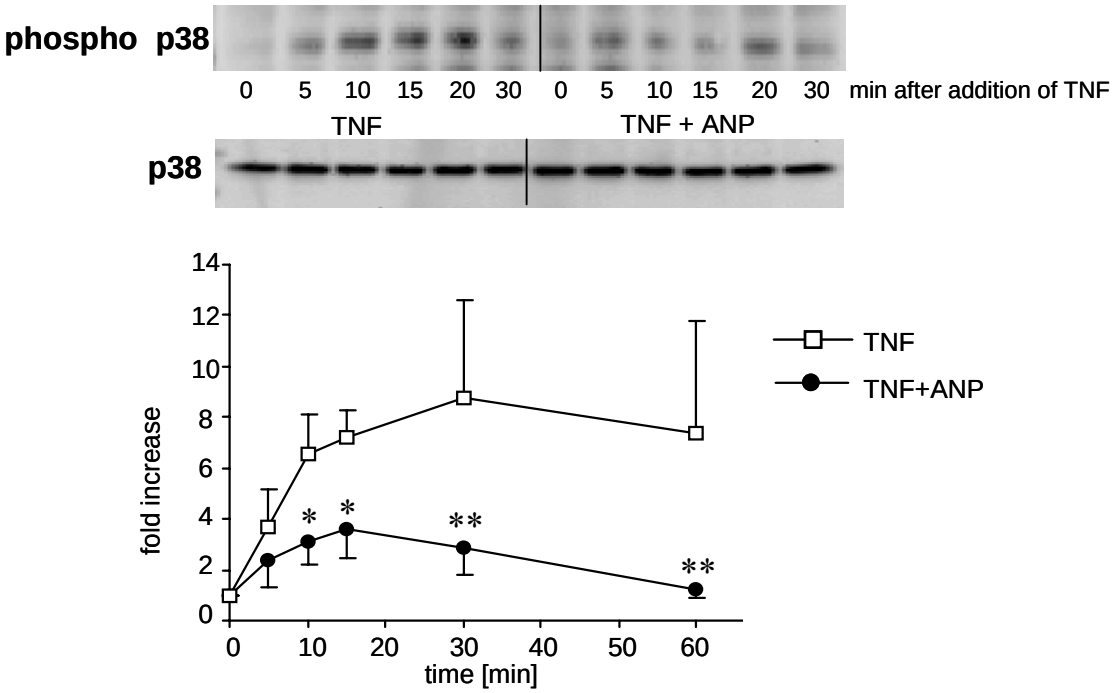


***figure 43: Influence of ANP on TNF-α-induced phosphorylation of p38***
HUVEC were treated with TNF-α (10 ng/ml) in the presence or absence of ANP ($10^{-6}$ mol/L) for the indicated times whereas ANP was added to the cells 30 min before TNF-α. Western blot was performed as described under "Materials and methods". The upper panel shows one representative out of three independent experiments from different cell preparations, each. Histogramm shows densitometric evaluation of signal intensities of three experiments whereby * $p<0.05$, ** $p<0.01$ represent significant differences compared to TNF-α treatment alone.

The inhibition of p38 MAPK phosphorylation by ANP was dose-dependent as shown by Western blot in figure 44.

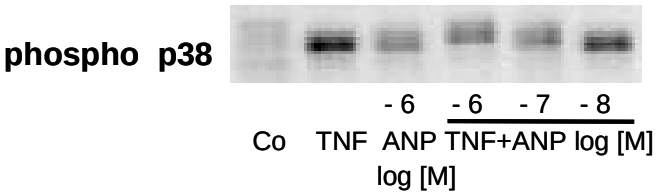


***figure 44: Dose dependent inhibition of activation of p38 by ANP***
HUVEC were either untreated (Co) or treated with TNF-α (10 ng/ml) in the presence or absence of ANP ($10^{-8}$-$10^{-6}$ mol/L) which was added to the cells 30 min before TNF-α (15 min). Western blot was performed as described under "Materials and methods". p38 MAPK activation was shown by demonstrating phosphorylated p38.

### 3.2.3.5 Mechanism of reduced p38 MAPK activation by ANP

In order to clarify a possible mechanism by which ANP reduces TNF-α-induced p38 MAPK activation two potential pathways were investigated. First the influence of ANP on the known upstream MAPKK of p38 MAPK, MKK 3/6, was investigated by Western blot (figure 45).

ANP had no influence on TNF-α-induced activation of MKK3/6 (figure 45).

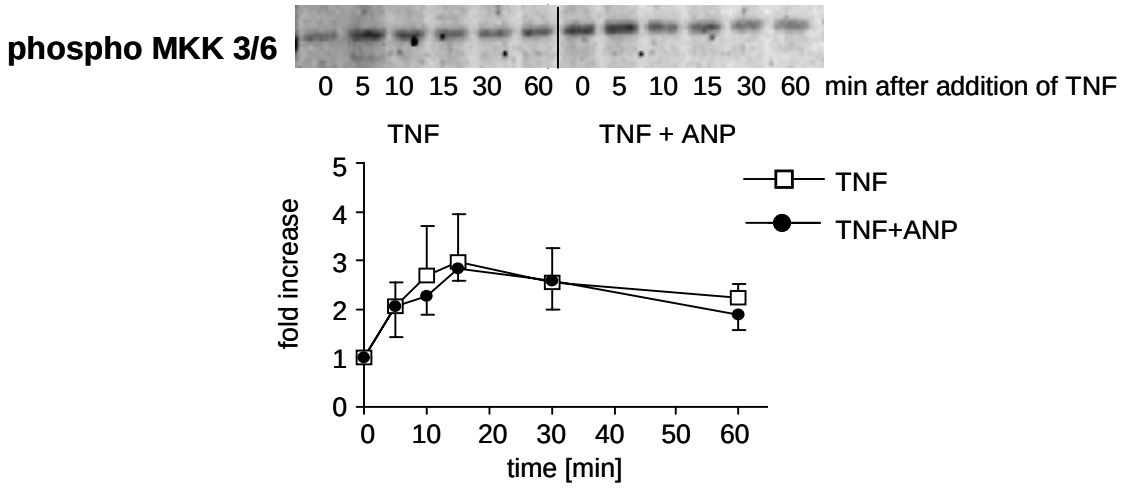


***figure 45: ANP treatment does not affect MKK3/6 activation***
Cells were activated with TNF-α (10 ng/ml) with or without ANP ($10^{-8}$-$10^{-6}$ mol/L) for the indicated times. MKK3/6 activation was determined by Western blot using an antibody against the activated form of MKK3/6. The upper panel shows one representative out of four independent experiments from different cell preparations. The lower panel shows the densitometric evaluation of signal intensities of four experiments.

As no effect of ANP on MKK3/6 was detectable, the second potential pathway for deactivating p38 MAPK was investigated. p38 MAPK can be deactivated by a dual-specificity MAPK phosphatase (MKP), which target the two critical phosphorylation sites in the activation loop of MAPK. From the known MKP, MKP-1 is known to be responsible for the dephosphorylation of p38 (Chen et al. 2001), which could not be shown for MKP-2 (Chu et al. 1996) or MKP-3 (Nichols et al. 2000). Therefore the effect of ANP on MKP-1 protein expression was investigated by Western blot (figure 46) and the effect of ANP on MKP-1 mRNA was examined by RT-PCR (figure 47).

ANP ($10^{-6}$ mol/L) significantly increased MKP-1 protein expression as early as 30 min, whereas TNF-α alone had no effect on MKP-1 expression (figure 46).

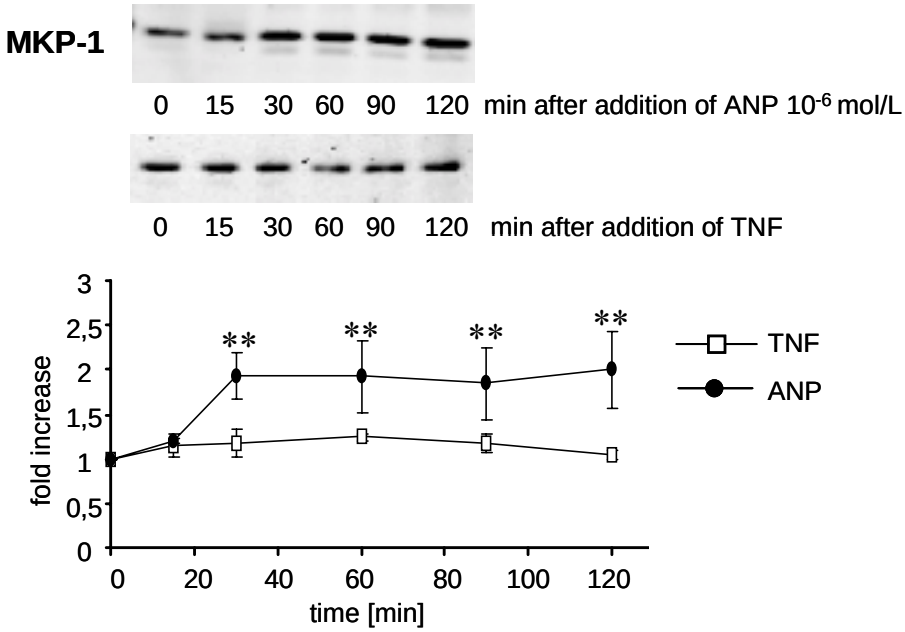


***figure 46: ANP induces MKP-1 protein expression***

Cells were treated with ANP ($10^{-6}$ mol/L) or TNF-α (10 ng/ml) for the indicated times. MKP-1 expression was investigated by Western blot. The blots show one representative out of four independent experiments from different cell preparations, each. The lower panel shows densitometric evaluation of signal intensities of three experiments whereby ** $p<0.01$ represent significant differences compared to the values seen at time point 0 min of the respective treatment.

**Regulation of MKP-1 induction by ANP**

As shown by Western blot ANP is able to induce MKP-1 protein levels. In order to demonstrate if the MKP-1 induction is mediated on the transcriptional level RT-PCR for MKP-1 was performed as described under "Materials and methods".

Figure 47 demonstrates that ANP ($10^{-6}$ mol/L) significantly elevated MKP-1 mRNA levels as early as 20 minutes and therefore suggests transcriptional regulation of MKP-1 induction by ANP.

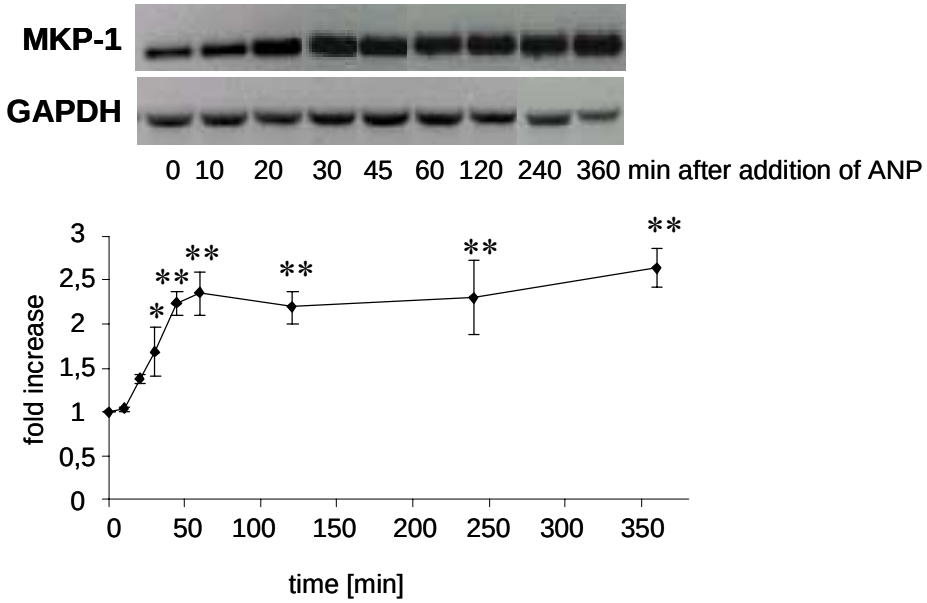


***figure 47: Transcriptional upregulation of MKP-1 by ANP***
HUVEC were treated with ANP ($10^{-6}$ mol/L) for the indicated times. RNA was isolated and MKP-1 and GAPDH mRNA was estimated by RT-PCR. Data show one representative out of three independent experiments from different cell preparations. Densitometric evaluation of ethidium bromide stained gels is shown whereby data are expressed as x-fold of values of cells at time point 0 min normalized for GAPDH. ** $p<0.01$ significantly different compared to the values seen at 0 min

## 3.2.4 Causal relationship between MKP-1 induction and p38 MAPK inhibition by ANP

In order to investigate if MKP-1 upregulation during ANP pretreatment does indeed contribute to a p38 inhibition, it was tested if addition of ANP simultaneously with TNF-α resulted in the same inhibitory action on p38.

A significant p38 inhibition by ANP occurred significantly only after 30 min or later (figure 48). This result indicates that preincubation with ANP (which leads to

increased expression of MKP-1) is indeed necessary for early inhibition of TNF-α-induced p38 activation.

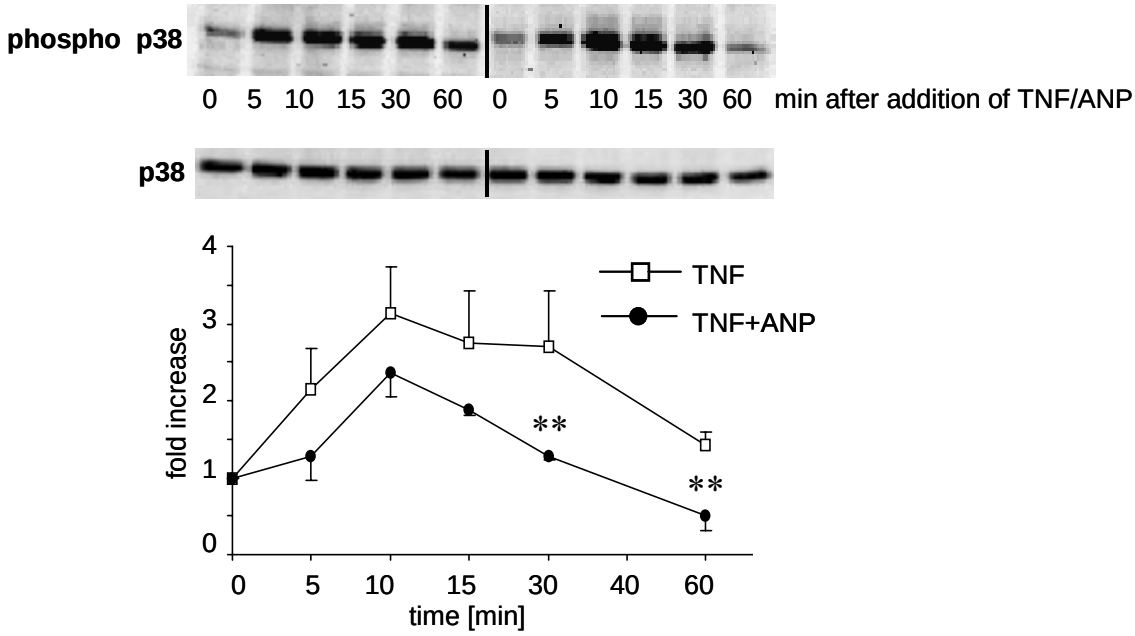


***figure 48: Involvement of MKP-1 induction in p38 inhibition***

HUVEC were treated with TNF-α (10 ng/ml) in the presence or absence of ANP ($10^{-6}$ mol/L) for the indicated times whereby ANP was given to the cells simultaneously with TNF-α. Cells were harvested in the presence of phosphatase inhibitors and Western blots were performed using antibodies against phosphorylated and non-phosphorylated p38. The blots show one representative out of three independent experiments from different cell preparations, each. The lower panel shows densitometric evaluation of signal intensities of three blots with ** $p<0.01$ representing significant differences compared to the values seen at time point 0 min.

The direct causal relationship between the MKP-1 induction by ANP and the p38 MAPK inhibition was demonstrated by antisense-experiments.

In a first control experiment the inhibition of MKP-1 translation after 3 h of incubation with antisense oligonucleotides in presence or absence of ANP ($10^{-6}$ mol/L) was shown by Western blot (figure 49). Use of sense oligonucleotides served as control for specificity of the experiment (figure 49).

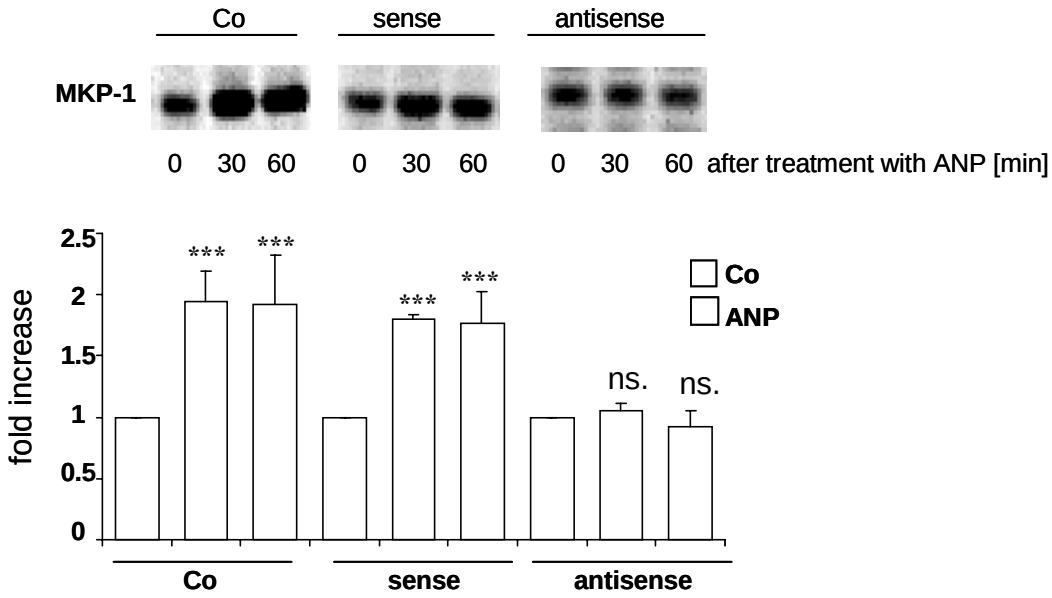


***figure 49: Blocking of MKP-1 expression by antisense-oligonucleotides***

Cells were treated with ANP ($10^{-6}$ mol/L) for the indicated time after transfection with antisense or sense oligonucleotides for MKP-1 as described under "Materials and methods". MKP-1 expression was investigated by Western blot. The blots show one representative out of four independent experiments from different cell preparations, each. Data show mean ± S.E.M. of four independent experiments with *** $p<0.001$ represent significant differences compared to the values seen in control cells.

The following Western blot of phospho p38 MAPK shows that the blockade of MKP-1 translation by antisense-oligonucleotides leads to the abolition of the inhibitory effects of ANP on p38 MAPK phosphorylation (figure 50).

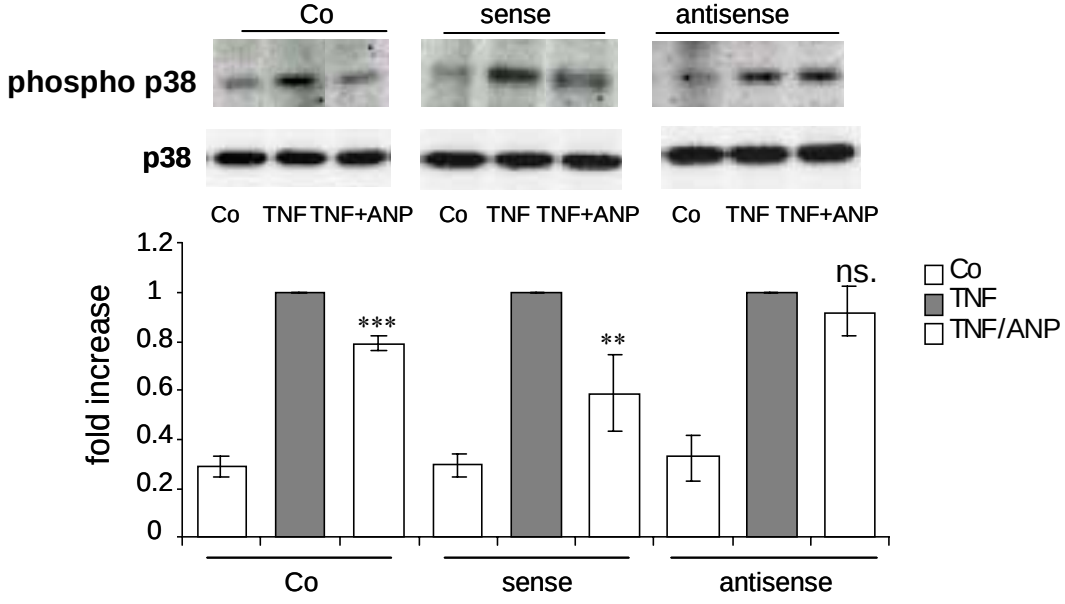


***figure 50: Abolition of ANP mediated p38 inhibition by blockade of MKP-1 with antisense-oligonucleotides***

HUVEC were either left untreated (Co) or treated with TNF-α (10 ng/ml) in the presence or absence of ANP ($10^{-6}$ mol/L) which was added to the cells 30 min before TNF-α (15 min) after transfection of cells with antisense or sense oligonucleotides for MKP-1 as described under "Materials and methods". The upper panel shows one representative Western blot out of four independent experiments with similar results, each. Values for TNF-α treatment only were referred to as 1. Data show mean ± S.E.M. of four independent experiments with ** $p<0.01$ and *** $p<0.001$ represent significant differences compared to the values seen in TNF-α-activated cells. p38 MAPK activation was shown by demonstrating phosphorylated p38 in Western blot, detection of unphosphorylated p38 in the lower blot served as loading control.

This result confirmes the results given in figure 48. It demonstrates that the transcriptional upregulation of MKP-1 by ANP is indeed necessary for early inhibition of TNF-α-induced p38 activation.

# 3.3 Monocyte chemoattractant protein (MCP-1)

As a proinflammatory cytokine TNF-α is able to induce the expression of chemokines, such as the monocyte chemoattractant protein (MCP-1). MCP-1 is a member of the CC chemokine subfamily and is critically involved in the recruitment of leukocytes to sites of the inflamed tissue, by binding to certain chemokine receptors that are expressed on the cell surface of several cells, such as endothelial cells, smooth muscle cells, or leukocytes. MCP-1 and other chemokines have been shown to play a key role in communication between different cells during the immune response under inflammatory conditions.

## 3.3.1 ANP inhibits TNF-α-induced secretion of MCP-1

In order to determine the influence of ANP on the TNF-α-induced secretion of the monocyte chemoattractant protein (MCP-1), secretion of MCP-1 in culture medium was investigated by enzyme-linked immunosorbent assay (ELISA) (figure 51).

ANP pretreatment dose-dependently ($10^{-10}$-$10^{-6}$mol/L) reduced MCP-1 protein (figure 51). ANP ($10^{-6}$ mol/L) alone significantly elevated basal MCP-1 expression.

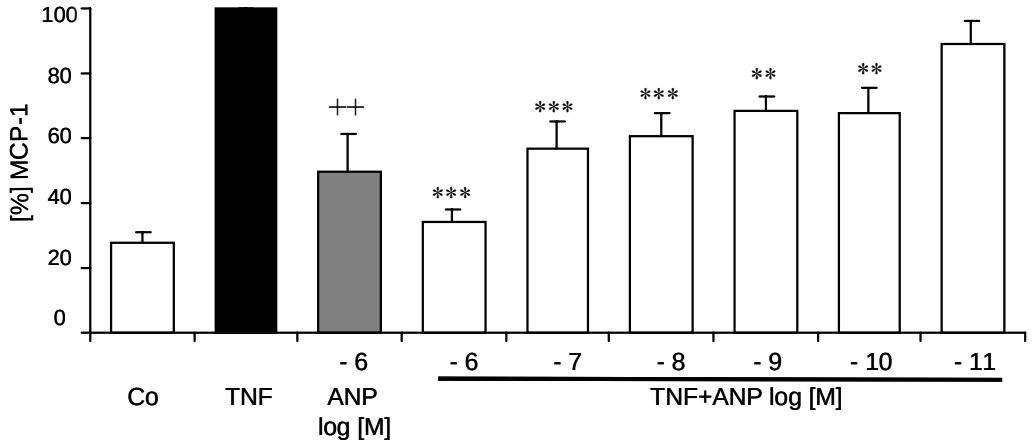


***figure 51: ELISA analysis of MCP-1 protein***

MCP-1 protein expression was detected by ELISA. Cells were left untreated, TNF-α-treated (6 h), and TNF-α + ANP ($10^{-11}$-$10^{-6}$ mol/L) treated, whereby ANP was added 30 min before TNF-α. Data show mean percentage MCP-1 ± S.E.M. of three independent experiments from different cell preparations. ** $p<0.01$ and *** $p<0.001$ represent significant differences compared to the values seen in TNF-α-activated cells, whereby TNF-α was set as 100%. $^{++}$ $p<0.01$ represents significant differences compared to the values seen in control cells.

## 3.3.2 Receptor specificity of the ANP effect on MCP-1

In order to clarify the receptor specificity of the inhibitory effect of ANP on TNF-α-induced expression of MCP-1, the following substances were tested for their influence on the TNF-α-induced MCP-1 release: The cell-permeable analogue of cGMP, 8-Br-cGMP, the specific NPR-C ligand cANF and the specific NPR-B ligand CNP. Experiments with the mentioned substances were carried out with TNF-α-treated cells by ELISA.

The cell-permeable analogue of cGMP, 8-Br-cGMP, significantly reduced TNF-α-induced MCP-1 expression in a dose-dependent manner (figure 52).

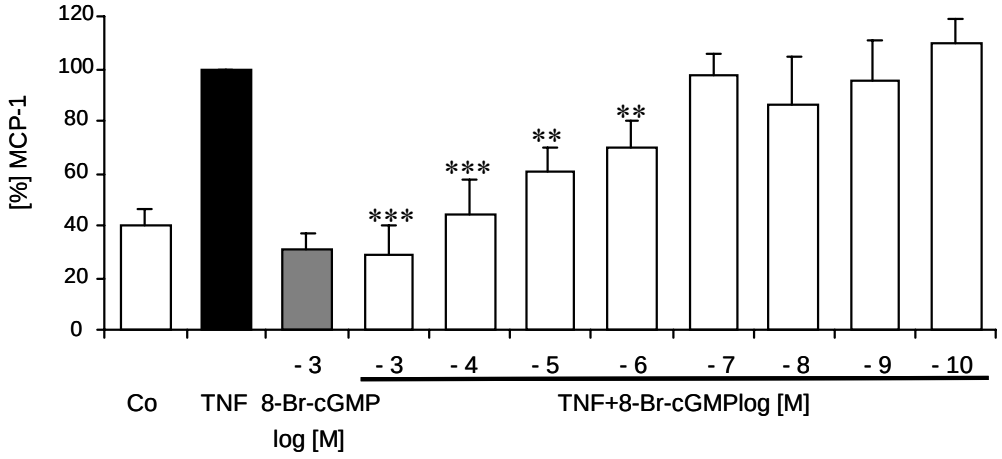


***figure 52: Effect of 8-Br-cGMP on MCP-1 expression***

MCP-1 expression of control cells (Co) or of cells treated with TNF-α (10 ng/ml, 6 h) was determined by ELISA as described under "Materials and Methodes". The effect of 8-Br-cGMP($10^{-10}$-$10^{-3}$ mol/L) on the expression of MCP-1 was determined for 8-Br-cGMP added to the cells 30 min before TNF-α, or for 8-Br-cGMP given to the cells alone ($10^{-3}$ mol/L) for 6 h. Data show mean percentage of MCP-1 ± S.E.M. of three independent experiments from different cell preparations, whereby TNF-α was set as 100%. *** $p<0.001$ and ** $p<0.01$ represent significant differences compared to the values seen in TNF-α-activated cells.

As demonstrated in figure 53 the NPR-C ligand cANF did not inhibit the TNF-α-induced MCP-1 expression, moreover it increased basal MCP-1 expression significantly (figure 53).

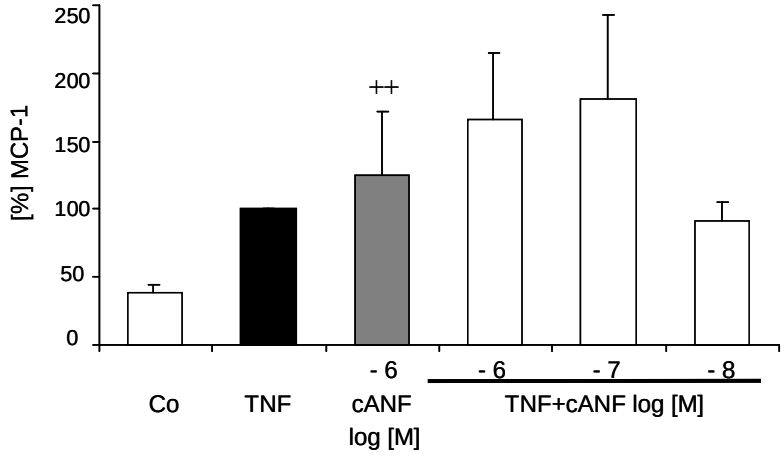


***figure 53: Effect of the NPR-C specific ligand cANF on MCP-1 expression***

MCP-1 expression of control cells (Co) or of cells treated with TNF-α (10 ng/ml, 6 h) was determined by ELISA as described under "Materials and methods". The effect of cANF ($10^{-8}$-$10^{-6}$ mol/L) on the expression of MCP-1 was determined for cANF added to the cells 30 min before TNF-α, or for cANF given to the cells alone for 6 hours. Data show mean percentage of MCP-1 ± S.E.M. of three

independent experiments from different cell preparations, whereby TNF-α was set as 100%. $^{++}$ $p<0.01$ represents significant differences compared to the values seen in control cells.

Interestingly the specific NPR-B ligand CNP exerted similar effects like ANP. CNP pretreatment ($10^{-7}$-$10^{-6}$mol/L) of the cells significantly reduced TNF-α-induced MCP-1 secretion (figure 54).

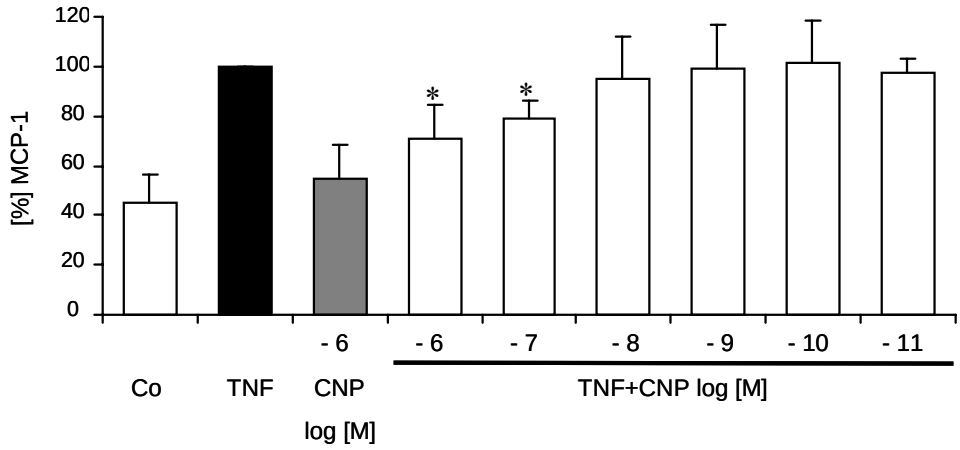


***figure 54: Effect of CNP on MCP-1 expression***

MCP-1 expression of control cells (Co), CNP treated, or of cells treated with TNF-α (10 ng/ml, 6 h) was determined by ELISA as described under "Materials and Methodes". The effect of CNP ($10^{-11}$-$10^{-6}$ mol/L) on the expression of MCP-1 was determined for CNP added to the cells 30 min before TNF-α, or for CNP given to the cells alone ($10^{-6}$ mol/L) for 6 h. Data show mean percentage of MCP-1 ± S.E.M. of three independent experiments from different cell preparations, whereby TNF-α was set as 100%. * $p<0.05$ represent significant differences compared to the values seen in TNF-α-activated cells.

## 3.3.3 Modulation of MCP-1 expression by NO

These data suggest a role for cGMP and therefore for the particulate guanylyl-cyclase-coupled NPR in the signal transduction of ANP-mediated effects. To examine if the soluble guanylyl-cyclase (sGC) also mediates this effect, we were interested if NO, an activator of the sGC affects TNF-α-induced MCP-1 production. Therefore we performed ELISA experiments using the NO-donor GSNO.

GSNO-pretreated cells showed indeed an attenuated TNF-α-induced MCP-1 expression (figure 55).

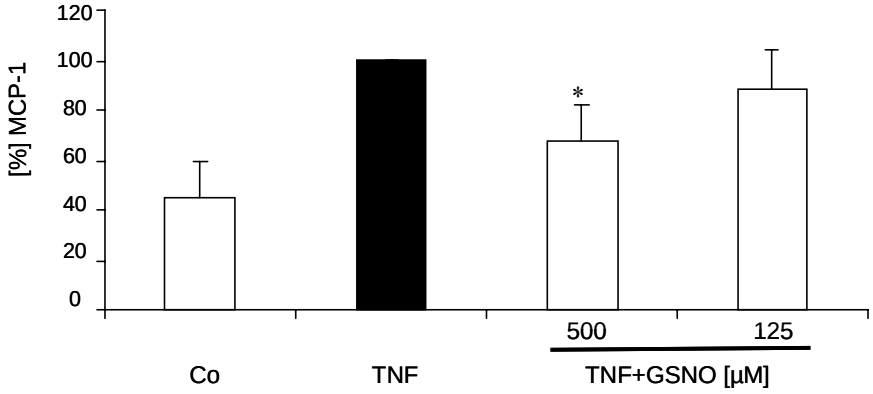


***figure 55: Modulation of MCP-1 expression by NO-donor GSNO***

HUVEC were cultured in either medium alone (Co), or in medium containing TNF-α (10 ng/ml, 6 h) with or without pretreatment (30 min) of the cells with two concentrations of GSNO (125 and 500 µmol/L). MCP-1 expression was detected by ELISA measurement as described under "Materials and methods". Data show mean ± S.E.M. of three independent experiments from different cell preparations. * $p<0.05$ represent significant differences compared to the values seen in TNF-α-activated cells, whereby TNF-α was set as 100%.

These data point to an inhibitory action of NO on TNF-α-induced MCP-1 secretion and further supports our observations of cGMP as second messenger in the signal transduction.

Furthermore we were interested in the potential role of TNF-α-induced NO production in the regulation of MCP-1 secretion. Inhibition of NO production by preincubation (30 min) with the NOS inhibitor, L-NNA (125 and 500 µmol/L) did not affect TNF-α-induced MCP-1 (figure 56).

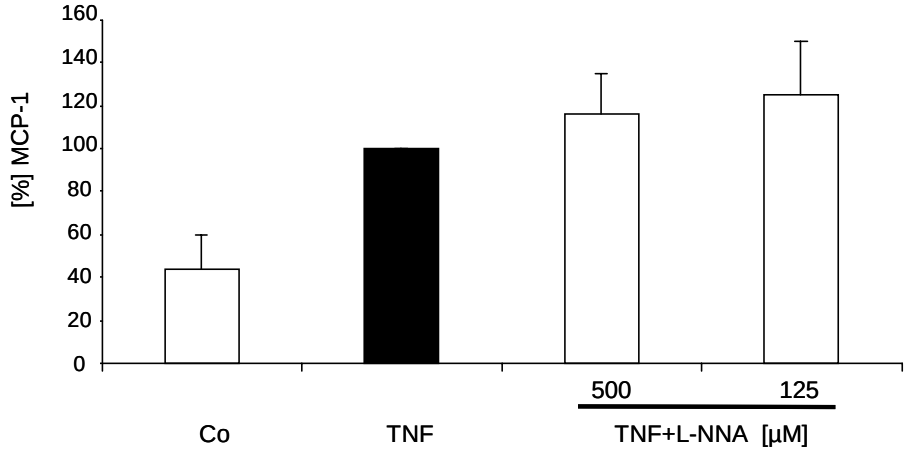


***figure 56: Modulation of MCP-1 expression by NOS inhibitor L-NNA***

HUVEC were cultured in either medium alone (Co), medium containing L-NNA, or in medium containing TNF-α (10 ng/ml, 6 h) with or without pretreatment (30 min) of the cells with two concentrations of L-NNA (125 and 500 µmol/L). MCP-1 expression was detected by ELISA measurement as described under "Materials and methods". Data show mean ± S.E.M. of three independent experiments from different cell preparations. $^{+}$ $p<0.05$ represents significant differences compared to the values seen in control cells.

## 3.3.4 ANP reduces TNF-α-induced MCP-1 mRNA expression

These data show a guanylyl-cyclase-mediated inhibition of TNF-α-induced MCP-1 secretion by ANP. The following experiments aimed to elucidate the molecular mechanism leading to this inhibitory action of ANP. In order to clarify whether the inhibition of TNF-α-induced MCP-1 secretion is regulated on a transcriptional level we performed semiquantitative RT-PCR.

TNF-α (10 ng/ml) significantly induced MCP-1 mRNA in HUVEC (figure 58). ANP pretreatment ($10^{-8}$-$10^{-6}$mol/L) indeed reduced TNF-α-induced expression of MCP-1 mRNA significantly, whereas ANP alone significantly elevated basal MCP-1 expression (figure 58).

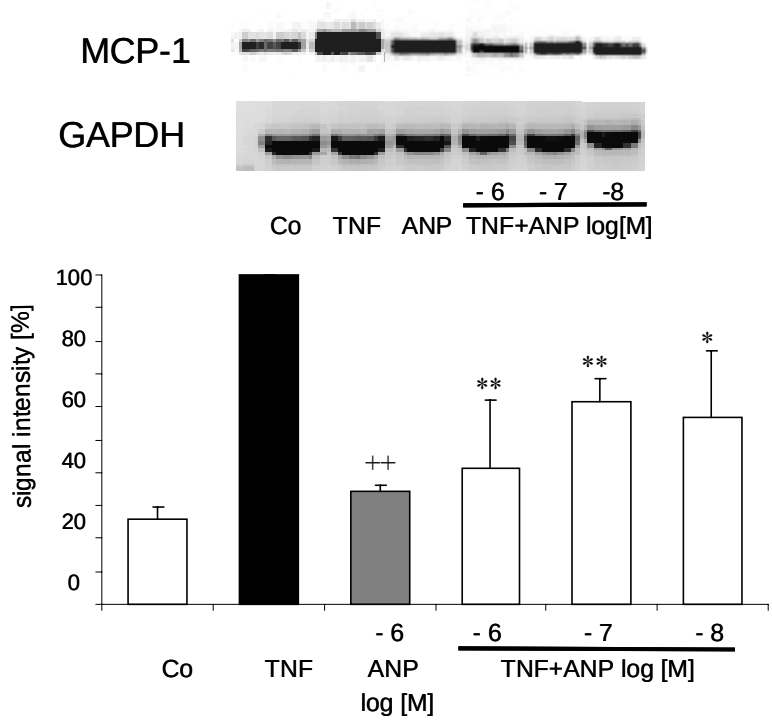


***figure 57: Dose-dependent inhibition of MCP-1 mRNA expression by ANP***

HUVEC were cultured in either medium alone (Co), medium containing ANP ($10^{-6}$ mol/L) or in medium containing TNF-α (10 ng/ml, 3 h) with or without pretreatment (30 min) of the cells with various concentrations of ANP ($10^{-8}$-$10^{-6}$ mol/L). RT-PCR was performed as described under "Materials and methods". Data show representative gels out of four independent experiments

performed, each. Histograms show densitometric evaluation of signal intensities normalized on GAPDH and are expressed as percentage of values for TNF-α treatment only. Data show mean ± S.E.M. of four independent experiments from different cell preparations. ** $p<0.01$ and * $p<0.05$ represent significant differences compared to the values seen in TNF-α-activated cells. $^{++}$ $p<0.01$ represents significant differences compared to the values seen in control cells.

## 3.3.5 Causal relationship between MKP-1-induced inactivation of p38 MAPK and reduced MCP-1 expression by ANP

The RT-PCR experiments suggest a transcriptional regulation of the ANP effects on TNF-α-induced MCP-1 expression. The p38 MAPK is known to play a pivotal role in the transcriptional regulation of MCP-1 expression. Since it is reported under 3.2 that ANP is able to inhibit TNF-α-induced phosphorylation of p38 MAPK *via* induction of MKP-1 we aimed to clarify a role for MKP-1 in the observed inhibition of MCP-1 expression by ANP.

HUVEC were transfected with either MKP-1 antisense or sense phosphorothioate-modified oligonucleotides. The functionality of the antisense experiment was examined by showing MKP-1 induction after antisense treatment in Western blot. Indeed, transfection with MKP-1 antisense, but not sense oligonucleotides abolished ANP-induced MKP-1 expression (figure 59).

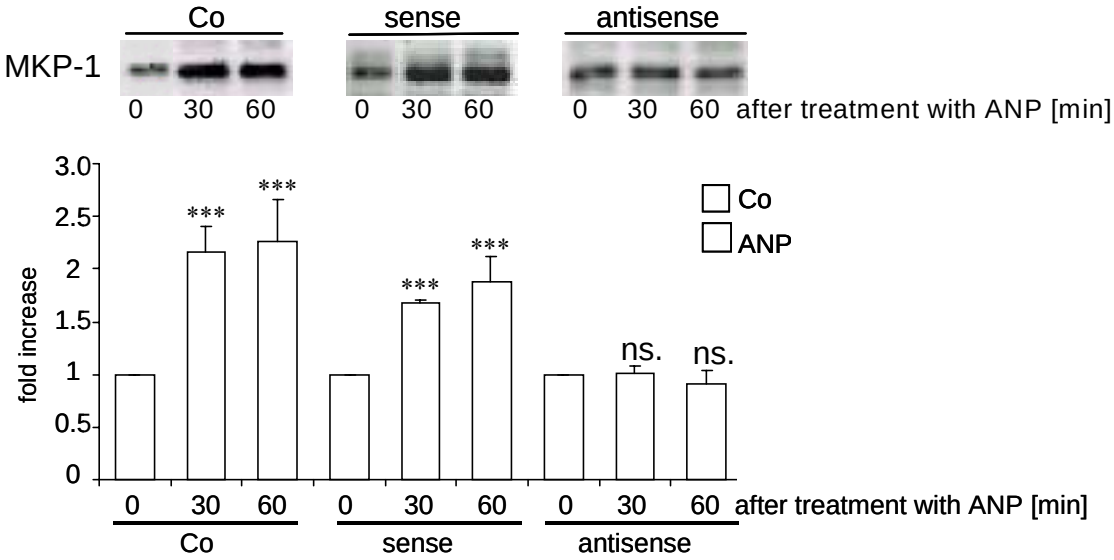


***figure 58: Blocking of MKP-1 expression by antisense-oligonucleotides***

HUVEC were transfected with antisense or sense MKP-1 oligonucleotides for 3 h or treated with transfection reagent without addition of DNA for the respective time (Co). After addition of fresh medium, cells were either left untreated or stimulated with ANP ($10^{-6}$ mol/L; 30 or 60 min). Western

blot for MKP-1 was performed as described under "Materials and methods". Data show one representative out of two independent experiments. Histogram shows densitometric evaluation of two independent experiments and represent mean ± S.E.M. whereby values of TNF-α treatment were set as 100%. *** $p<0.001$ represent significant differences from values in control cells.

As demonstrated by figure 59 transfection with MKP-1 antisense, but not sense oligonucleotides abrogated the inhibitory effect of ANP on MCP-1 expression. These data provided a causal relationship between ANP-mediated induction of MKP-1 and inhibition of TNF-α-induced expression of MCP-1 by ANP, suggesting a role for p38 MAPK in the signal transduction pathway.

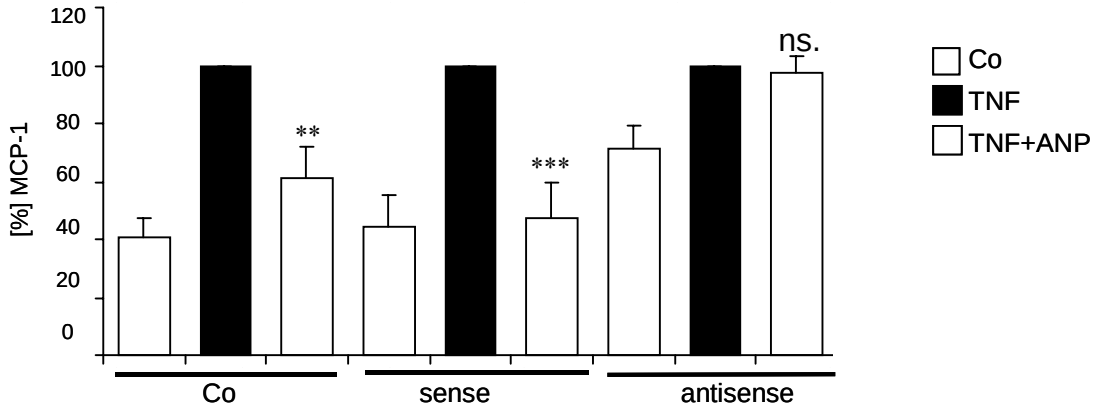


***figure 59: Blocking of MCP-1 expression by MKP-1 antisense-oligonucleotides***
HUVEC were transfected with antisense or sense MKP-1 oligonucleotides for 3 h or treated with transfection reagent without addition of DNA for the respective time (Co). After addition of fresh medium, cells were either left untreated or stimulated with TNF-α (10 ng/ml; 6 h) in presence or absence of ANP ($10^{-6}$ mol/L), which was added to the cells 30 min before TNF-α. ELISA for MCP-1 was performed as described under "Materials and methods". Histogram shows densitometric evaluation of three independent ELISA experiments and represents mean ± S.E.M. whereby values of TNF-α treatment were set as 100%. ** $p<0.01$ and *** $p<0.001$ represent significant difference from values in TNF-α-activated cells.

# 4 DISCUSSION

# 4.1 Adhesion molecules

## 4.1.1 ANP inhibits TNF-α-induced expression of adhesion molecules due to IκB induction

The recruitment of leukocytes into infected tissue is part of the immune defense against external pathogenes. However, an excessive diapedesis of leukocytes to the damaged tissue represents a central step in the development of inflammatory conditions. In this context the adhesive properties of the endothelium play a crucial role and cellular adhesion molecules, such as ICAM-1, VCAM-1, and E-selectin are critically upregulated by several stimuli (Gimbrone, Jr. et al. 1997). The inflammatory cytokine TNF-α has been shown to modulate the expression of cell adhesion molecules. The hypothesis of the first section of the present work was that ANP might influence the TNF-α-induced expression of CAM.

### 4.1.1.1 ANP inhibits expression of ICAM-1 and E-selectin

The results of the present work demonstrated that ANP inhibits a crucial step in the pathogenesis of inflammatory states, the expression of CAM. Interestingly, ANP dose-dependently only affected the expression of ICAM-1 and E-selectin mRNA and protein levels, whereas it showed no effect on VCAM-1 expression. These results may not surprise taking into account the knowledge about the transcriptional regulation of the three CAM. The proinflammatory transcription factor NF-κB has been identified to be a key component of the cytokine-inducible expression of ICAM-1 and E-selectin (Collins et al. 1995). Despite the knowledge that NF-κB is also involved in regulation of VCAM-1 expression, VCAM-1 has previously been shown to be regulated *via* pathways including other proinflammatory transcription factors besides NF-κB, too (Lawson et al. 1999). The regulatory regions of the VCAM-1 gene are composed of multiple binding elements, which are recognized by a large number of transcription factors. The cytokine-induced transcriptional enhancer in the VCAM-1 promoter requires combinatorial interactions of NF-κB with other nuclear activators, such as stimulatory protein-1, interferon regulatory factor-1, and activator protein-1 (Neish et al. 1995a; Neish et al. 1995b; Ahmad et al. 1998). Considering these facts the transcriptional regulation of VCAM-1 can not solely be connected to the transcriptional activity of NF-κB.

### 4.1.1.2 cGMP-mediated inhibition of CAM expression

ANP is known to mediate most of its cardiovascular and renal effects through interaction with the guanylyl-cyclase-coupled natriuretic peptide A-receptor, NPR-A, *via* cGMP as second messenger (Levin et al. 1998). However, ANP has also been shown to act through binding the non-guanylyl-cyclase-linked natriuretic peptide receptor (NPR-C) (Levin 1993). Taking these facts into account it seemed to be important to clarify the receptor specificity of the observed ANP effects. The use of the NPR-A antagonist, HS-142-1, the cell permeable cGMP analogue, 8-Br-cGMP, and the specific NPR-C agonist cANF, indicate that the inhibitory action of ANP on CAM expression is mediated *via* cGMP. The NPR-A antagonist HS-142-1 abrogated, whereas the cGMP analogue 8-Br-cGMP mimicked the effect of ANP on CAM expression. Moreover, the specific NPR-C agonist cANF had no influence on TNF-α-induced CAM expression. Interestingly, CNP, a specific ligand for the other guanylyl-cyclase-coupled receptor, NPR-B, also showed inhibitory action on CAM.
cGMP has been described before to attenuate hypoxia/reoxygenation-mediated VCAM-1 expression in HUVEC (Collard et al. 1999). However, cGMP analogues have also been shown not to interfere with CAM expression induced by TNF-α (Spiecker et al. 1998) or other cytokines in human saphenous vein endothelial cells (De Caterina et al. 1995) or by IL-1β in HUVEC (Takahashi et al. 1996). These contradictory observations might reflect cell type-, species-, and stimulus-dependent differences in the regulation of CAM expression.

### 4.1.1.3 cGMP-mediated inhibition of NF-κB activation

The proinflammatory transcription factor NF-κB is recognized as a ubiquitously expressed transcription factor. Upon stimulation NF-κB is rapidly activated and regulates the expression of a wide variety of genes, including genes coding for cell adhesion molecules (ICAM-1 and E-selectin) and chemokines (MCP-1). Due to the central role of NF-κB in the regulation of CAM expression, the effects of ANP on TNF-α-induced DNA binding activity of NF-κB were assessed. The results of the present work show an attenuated TNF-α-induced activation of NF-κB in endothelial cells upon pretreatment with ANP. Interestingly, the specific ligand for NPR-B, CNP, also showed this inhibitory property. These observations suggested a role for cGMP in regulating NF-κB activation. In fact the use of the cell permeable cGMP analogue 8-Br-cGMP, and the specific NPR-C agonist cANF, confirmed that the inhibitory action of ANP on TNF-α-induced activation of NF-κB is mediated *via* cGMP: The

cGMP analogue 8-Br-cGMP mimicked the effect of ANP and CNP, whereas the specific NPR-C agonist cANF had no influence on TNF-α-induced NF-κB DNA-binding activity. These data provide evidence that ANP and CNP mediate their NF-κB inhibiting action *via* the guanylyl-cyclase-coupled receptors NPR-A and NPR-B. Previous works communicated the inhibitory action of ANP on NF-κB in LPS-stimulated macrophages and reperfused rat livers (Kiemer and Vollmar 1998; Kiemer et al., 2000b). Tsukagoshi and coworkers were also able to show a decreased NF-κB DNA-binding activity by ANP in IFN-γ-stimulated macrophages (Tsukagoshi et al. 2001). Our observations are additionally supported by reports of other research groups that demonstrated an attenuated activation of NF-κB by cGMP (Collard et al. 1999; Ghiso et al. 1999).

#### 4.1.1.4 ANP induces expression of IκB-α and -ε

The activation of NF-κB is known to be regulated by its cytoplasmic inhibitor IκB (Ghosh et al. 1998). In unstimulated cells, inhibitory protein IκB binds NF-κB and masks its nuclear localization signal, thus retaining it in the cytoplasm (Ghosh et al. 1998). IκB is a member of a large family of inhibitory molecules that have been identified in the last years existing as IκB-α, -β, -ε, and -γ isoforms. To date the best characterized IκB is IκB-α, because it was the first identified inhibitor of NF-κB (Ghosh et al. 1998).

As mentioned above, other works demonstrate the inhibitory action of ANP on NF-κB in other cell systems. However, the mechanisms involved in this inhibitory action of ANP have been completely unknown (Kiemer and Vollmar 1998; Kiemer et al. 2000b; Kiemer and Vollmar 2001b; Tsukagoshi et al. 2001). The data presented here provide substantial information about the underlying mechanisms involving the induction of the IκB isoforms for the first time. This induction of IκB is demonstrated to be mediated most likely *via* a transcriptional regulation, as shown by RT-PCR and the use of the transcription inhibitor, actinomycin D. These data are supported by the fact that other endogenous substances, such as glucocorticoids (Costas et al. 2000), IL-17 (Kehlen et al. 1999), and TGF-β1 (Azuma et al. 1999), were also described to attenuate NF-κB activation *via* this pathway. Interestingly, ANP specifically induces expression of IκB-α and -ε without increasing IκB-β expression. However, the specific regulation of IκB isoforms and the individual relevance is not well-understood and current reports are rather rare. Bourke et al. for instance reported IκB-β as the crucial inhibitor of NF-κB translocation in glial cells (Bourke et al. 2000). This observation is supported by Ghosh and coworkers who describe IκB-β but not IκB-α

as the classical cytoplasmic inhibitor of NF-κB in mouse endothelial fibroblast cells. Additionally, one work suggests that IκB-ε might be specifically involved in the expression of ICAM-1 (Spiecker et al. 2000). These facts may reflect the complexity of the regulatory pathway of NF-κB activity by the different IκB isoforms. Moreover, species and cell-type seem to play a pivotal role in the regulation of different IκB isoforms.

#### 4.1.1.5 ANP induces basal NF-κB activation

Due to the observation that ANP is able to induce IκB isoforms the question came up how this transcriptional induction of IκB is regulated. In the present work it could be demonstrated that ANP significantly increased basal NF-κB activation. Due to the fact that the transcription of IκB is known to be mainly regulated by NF-κB (Read et al. 1994), this basal activation of NF-κB is suggested to represent a crucial step in inhibition of later TNF-α-induced NF-κB activation. This supposition is confirmed by other groups. For example, De Martin and coworkers showed that the upregulation of IκB-α, as the inhibitor protein of NF-κB, is kind of an autoregulatory loop of NF-κB activity by an autocrine fashion (De Martin et al. 2000). The activation of NF-κB by ANP has very recently been shown in a model of cardiac ischemia (Izumi et al. 2001) and therefore supports our observation. In addition to the well-known pathway of IκB regulation by NF-κB it has recently been shown that induction of IκB occurs as a response to heat shock, suggesting IκB as a heat shock protein (DeMeester et al. 1997). In this context it is interesting to note that ANP treatment has been shown to exert a heat shock response-like state in livers (Kiemer et al. 2002a). However, the roles of specific IκB isoforms in regulating NF-κB activity, and being regulated by NF-κB in endothelial cells are not yet defined.

### 4.1.2 Influence of ANP on AP-1

Activator protein-1 (AP-1) is an important transcription factor known to play a key role in cellular proliferation, differentiation, and in inflammatory processes (Rahman and MacNee 1998). In order to characterize the specificity of the observed inhibitory potential of ANP on TNF-α-induced NF-κB DNA-binding activity, effects of ANP on AP-1 were investigated in the present work.

#### 4.1.2.1 ANP had no effect on TNF-α-induced AP-1 DNA-binding activity

The results showed that ANP had no effect on the TNF-α-induced AP-1 DNA binding activity. In contrast to this result ANP has previously been shown to possess an inhibitory potential on AP-1 DNA-binding activity. This was demonstrated for LPS-activated murine macrophages (Kiemer et al. 2000a) and reperfused rat livers (Kiemer et al. 2000b). These different observations may reflect cell-type, -species, and stimuli-dependent differences in the action of ANP.
These data show that ANP is not an overall inhibitor of TNF-α-induced signaling pathways in endothelial cells but suggests a certain specificity of the inhibitory action of ANP on the NF-κB DNA-binding activity.

#### 4.1.2.2 ANP-induced DNA-binding activity of AP-1

Interestingly, the results of the present work concerning the effects of ANP on basal AP-1 DNA-binding activity indicate that ANP is able to increase the basal activity of AP-1. These first observations were confirmed by the use of an inhibitor of AP-1 transcription, U0126, which was able to completely attenuate the ANP induced AP-1 DNA-binding activity. These data are supported by reports that cGMP induces AP-1-related transcriptions (Pilz et al. 1995). AP-1 is described as the main transcription factor involved in the induction of the cytoprotective HSP32/HO-1 (Immenschuh et al. 1998). Since AP-1 plays a key role in proliferation, differentiation, and transcription of cytoprotective genes, e.g. HO-1, the observed effects may have an impact on cytoprotective properties exerted by ANP (Kiemer et al. 2002a). The role of ANP mediated AP-1 activation in endothelial cells will be further characterized by Nicole Bildners doctoral thesis.

# 4.2 Cytoskeleton

## 4.2.1 ANP reduces TNF-α-induced stress fiber formation and endothelial permeability *via* induction of MKP-1

The TNF-α-induced increase in vascular permeability is commonly attributed to the reorganization of F-actin filaments into stress fibers followed by contraction of cells and formation of intercellular gaps (Brett et al. 1989; Lum and Malik 1996; van Hinsbergh 1997; Wojciak-Stothard et al. 1998). The underlying molecular mechanisms of a potential protective action of ANP on the detrimental action of TNF-α on the endothelial cytoskeleton are not completely understood. In this context the second section of the present work aimed to clarify the effects of ANP on TNF-α-mediated pathophysiological cytoskeleton changes. Potentially involved signal transduction mediators (e.g. p38 MAPK, HSP27, MKK 3/6, and MAPK-phosphatase-1) were investigated in order to clarify the molecular mechanism of the observed effects.

### 4.2.1.1 ANP reduces TNF-α-induced changes in endothelial morphology, cytoskeleton, and function

The present work provides evidence that the cardiovascular hormone ANP can abrogate TNF-α-induced changes in endothelial morphology and macromolecule permeability. These inhibitory properties of ANP were shown to be mediated *via* cGMP. The observed effects of ANP are supported by a paper showing a protective effect of ANP against lysophosphatidylcholine-induced endothelial dysfunction (Murohara et al. 1999). Moreover, a cGMP-dependent inhibition of thrombin induced increase in permeability has been described in bovine aortic endothelial cells (Lofton et al. 1990). Furthermore, there exist *in vivo* data which suggest that cGMP can have both positive and negative effects on endothelial permeability (van Hinsbergh 1997). For instance one work demonstrates that cGMP-elevating agents cause a decrease of vascular leakage after oxidative damage in bovine aortic endothelial cells and perfused rabbit lungs in the lung circulation (Lofton et al. 1991), whereas in the peripheral circulation cGMP-elevating agents worsen the vascular leakage (Zimmerman et al. 1990; Lofton et al. 1991). These different observations may demonstrate cell-type-, species-, and stimuli-dependent differences in the action of ANP, respectively cGMP, on cytoskeleton and permeability changes. Since TNF-α plays a pivotal role in formation of atheromatous plaques, the ability of ANP to abrogate TNF-α-induced

increase in permeability is of special interest suggesting an antiatherogenic action for this cardiovascular hormone. The following sections elucidate the mechanisms underlying this protective action of ANP on TNF-α-exposed endothelium.

### 4.2.1.2 ANP inhibits TNF-α-induced actin polymerization *via* cGMP

The fact that ANP is able to abolish TNF-α-induced morphological changes and increased macromolecule permeability combined with the knowledge that increased permeability is closely associated with increased formation of F-actin (Brett et al. 1989; Lum and Malik 1996; van Hinsbergh 1997; Wojciak-Stothard et al. 1998) and the development of stress fibers (Brett et al. 1989; van Hinsbergh 1997; Wojciak-Stothard et al. 1998) leads to investigations that focus on effects of ANP on actin polymerization and the subsequent development of F-actin stress fibers.
The results showed no effect of ANP on basal F-actin content in endothelial cells whereas TNF-α-induced formation of F-actin was dose-dependently reduced by ANP. The effects of ANP on F-actin content could be confirmed by microscopic investigations using a specific F-actin staining dye (rhodamin phalloidin). It was indeed possible to show a reduced formation of F-actin stress fibers upon pretreatment with ANP. In order to clarify the receptor specificity of the observed inhibitory action of ANP on TNF-α-induced F-actin content and stress fiber formation, NPR-A second messenger analogue 8-Br-cGMP was tested for its effect on these parameters. The results clearly indicate the involvement of cGMP in the effects exerted by ANP, since 8-Br-cGMP at least partially mimicked the effects. So far little information exists on actions of ANP on F-actin content and stress fiber formation. Only a single paper by Sharma and coworkers demonstrated that incubation of glomerular epithelial cells with ANP resulted in an apparent disassembly of stress fibers mediated *via* cGMP (Sharma et al. 1992).
These results of reduced TNF-α-induced F-actin polymerization by ANP seemed to be part of a potential mechanism by which ANP can regulate TNF-α-induced changes in endothelial cell morphology and macromolecule permeability. The following studies aimed to clarify the signal transduction pathway underlying the observed effects.

### 4.2.1.3 ANP inhibits p38 MAPK activation *via* induction of MKP-1

In the present work it is reported for the first time that ANP inhibits TNF-α-induced phosphorylation of the actin capping protein HSP27. This inhibition of the HSP27 phosphorylation by ANP is suggested as the crucial step in the signal transduction

mechanism underlying the inhibitory property of ANP on TNF-α-induced endothelial cell cytoskeleton changes. HSP27 has been closely associated with the regulation of actin polymerization (Landry and Huot 1995; Razandi et al. 2000) which represents a key step in the formation of stress fibers (Wojciak-Stothard et al. 1998). The function of HSP27 in regulating the actin cytoskeleton has indeed been shown to be dependent on the phosphorylation state of this protein (Lavoie et al. 1993).

Diverse physiological stimuli, such as cytokines have been shown to dramatically increase the phosphorylation of HSP27 (Gaestel et al. 1991). The phosphorylation of HSP27 is known to be catalyzed by a member of the family of mitogen activated protein kinases (MAPK), the p38 MAPK (Kyriakis and Avruch 1996). The present work shows an inhibition of TNF-α-induced activation of p38 MAPK by ANP, suggested to be the mechanism responsible for the inhibited phosphorylation of HSP27 by ANP. The observation of a decreased activation of p38 MAPK by ANP has been described in the literature before: the inhibitory action of ANP on TNF-α production was demonstrated to be mediated *via* an attenuation of LPS-induced activation of p38 MAPK in macrophages (Tsukagoshi et al. 2001). Moreover, ANP was shown to reduce VEGF-induced activation of p38 MAPK in bovine aortic endothelial cells (Pedram et al. 2001). These papers support our observation of ANP as an inhibitor of p38 MAPK. However, no information exists on the ANP-induced signaling leading to suppressed p38 activity.

In order to clarify the mechanism which is responsible for suppressed p38 phosphorylation two possible targets for ANP were investigated. On the one hand p38 MAPK is known to be regulated by its upstream kinase MKK3/6 (Herlaar and Brown 1999). On the other hand dual-specific MAPK phosphatases (MKP) are known to dephosphorylate and therefore deactivate MAPK. From the known MKP, MKP-1 (CL100) has been shown to be specifically responsible for the dephosphorylation of p38 (Chen et al. 2001), which could neither be shown for MKP-2 (Chu et al. 1996) nor MKP-3 (Nichols et al. 2000).

Interestingly, the results of the present work indicate that ANP does not affect the activation of MKK3/6 upstream of p38 MAPK, but induces MKP-1 *via* an elevation of MKP-1 mRNA. MKP-1 mRNA was induced by ANP after only 20 min and moreover the protein levels were elevated after only 30 min. These observations of MKP-1 as an immediate early gene product were supported by others, since ANP has been described to induce MKP-1 mRNA after 30 min in mesangial cells (Sugimoto et al. 1996) and MKP-1 protein after only 30 min in renal tubular cells (Hannken et al. 2001) as well. Furthermore, other stimuli than ANP were reported to induce MKP-1 mRNA in less than 30 min. For instance Metzler and coworkers showed an increased MKP-1 expression after only 20 min treatment with arachidonic acid in VSMC (Metzler et al.

1998). The fact that the human MKP-1 gene (CL100) contains one AP-1 binding site (Kwak et al. 1994) and the discussed data concerning AP-1 activation by ANP led to the hypothesis that ANP may induce MKP-1 *via* activation of this AP-1 site. Although ANP has been reported before to induce MKP-1 in other cell systems, it was not clarified whether induction of MKP-1 by ANP is causally linked to the observed inhibition of p38 MAPK as suggested by our experiments. To investigate this causal link seemed essential since there exist data that indicate that an increased MKP-1 expression does not inevitably contribute to the deactivation of MAPK (Wu et al. 1994; Jeon et al. 1998). Therefore we performed MKP-1 antisense experiments to clarify the causal role of MKP-1 induction in ANP-mediated p38 MAPK inhibition. MKP-1 antisense but not sense oligonucleotides abrogated the inhibitory effect of ANP on p38 MAPK activation. This fact demonstrates for the first time that the rapid transcriptional up-regulation of MKP-1 by ANP is necessary for early inhibition of TNF-α-induced p38 activation in human endothelial cells.

#### 4.2.1.4 Causal relationship between the MAPK pathway, F-actin polymerization, and macromolecule permeability

After characterization of the signaling pathway leading to attenuated p38 MAPK activation, however, the inhibitory action of ANP on the TNF-α-induced p38 MAPK activation was not causally linked to the observed effects of ANP on F-actin polymerization and macromolecule permeability. In order to elucidate the potential involvement of the p38 MAPK signaling pathway in ANP-mediated effects on cytoskeleton and permeability changes, the p38 MAPK inhibitor, SB203580, was tested for its effects on TNF-α-induced F-actin polymerization and increased macromolecule permeability. As shown by the results SB203580 abrogates both F-actin polymerization as well as TNF-α-induced elevation of macromolecule permeability. These facts suggest a direct involvement of p38 MAPK in both signaling pathways and causally connect TNF-α-induced alterations in HUVEC with the p38 MAPK signaling cascade. Moreover and importantly, it is shown here that ANP counteracts the TNF-α-induced formation of stress fibers and increased permeability by inhibiting p38 MAPK signaling.

## 4.3 Monocyte chemoattractant protein MCP-1

MCP-1 has been shown to play a key role in inflammation. In this context it has been demonstrated to be critically involved in the pathogenesis of atherosclerosis (Reape and Groot 1999) and it is highly recognized to be expressed in human atherosclerotic lesions (Nelken et al. 1991; Yla-Herttuala et al. 1991).
In the present study it is demonstrate that the cardiovascular hormone ANP is able to suppress the TNF-α-induced expression of MCP-1 *via* induction of MKP-1 in endothelial cells. Thus, this inhibitory action of ANP on MCP-1 secretion in human endothelial cells might contribute to an antiinflammatory and especially antiatherogenic potential of this cardiovascular hormone.

### 4.3.1 cGMP-mediated inhibition of TNF-α-induced MCP-1 release

The results presented here indicate that the inhibitory action of ANP on TNF-α-induced MCP-1 expression is mediated *via* cGMP. 8-Br-cGMP mimicked the effect of ANP on MCP-1 release and CNP, the ligand for the other guanylyl-cyclase-coupled receptor, NPR-B, also shows inhibitory action on MCP-1 secretion. Furthermore the specific NPR-C agonist cANF did not affect TNF-α-induced MCP-1 secretion confirming the role for a guanylyl-cyclase-dependent pathway. To our knowledge the regulatory action of cGMP on TNF-α-induced MCP-1 release has yet been comletely unknown. Therefore our data are the first to report the inhibitory action of cGMP on TNF-α-induced MCP-1.
More information exists on the regulatory mechanisms of MCP-1 expression in endothelial cells induced by stimuli other than TNF-α. For instance Chien and coworkers reported that cGMP plays no role in the regulation of mechanical strain stress-induced MCP-1 expression in HUVEC (Wang et al. 1995). Another report by Okada et al. showed no influence of cGMP on cyclic stretch-induced upregulation of MCP-1 in HUVEC (Okada et al. 1998). These contradictory data may reflect especially stimulus- dependent differences in MCP-1 regulation.

## 4.3.2 Modulation of TNF-α-induced MCP-1 release by NO

The observation that the ANP-mediated inhibition of TNF-α-induced MCP-1 secretion is most likely regulated via guanylyl-cyclase-dependent pathways led us to focus on an important activator of cGMP release, NO. NO activates the soluble guanylyl-cyclase and thereby increases intracellular cGMP. Therefore, we were interested in the effect of NO-modulating substances on TNF-α-induced MCP-1 secretion. The data presented here show indeed an attenuated TNF-α-induced MCP-1 release in HUVEC pre-treated with the NO-donor GSNO. This result confirms our hypothesis of a signal transduction pathway involving cGMP as second messenger mediating an inhibitory action on MCP-1 induction. To our knowledge so far nothing is known about an inhibitory property of NO on TNF-α-induced MCP-1 expression in HUVEC. Therefore the data presented here show for the first time that NO is able to inhibit TNF-α-induced MCP-1 expression.

## 4.3.3 Regulation of basal MCP-1 production

Interstingly, NO has been recognized to regulate basal MCP-1 expression in HUVEC. Zeiher et al. report a NO-dependent decrease in basal MCP-1 expression (Zeiher et al. 1995). However, in our experimental settings the NO-Donor GSNO did not affect basal MCP-1 release. This discrepance of our data to the literature may be due to the use of different NO-donors and stimulation times.
8-Bromo-cGMP did not affect basal MCP-1 expression in our experiments excluding a role for cGMP in basal regulation of MCP-1. These observations are supported by the group of Zeiher who demonstrated that elevation of endothelial cGMP levels have no effect on basal MCP-1 expression (Zeiher et al. 1995).
Interstingly, ANP and the specific NPR-C agonist cANF increased basal MCP-1 secretion. The activation of NPR-C by ANP was shown to result in an inhibition of adenylyl-cyclase and decreased cAMP levels in endothelial cells (Hu et al. 1992). Therefore our data strongly suggest a role for NPR-C and cAMP in the signal transduction pathway of basal MCP-1 expression. Contradictory to these results some groups describe an increased MCP-1 expression as result of increased cAMP levels. For example leptin was shown to clearly activate MCP-1 secretion via activation of the cAMP-dependend PKA in bovine aortic endothelial cells (Yamagishi et al. 2001). This work is supported by two other works demonstrating that an increased level of intracellular cAMP induces MCP-1 expression in human endothelial cells (Shyy et al.

1993; Zeiher et al. 1995). These different data may reflect stimulus- and cell-type-dependent differences in basal MCP-1 release.
Nevertheless a regulatory role for NPR-C and cAMP in the secretion of basal MCP-1 in endothelial cells has yet not been described.
Since endothelial cells themselves represent a source of NO production (Preli et al. 2002) we aimed to exclude a potential role for TNF-α-induced endogenous NO production in our cell system. Since the NOS inhibitor L-NNA did not affect TNF-α-induced MCP-1 release, endogenous NO production appeares not to be involved in regulating MCP-1 induction.

### 4.3.4 Molecular mechanism of reduced TNF-α-induced MCP-1 expression by ANP

The inhibitory action of ANP on MCP-1 release is regulated most likely on a transcriptional level due to the observed decrease in TNF-α-induced MCP-1 mRNA levels. The transcriptional regulation of MCP-1 expression has been increasingly recognized to be mediated via the p38 MAPK pathway (Goebeler et al. 2001; Marin et al. 2001). For instance Goebeler and coworkers recently reported the involvement of p38 MAPK in TNF-α-induced MCP-1 expression in endothelial cells(Goebeler et al. 1999). The group of Nakamura showed an inhibitory action of circulating thioredoxin on LPS-induced MCP-1 expression via suppressed p38 phosphorylation (Nakamura et al. 2001).
As it is demonstrated in the present work, ANP inhibits TNF-α-induced p38 MAPK activation in HUVEC. We show that this inhibitory action of ANP was mediated via an early transcriptional induction of MKP-1 by ANP (Kiemer et al. 2 A.D.). Considering these facts we were interested in the causal relationship between MKP-1 induction by ANP and the observed inhibition of MCP-1 release. The data presented here show indeed a causal role for MKP-1 induction in ANP-mediated MCP-1 inhibition since MKP-1 antisense but not sense oligonucleotides abrogated the inhibitory effect of ANP on TNF-α-induced MCP-1 expression. These results causally connect ANP-mediated inhibition of TNF-α-induced MCP-1 expression to the p38 MAPK pathway.

# 5 SUMMARY

# 5.1 Summary

The present work deals with the inhibitory action of ANP on TNF-α-induced expression of adhesion molecules (ICAM-1, VCAM-1, E-selectin), chemokines (MCP-1), and cytoskeleton changes in human endothelial cells.

## 5.1.1 Effect of ANP on TNF-α-induced CAM expression

The following diagram shows a schematic outdraw of the summerized results of the first part of the present work.

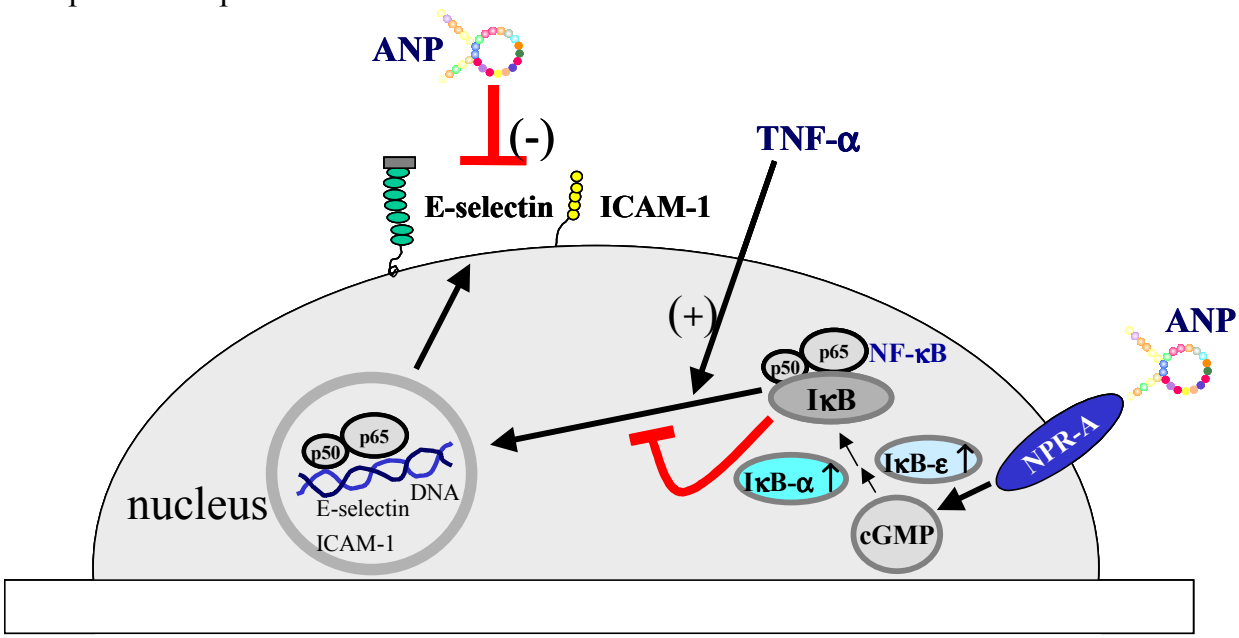


***figure 1 summary:*** *schematic diagram of the signal transduction pathways clarified by the first section of the present work*

It has been shown before that TNF-α increases the expression of cell adhesion molecules E-selectin and ICAM-1 *via* activation of the transcription factor NF-κB.
We could show that ANP is able to inhibit the activation of NF-κB *via* binding its guanylyl-cyclase-coupled NPR-A and -B receptor. We could further elucidate the molecular mechanism leading to the inhibition of NF-κB activation by ANP. ANP was shown to transcriptionally activate the expression of IκB isoforms. In consequence of the ANP mediated inhibition of NF-κB DNA-binding activity we could demonstrate an attenuated surface expression of E-selectin and ICAM-1.

### 5.1.2 Effect of ANP on TNF-α-induced cytoskeleton and permeability changes

The following figure shows an outdraw of the summerized results of the second part of the present work.

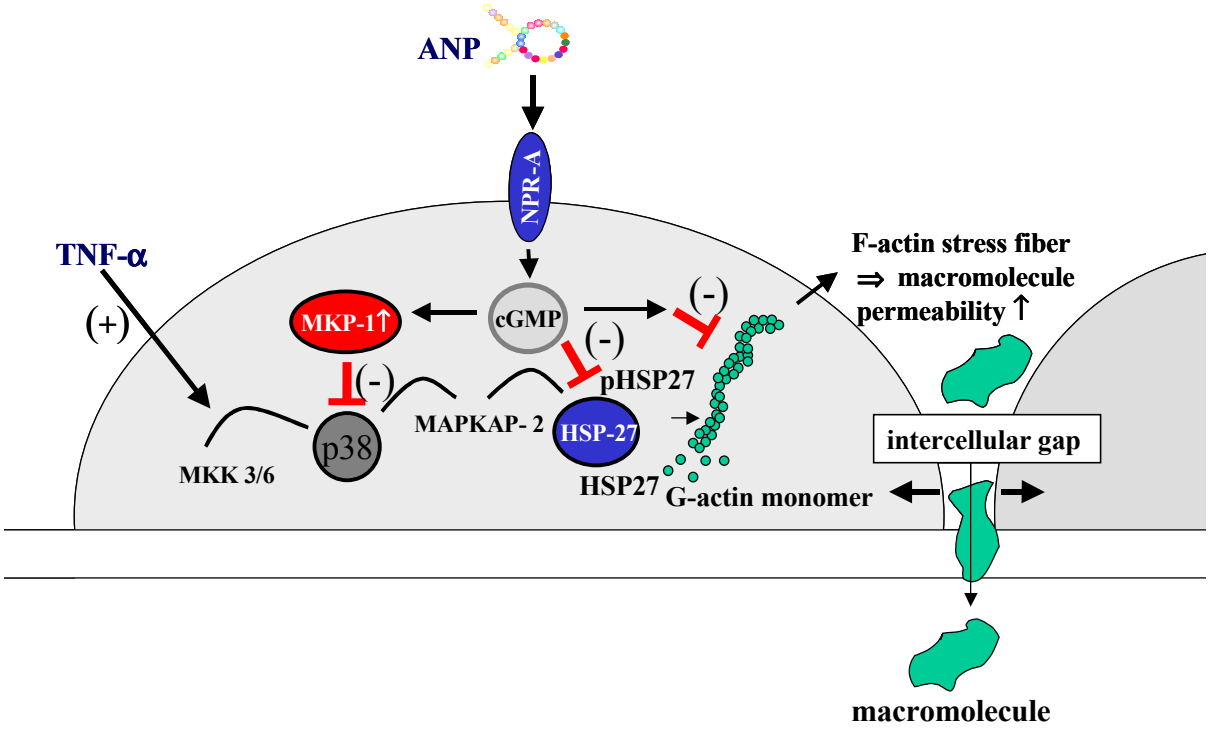


***figure 2 summary:*** *schematic diagram of the signal transduction pathways clarified by the second section of the present work*

TNF-α has been shown to induce changes in cytoskeleton and macromolecule permeability of endothelial cells.

We have shown here for the first time that ANP is able to abrogate both TNF-α-induced effects *via* its guanylyl-cyclase-coupled NPR-A receptor. Moreover, ANP was shown to reduce TNF-α-induced F-actin polymerization and stress fiber formation *via* the inhibition of p38 MAPK and its downstream target HSP27. Furthermore we could report here for the first time a decrease in TNF-α-induced macromolecule permeability by ANP. The deactivation of p38 MAPK was demonstrated to be mediated *via* a significant transcriptional induction of the MKP-1 by ANP.

### 5.1.3 Effect of ANP on TNF-α-induced MCP-1 expression

The results of the third part of the present work are summerized in figure 3.

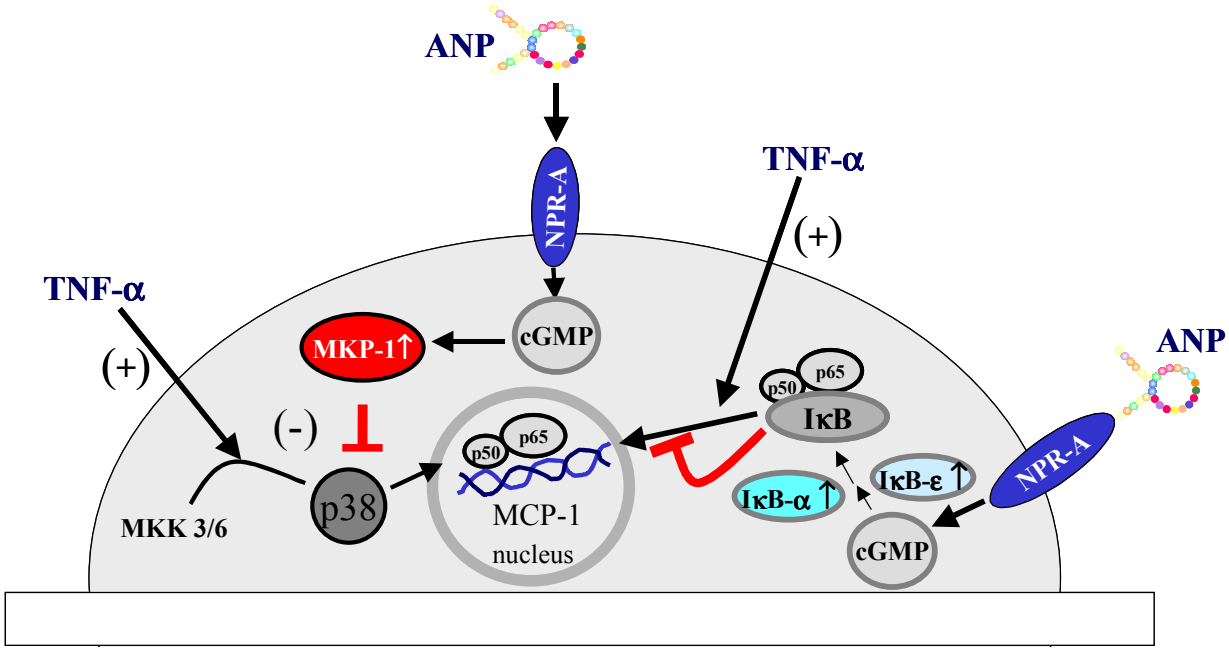


***figure 3 summary**: schematic diagram of the signal transduction pathways clarified by the first and third section of the present work*

It is known that TNF-α induces the release of MCP-1 during inflammatory processes *via* influencing the transcription factor NF-κB and the p38 MAPK pathway.
We could report here for the first time a decreased TNF-α-induced MCP-1 expression by treatment of endothelial cells with ANP. The observed ANP effect was shown to be mediated *via* the particulate guanylyl-cyclase-coupled NPR. Furthermore we show that trancriptional induction of MKP-1 by ANP is essential for inhibition of TNF-α-induced MCP-1 expression by ANP.

In summary the data presented here provides evidence that ANP is able to preserve the structure and function of endothelial cells. These observations are of special importance because there is clear evidence that endothelial cell dysfunction is the cause for many acute and chronic vascular diseases (Biegelsen and Loscalzo 1999). The potency of an endogenous compound, i.e. ANP, to protect against such endothelial dysfunction points to an antiinflammatory and antiatherogenic potential of this cardiovascular hormone.

This work has been supported by the DFG (Vo376/8-1).

# 6 APPENDIX

# 6.1 Abbreviations

| | |
|---|---|
| A | Ampere |
| AB | Antibody |
| ANP | Atrial natriuretic peptid |
| AP-1/2 | Activator protein 1/2 |
| APS | Ammonium persulfate |
| ATP | Adenosine-5`-triphosphate |
| BNP | Brain natriuretic peptid |
| bp | Basepair |
| Bq | Bequerel |
| BSA | Bovine serum albumine |
| CAM | Cell Adhesion Molecule |
| cAMP | cyclic Adenosine-5`-monophosphate |
| cDNA | complementary DNA |
| cGMP | Cyclic Guanosin-5´-monophosphate |
| cpm | Counts per minute |
| cRNA | complementary RNA |
| Ci | Curie (1 Ci=3.7x$10^{10}$ Bequerel) |
| CNP | C-type natriuretic peptide |
| Co | Control |
| Da | Dalton |
| dATP | 2`-Desoxyadenosine-5`-triphosphate |
| dCTP | 2`-Desoxycytosine-5`-triphosphate |
| dGTP | 2`-Desoxyguanosine-5`-triphosphate |
| DMSO | Dimethylsulfoxide |
| DNA | Desoxyribonucleic acid |
| dNTP | Desoxynucleosidtriphosphate |
| DTT | Dithioerythriol |
| ECL | Enhanced Chemoluminescence reagent |
| EDTA | Ethylene diamine-N,N,N´,N´ tetra acid |
| EGTA | Bis(aminoehyl)glycolether-N,N,N´,N´-tetra acid |
| EMSA | Electrophoretic mobility shift assay |
| EtBr | Ethidium bromide |
| EtOH | Ethanol |
| FITC | Fluoresceinisothiocyanate |
| FCS | Fetal calf serum |

| | |
|---|---|
| GTP | Guanosin-5`-triphosphate |
| h | Hour |
| HUVEC | Human Umbilical Vein Endothelial Cells |
| ICAM | Intracellular Cell Adhesion Molecule |
| IκB (α-ε) | Inhibitory protein (α-ε) |
| kDa | kilo Dalton |
| L | Liter |
| m | Milli ($10^{-3}$) |
| M | Molar |
| MeOH | Methanol |
| µ | Micro ($10^{-6}$) |
| min | Minute |
| MCP-1 | Monocyte chemoattractant protein |
| mRNA | messenger Ribonucleinic acid |
| % (m/v) | mass per volume per cent |
| n | nano ($10^{-9}$) |
| NF-κB | Nuclear Factor κB |
| NP | Natriuretic Peptides |
| NPR | Natriuretic Peptide Receptor |
| NTP | ATP, CTP, GTP, or TTP |
| OD | Optical Density |
| PAA | Polyacrylamide |
| PAGE | Polyacrylamide-gel electrophoresis |
| PBS | Phosphate buffered saline solution |
| PCR | Polymerase chain reaction |
| PMSF | Phenylmethylsulfonylfluoride |
| Poly[dIdC] | Polydesoxyinosine-desoxycytosine |
| RNA | Ribonucleinic acid |
| RNase | Ribonuclease |
| rpm | Rotations per minute |
| RT | Room temperature |
| sec | Second |
| SEM | Standard error of the mean value |
| SDS | Sodium dodecyl sulfate |
| SMC | Smooth muscle cells |
| STE | Sodium chloride, Tris, EDTA buffer |
| TAE | Tris, acetate, EDTA buffer |
| TBE | Tris, borate, EDTA buffer with Triton X-100 |

| | |
|---|---|
| TBS-T | Phosphate buffered saline solution with Tween |
| TE | Tris-EDTA buffer |
| TEMED | N,N,N´,N´-tetramethylethylendiamine |
| TNF-α | Tumor necrosis factor alpha |
| tot RNA | total RNA |
| Tris | Tris-hydroxymethyl-aminomethan |
| U | Unit |
| UTP | Uridine-5`-triphosphate |
| V | Volt |
| VCAM | Vascular Cell Adhesion Molecule |
| % (v/v) | Volume per volume |
| W | Watt |

## 6.2 Alphabetical order of companies

| | |
|---|---|
| Alexis Biochemicals | (Grünberg, Germany) |
| Amersham | (Braunschweig, Germany) |
| Beckmann Instruments | (Munich, Germany) |
| Becton Dickinson | (San Jose, CY, USA) |
| Biochrom | (Berlin, Germany) |
| Biometra | (Göttingen, Germany) |
| BioRad Laboratories | (Munich, Germany) |
| Biosource | (Nivelles, Belgium) |
| Bio Whittaker Bioproducts | (Heidelberg, Germany) |
| Biozym Diagnostics | (Oldendorf, Germany) |
| Calbiochem | (Schwalbach, Germany) |
| Carl Roth | (Karlsruhe, Germany) |
| Cell Signaling | (Frankfurt/M, Germany) |
| Dianova | (Hamburg, Germany) |
| Eppendorf | (Maintal, Germany) |
| Gibco/BRL | (Eggenstein, Germany) |
| Gilson | (Villiers-Le Bel, France) |
| Greiner | (Nürtingen, Germany) |
| ICN Biomedicals | (Eschwege, Germany) |
| Jackson Immunolab | (Hamburg, Germany) |
| Merck-Eurolab | (Munich, Germany) |
| Millipore | (Eschborn, Germany) |

| | |
|---|---|
| Molecular probes | (Göttingen, Germay) |
| MWG-biotech | (Ebersberg, Germany) |
| NEN | (Cologne, Germany) |
| NUNC | (Wiesbaden, Germany |
| PAN | (Aidenbach, Germany) |
| Peske | (Aindling-Pichl, Germany) |
| Pharmacia Biotec | (Heidelberg, Germany) |
| Promocell | (Heidelberg, Germany) |
| Qiagen | (Hilden, Germany) |
| Roche | (Mannheim, Germany) |
| Santa Cruz | (Heidelberg, Germany) |
| Saxon Biochemicals | (Hannover, Germany) |
| Shimadzu | (Duisburg, Germany) |
| Schleicher & Schüll | (Dassel, Germany) |
| Serotec LTD | (Wiesbaden, Germany) |
| Sigma | (Taufkirchen, Germany) |
| Stratagene | (Heidelberg, Germany) |
| Stressgen | (San Diego, USA) |

# 6.3 Publications

**Parts of this work are published or are in preparation for publication**:

Poster:

Nina C. Weber, Nicole Bildner, Angelika M. Vollmar, Alexandra K. Kiemer, **2002,** ANP inhibits TNF-α-induced expression of adhesion molecules in endothelial cells *via* induction of IκB. Poster presentation at the 43. Tagung der Deutschen Gesellschaft für klinische Pharmakologie und Toxikologie in Mainz.

Alexandra K. Kiemer, Nina C. Weber, Nicole Bildner, Angelika M. Vollmar, **1999,** ANP verhindert TNF-α-induzierte Veränderungen von Morphologie und Zytoskelett in Endothelzellen. Poster presentation at the 7. Tagung für Zell und Gewebeschädigung in Weinheim.

Lecture:

Nina C. Weber, Alexandra K. Kiemer, Robert Fürst, Angelika M. Vollmar, **2001,** The atrial natriuretic peptide reduces TNF-α-induced actin polymerization and permeability in endothelial cells. Lecture at the 8. Tagung für Zell und Gewebeschädigung in Halle.

Original publications:

Nina C. Weber, Angelika M. Vollmar, Thomas Hartung, Alexandra K. Kiemer, **2002.** The atrial natriuretic peptide inhibits TNF-α-induced expression of MCP-1 *via* induction of MKP-1. *Arteriosc.Throm.Vasc. Biol. Submitted for publication*.

Alexandra K. Kiemer, Nina C. Weber, Robert Fürst, Nicole Bildner, Stefanie Kulhanek-Heinze , Angelika M. Vollmar, **2002.** Inhibition of p38 MAPK activation *via* induction of MKP-1: Atrial Natriuretic Peptide reduces TNF-α-induced actin polymerization and endothelial permeability. *Circulation Research, May 2002.*

Alexandra K. Kiemer, Nina C. Weber, Angelika M. Vollmar, **2002.** Induction of IκB: Atrial Natriuretic Peptide inhibits endothelial expression of adhesion molecules. *Mol. Pharmacol. Submitted for publication.*

Alexandra K. Kiemer, Nicole Bildner, Nina C. Weber, Angelika M. Vollmar, **2002.** Induction of heme oxygenase-1 (HO-1) by the Atrial Natriuretic Peptide does not confer resistance against TNF-α-induced apoptosis in endothelial cells. *In preparation*.

# 7 REFERENCES

# 7.1 References


1. **Ahmad, M., Theofanidis, P., and Medford, R. M.** (1998). Role of activating protein-1 in the regulation of the vascular cell adhesion molecule-1 gene expression by tumor necrosis factor-alpha. *J Biol.Chem.* **273**, 4616-4621.

2. **Albelda, S. M., Muller, W. A., Buck, C. A., and Newman, P. J.** (1991). Molecular and cellular properties of PECAM-1 (endoCAM/CD31): a novel vascular cell-cell adhesion molecule. *J.Cell Biol.* **114**, 1059-1068.

3. **Alessi, D. R., Smythe, C., and Keyse, S. M.** (1993). The human CL100 gene encodes a Tyr/Thr-protein phosphatase which potently and specifically inactivates MAP kinase and suppresses its activation by oncogenic ras in Xenopus oocyte extracts. *Oncogene* **8**, 2015-2020.

4. **Alexander, B. T., Cockrell, K. L., Massey, M. B., Bennett, W. A., and Granger, J. P.** (2002). Tumor necrosis factor-alpha-induced hypertension in pregnant rats results in decreased renal neuronal nitric oxide synthase expression. *Am.J Hypertens.* **15**, 170-175.

5. **Aplin, A. E., Howe, A., Alahari, S. K., and Juliano, R. L.** (1998). Signal transduction and signal modulation by cell adhesion receptors: the role of integrins, cadherins, immunoglobulin-cell adhesion molecules, and selectins. *Pharmacol.Rev* **50**, 197-263.

6. **Azuma, M., Motegi, K., Aota, K., Yamashita, T., Yoshida, H., and Sato, M.** (1999). TGF-beta1 inhibits NF-kappaB activity through induction of IkappaB-alpha expression in human salivary gland cells: a possible mechanism of growth suppression by TGF-beta1. *Exp.Cell Res.* **250**, 213-222.

7. **Baggiolini, M.** (1998). Chemokines and leukocyte traffic. *Nature* **392**, 565-568.

8. **Baggiolini, M., Walz, A., and Kunkel, S. L.** (1989). Neutrophil-activating peptide-1/interleukin 8, a novel cytokine that activates neutrophils. *J.Clin.Invest* **84**, 1045-1049.

9. **Bazan, J. F., Bacon, K. B., Hardiman, G., Wang, W., Soo, K., Rossi, D., Greaves, D. R., Zlotnik, A., and Schall, T. J.** (1997). A new class of membrane-bound chemokine with a CX3C motif. *Nature* **385**, 640-644.

10. **Benjamin, I. J. and McMillan, D. R.** (1998). Stress (heat shock) proteins: molecular chaperones in cardiovascular biology and disease. *Circ.Res.* **83**, 117-132.

11. **Benndorf, R., Hayess, K., Ryazantsev, S., Wieske, M., Behlke, J., and Lutsch, G.** (1994). Phosphorylation and supramolecular organization of murine small heat shock protein HSP25 abolish its actin polymerization-inhibiting activity. *J.Biol.Chem.* **269**, 20780-20784.

12. **Berlin, C., Bargatze, R. F., Campbell, J. J., von Andrian, U. H., Szabo, M. C., Hasslen, S. R., Nelson, R. D., Berg, E. L., Erlandsen, S. L., and Butcher, E. C.** (1995). alpha 4 integrins mediate lymphocyte attachment and rolling under physiologic flow. *Cell* **80**, 413-422.

13. **Bevilacqua, M. P.** (1993). Endothelial-leukocyte adhesion molecules. *Annu.Rev.Immunol.* **11**, 767-804.

14. **Biegelsen, E. S. and Loscalzo, J.** (1999). Endothelial function and atherosclerosis. *Coron.Artery Dis.* **10**, 241-256.

15. **Bourke, E., Kennedy, E. J., and Moynagh, P. N.** (2000). Loss of Ikappa B-beta is associated with prolonged NF-kappa B activity in human glial cells. *J Biol.Chem.* **275**, 39996-40002.

16. **Brett, J., Gerlach, H., Nawroth, P., Steinberg, S., Godman, G., and Stern, D.** (1989). Tumor necrosis factor/cachectin increases permeability of endothelial cell monolayers by a mechanism involving regulatory G proteins. *J Exp.Med.* **169**, 1977-1991.

17. **Cantin, M., Gutkowska, J., Thibault, G., Garcia, R., Anand-Srivastava, M., Hamet, P., Schiffrin, E., and Genest, J.** (1984). The heart as an endocrine gland. *J.Hypertens.Suppl* **2**, S329-S331.

18. **Carpenter, C. L.** (2000). Actin cytoskeleton and cell signaling. *Crit Care Med* **28**, N94-N99.

19. **Chen, P., Hutter, D., Yang, X., Gorospe, M., Davis, R. J., and Liu, Y.** (2001). Discordance between the binding affinity of mitogen-activated protein kinase subfamily members for MKP-2 and their ability to catalytically activate the phosphatase. *J Biol.Chem.*

20. **Chinkers, M. and Garbers, D. L.** (1989). The protein kinase domain of the ANP receptor is required for signaling. *Science* **245**, 1392-1394.

21. **Chinkers, M. and Wilson, E. M.** (1992). Ligand-independent oligomerization of natriuretic peptide receptors. Identification of heteromeric receptors and a dominant negative mutant. *J.Biol.Chem.* **267**, 18589-18597.

22. **Chu, Y., Solski, P. A., Khosravi-Far, R., Der, C. J., and Kelly, K.** (1996). The mitogen-activated protein kinase phosphatases PAC1, MKP-1, and MKP- 2 have unique substrate specificities and reduced activity in vivo toward the ERK2 sevenmaker mutation. *J Biol.Chem.* **271**, 6497-6501.

23. **Cohen, D., Koh, G. Y., Nikonova, L. N., Porter, J. G., and Maack, T.** (1996). Molecular determinants of the clearance function of type C receptors of natriuretic peptides. *J.Biol.Chem.* **271**, 9863-9869.

24. **Collard, C. D., Agah, A., Reenstra, W., Buras, J., and Stahl, G. L.** (1999). Endothelial nuclear factor-kappaB translocation and vascular cell adhesion molecule-1 induction by complement: inhibition with anti-human C5 therapy or cGMP analogues. *Arterioscler.Thromb.Vasc.Biol.* **19**, 2623-2629.

25. **Collins, T., Read, M. A., Neish, A. S., Whitley, M. Z., Thanos, D., and Maniatis, T.** (1995). Transcriptional regulation of endothelial cell adhesion molecules: NF- kappa B and cytokine-inducible enhancers. *FASEB J* **9**, 899-909.

26. **Connolly, J. A., Kalnins, V. I., and Barber, B. H.** (1981). Microtubules and microfilaments during cell spreading and colony formation in PK 15 epithelial cells. *Proc.Natl.Acad.Sci.U.S.A* **78**, 6922-6926.

27. **Costas, M. A., Muller, I. L., Holsboer, F., and Arzt, E.** (2000). Transrepression of NF-kappaB is not required for glucocorticoid- mediated protection of TNF-alpha-induced apoptosis on fibroblasts. *Biochim.Biophys.Acta* **1499**, 122-129.

28. **Dagnino, L., Drouin, J., and Nemer, M.** (1991). Differential expression of natriuretic peptide genes in cardiac and extracardiac tissues. *Mol.Endocrinol.* **5**, 1292-1300.

29. **de Bold, A. J., Borenstein, H. B., Veress, A. T., and Sonnenberg, H.** (1981). A rapid and potent natriuretic response to intravenous injection of atrial myocardial extract in rats. *Life Sci.* **28**, 89-94.

30. **De Caterina, R., Libby, P., Peng, H. B., Thannickal, V. J., Rajavashisth, T. B., Gimbrone, M. A., Jr., Shin, W. S., and Liao, J. K.** (1995). Nitric oxide decreases cytokine-induced endothelial activation. Nitric oxide selectively reduces endothelial expression of adhesion molecules and proinflammatory cytokines. *J Clin.Invest* **96**, 60-68.

31. **De Martin, R., Hoeth, M., Hofer-Warbinek, R., and Schmid, J. A.** (2000). The transcription factor NF-kappa B and the regulation of vascular cell function. *Arterioscler.Thromb.Vasc.Biol.* **20**, E83-E88.

32. **DeMeester, S. L., Buchman, T. G., Qiu, Y., Jacob, A. K., Dunnigan, K., Hotchkiss, R. S., Karl, I., and Cobb, J. P.** (1997). Heat shock induces IkappaB-alpha and prevents stress-induced endothelial cell apoptosis. *Arch.Surg.* **132**, 1283-1287.

33. **Denk, A., Goebeler, M., Schmid, S., Berberich, I., Ritz, O., Lindemann, D., Ludwig, S., and Wirth, T.** (2001). Activation of NF-kappa B via the Ikappa B kinase complex is both essential and sufficient for proinflammatory gene expression in primary endothelial cells. *J.Biol.Chem.* **276**, 28451-28458.

34. **Diamond, M. S., Staunton, D. E., Marlin, S. D., and Springer, T. A.** (1991). Binding of the integrin Mac-1 (CD11b/CD18) to the third immunoglobulin- like domain of ICAM-1 (CD54) and its regulation by glycosylation. *Cell* **65**, 961-971.

35. **Elices, M. J., Osborn, L., Takada, Y., Crouse, C., Luhowskyj, S., Hemler, M. E., and Lobb, R. R.** (1990). VCAM-1 on activated endothelium interacts with the leukocyte integrin VLA-4 at a site distinct from the VLA-4/fibronectin binding site. *Cell* **60**, 577-584.

36. **Forssmann, W., Meyer, M., and Forssmann, K.** (2001). The renal urodilatin system: clinical implications. *Cardiovasc.Res.* **51**, 450-462.

37. **Gaestel, M., Schroder, W., Benndorf, R., Lippmann, C., Buchner, K., Hucho, F., Erdmann, V. A., and Bielka, H.** (1991). Identification of the phosphorylation sites of the murine small heat shock protein hsp25. *J.Biol.Chem.* **266**, 14721-14724.

38. **Georgopoulos, C. and Welch, W. J.** (1993). Role of the major heat shock proteins as molecular chaperones. *Annu.Rev.Cell Biol.* **9**, 601-634.

39. **Ghiso, N., Rohan, R. M., Amano, S., Garland, R., and Adamis, A. P.** (1999). Suppression of hypoxia-associated vascular endothelial growth factor gene expression by nitric oxide via cGMP. *Invest Ophthalmol.Vis.Sci.* **40**, 1033-1039.

40. **Ghosh, S., May, M. J., and Kopp, E. B.** (1998). NF-kappa B and Rel proteins: evolutionarily conserved mediators of immune responses. *Annu.Rev Immunol* **16**, 225-260.

41. **Gimbrone, M. A., Jr., Nagel, T., and Topper, J. N.** (1997). Biomechanical activation: an emerging paradigm in endothelial adhesion biology. *J Clin.Invest* **100**, S61-S65.

42. **Goebeler, M., Gillitzer, R., Kilian, K., Utzel, K., Brocker, E. B., Rapp, U. R., and Ludwig, S.** (2001). Multiple signaling pathways regulate NF-kappaB-dependent transcription of the monocyte chemoattractant protein-1 gene in primary endothelial cells. *Blood* **97**, 46-55.

43. **Goebeler, M., Kilian, K., Gillitzer, R., Kunz, M., Yoshimura, T., Brocker, E. B., Rapp, U. R., and Ludwig, S.** (1999). The MKK6/p38 stress kinase cascade is critical for tumor necrosis factor-alpha-induced expression of monocyte-chemoattractant protein-1 in endothelial cells. *Blood* **93**, 857-865.

44. **Guan, K., Hakes, D. J., Wang, Y., Park, H. D., Cooper, T. G., and Dixon, J. E.** (1992). A yeast protein phosphatase related to the vaccinia virus VH1 phosphatase is induced by nitrogen starvation. *Proc.Natl.Acad.Sci.U.S.A* **89**, 12175-12179.

45. **Gupta, S. K., Lysko, P. G., Pillarisetti, K., Ohlstein, E., and Stadel, J. M.** (1998). Chemokine receptors in human endothelial cells. Functional expression of CXCR4 and its transcriptional regulation by inflammatory cytokines. *J.Biol.Chem.* **273**, 4282-4287.

46. **Hale, K. K., Trollinger, D., Rihanek, M., and Manthey, C. L.** (1999). Differential expression and activation of p38 mitogen-activated protein kinase alpha, beta, gamma, and delta in inflammatory cell lineages. *J.Immunol.* **162**, 4246-4252.

47. **Hannken, T., Schroeder, R., Stahl, R. A., and Wolf, G.** (2001). Atrial natriuretic peptide attenuates ANG II-induced hypertrophy of renal tubular cells. *Am.J Physiol Renal Physiol* **281**, F81-F90.

48. **Hayes, I. M., Jordan, N. J., Towers, S., Smith, G., Paterson, J. R., Earnshaw, J. J., Roach, A. G., Westwick, J., and Williams, R. J.** (1998). Human vascular smooth muscle cells express receptors for CC chemokines. *Arterioscler.Thromb.Vasc.Biol.* **18**, 397-403.

49. **Heller, R. A. and Kronke, M.** (1994). Tumor necrosis factor receptor-mediated signaling pathways. *J Cell Biol.* **126**, 5-9.

50. **Herlaar, E. and Brown, Z.** (1999). p38 MAPK signalling cascades in inflammatory disease. *Mol.Med Today* **5**, 439-447.

51. **Hession, C., Tizard, R., Vassallo, C., Schiffer, S. B., Goff, D., Moy, P., Chi-Rosso, G., Luhowskyj, S., Lobb, R., and Osborn, L.** (1991). Cloning of an alternate form of vascular cell adhesion molecule-1 (VCAM1). *J.Biol.Chem.* **266**, 6682-6685.

52. **Hu, R. M., Levin, E. R., Pedram, A., and Frank, H. J.** (1992). Atrial natriuretic peptide inhibits the production and secretion of endothelin from cultured endothelial cells. Mediation through the C receptor. *J.Biol.Chem.* **267**, 17384-17389.

53. **Huot, J., Houle, F., Marceau, F., and Landry, J.** (1997). Oxidative stress-induced actin reorganization mediated by the p38 mitogen-activated protein kinase/heat shock protein 27 pathway in vascular endothelial cells. *Circ.Res.* **80**, 383-392.

54. **Immenschuh, S., Hinke, V., Ohlmann, A., Gifhorn-Katz, S., Katz, N., Jungermann, K., and Kietzmann, T.** (1998). Transcriptional activation of the haem oxygenase-1 gene by cGMP via a cAMP response element/activator protein-1 element in primary cultures of rat hepatocytes. *Biochem.J.* **334 ( Pt 1)**, 141-146.

55. **Inagami, T., Misono, K. S., Maki, M., Fukumi, H., Takayanagi, R., Grammer, R. T., Tibbetts, C., Pandey, K., Sugiyama, M., Yabe, Y., and .** (1984). Atrial natriuretic factor: purification of active peptides, cloning of cDNA and determination of structures of active peptides and precursors. *J.Hypertens.Suppl* **2**, S317-S319.

56. **Ishibashi, T., Bottaro, D. P., Chan, A., Miki, T., and Aaronson, S. A.** (1992). Expression cloning of a human dual-specificity phosphatase. *Proc.Natl.Acad.Sci.U.S.A* **89**, 12170-12174.

57. **Isobe, H., Okajima, K., Uchiba, M., Harada, N., and Okabe, H.** (2002). Antithrombin prevents endotoxin-induced hypotension by inhibiting the induction of nitric oxide synthase in rats. *Blood* **99**, 1638-1645.

58. **Izumi, T., Saito, Y., Kishimoto, I., Harada, M., Kuwahara, K., Hamanaka, I., Takahashi, N., Kawakami, R., Li, Y., Takemura, G., Fujiwara, H., Garbers, D. L., Mochizuki, S., and Nakao, K.** (2001). Blockade of the natriuretic peptide receptor guanylyl cyclase-A inhibits NF-kappaB activation and alleviates myocardial ischemia/reperfusion injury. *J Clin.Invest* **108**, 203-213.

59. **Jeon, S. H., Yoo, B. H., Kang, U. K., Ahn, Y. M., Bae, C. D., Park, J. B., and Kim, Y. S.** (1998). MKP-1 induced in rat brain after electroconvulsive shock is independent of regulation of 42- and 44-kDa MAPK activity. *Biochem.Biophys.Res.Commun.* **249**, 692-696.

60. **Karin, M.** (1999). How NF-kappaB is activated: the role of the IkappaB kinase (IKK) complex. *Oncogene* **18**, 6867-6874.

61. **Kehlen, A., Thiele, K., Riemann, D., Rainov, N., and Langner, J.** (1999). Interleukin-17 stimulates the expression of IkappaB alpha mRNA and the secretion of IL-6 and IL-8 in glioblastoma cell lines. *J Neuroimmunol.* **101** , 1-6.

62. **Keyse, S. M.** (1995). An emerging family of dual specificity MAP kinase phosphatases. *Biochim.Biophys.Acta* **1265**, 152-160.

63. **Keyse, S. M.** (2000). Protein phosphatases and the regulation of mitogen-activated protein kinase signalling. *Curr.Opin.Cell Biol.* **12**, 186-192.

64. **Keyse, S. M. and Ginsburg, M.** (1993). Amino acid sequence similarity between CL100, a dual-specificity MAP kinase phosphatase and cdc25. *Trends Biochem.Sci.* **18**, 377-378.

65. Kiemer, A. K., Baron, A., Gerbes, A. L., Bilzer, M., and Vollmar, A. M. The Atrial Natriuretic Peptide as a Regulator of Kupffer Cell Functions. Shock . 2001. Ref Type: In Press

66. **Kiemer, A. K., Gerbes, A. L., Bilzer, M., and Vollmar, A. M.** (2002a). The atrial natriuretic peptide and cGMP: novel activators of the heat shock response in rat livers. *Hepatology* **35**, 88-94.

67. **Kiemer, A. K., Hartung, T., and Vollmar, A. M.** (2000a). cGMP-mediated inhibition of TNF-alpha production by the atrial natriuretic peptide in murine macrophages. *J Immunol.* **165**, 175-181.

68. **Kiemer, A. K., Lehner, M. D., Hartung, T., and Vollmar, A. M.** (2002b). Inhibition of cyclooxygenase-2 by natriuretic peptides. *Endocrinology* **143**, 846-852.

69. **Kiemer, A. K. and Vollmar, A. M.** (1997). Effects of different natriuretic peptides on nitric oxide synthesis in macrophages. *Endocrinology* **138**, 4282-4290.

70. **Kiemer, A. K. and Vollmar, A. M.** (1998). Autocrine regulation of inducible nitric-oxide synthase in macrophages by atrial natriuretic peptide. *J Biol.Chem.* **273**, 13444-13451.

71. **Kiemer, A. K. and Vollmar, A. M.** (2001a). Elevation of intracellular calcium levels contributes to the inhibition of nitric oxide production by atrial natriuretic peptide. *Immunol.Cell Biol.* **79**, 11-17.

72. **Kiemer, A. K. and Vollmar, A. M.** (2001b). Induction of L-arginine transport is inhibited by ANP: a peptide hormone as a novel regulator of iNOS substrate availability. *Mol.Pharmacol.* **60**, 421-426.

73. **Kiemer, A. K., Vollmar, A. M., Bilzer, M., Gerwig, T., and Gerbes, A. L.** (2000b). Atrial natriuretic peptide reduces expression of TNF-alpha mRNA during reperfusion of the rat liver upon decreased activation of NF-kappaB and AP-1. *J Hepatol.* **33**, 236-246.

74. **Kiemer, A. K., Weber N.C., Fürst R., Bildner N., Kulhanek-Heinze S., and Vollmar, A. M.** (2002) Inhibition of p38 MAPK activation *via* induction of MKP-1: Atrial Natriuretic Peptide reduces TNF-α-induced actin polymerisation and endothelial permeability. *Circ.Res.***90**, 874-881

**Kwak, S. P., Hakes, D. J., Martell, K. J., and Dixon, J. E.** (1994). Isolation and characterization of a human dual specificity protein- tyrosine phosphatase gene. *J.Biol.Chem.* **269**, 3596-3604.

76. **Kyriakis, J. M. and Avruch, J.** (1996). Sounding the alarm: protein kinase cascades activated by stress and inflammation. *J.Biol.Chem.* **271**, 24313-24316.

77. **Landry, J. and Huot, J.** (1995). Modulation of actin dynamics during stress and physiological stimulation by a signaling pathway involving p38 MAP kinase and heat- shock protein 27. *Biochem.Cell Biol.* **73**, 703-707.

78. **Landry, J., Lambert, H., Zhou, M., Lavoie, J. N., Hickey, E., Weber, L. A., and Anderson, C. W.** (1992). Human HSP27 is phosphorylated at serines 78 and 82 by heat shock and mitogen-activated kinases that recognize the same amino acid motif as S6 kinase II. *J.Biol.Chem.* **267**, 794-803.

79. **Lavoie, J. N., Hickey, E., Weber, L. A., and Landry, J.** (1993). Modulation of actin microfilament dynamics and fluid phase pinocytosis by phosphorylation of heat shock protein 27. *J.Biol.Chem.* **268**, 24210-24214.

80. **Lawson, C., Ainsworth, M., Yacoub, M., and Rose, M.** (1999). Ligation of ICAM-1 on endothelial cells leads to expression of VCAM-1 via a nuclear factor-kappaB-independent mechanism. *J.Immunol* **162**, 2990-2996.

81. **Leitman, D. C., Andresen, J. W., Kuno, T., Kamisaki, Y., Chang, J. K., and Murad, F.** (1986). Identification of two binding sites for atrial natriuretic factor in endothelial cells: evidence for a receptor subtype coupled to guanylate cyclase. *Trans.Assoc.Am.Physicians* **99**, 103-113.

82. **Leitman, D. C. and Murad, F.** (1986). Comparison of binding and cyclic GMP accumulation by atrial natriuretic peptides in endothelial cells. *Biochim.Biophys. Acta* **885**, 74-79.

83. **Levin, E. R.** (1993). Natriuretic peptide C-receptor: more than a clearance receptor. *Am.J Physiol* **264**, E483-E489.

84. **Levin, E. R., Gardner, D. G., and Samson, W. K.** (1998). Natriuretic peptides. *N.Engl.J Med.* **339**, 321-328.

85. **Lofton, C. E., Baron, D. A., Heffner, J. E., Currie, M. G., and Newman, W. H.** (1991). Atrial natriuretic peptide inhibits oxidant-induced increases in endothelial permeability. *J Mol.Cell Cardiol.* **23**, 919-927.

86. **Lofton, C. E., Newman, W. H. a., and Currie, M. G.** (1990). Atrial Natriuretic Peptide Regulation of Endothelial Permeability is Mediated by cGMP. *Biochemical and Biophysical Research Communications* **172**, 793-799.

87. **Lowry OH** (1951). Protein measurement with the Folin phenol reagent. *J Biol. Chem.* **193**, 265-270.

88. **Lum, H. and Malik, A. B.** (1996). Mechanisms of increased endothelial permeability. *Can.J Physiol Pharmacol.* **74**, 787-800.

89. **Luster, A. D.** (1998). Chemokines--chemotactic cytokines that mediate inflammation. *N.Engl.J.Med.* **338**, 436-445.

90. **Marin, V., Farnarier, C., Gres, S., Kaplanski, S., Su, M. S., Dinarello, C. A., and Kaplanski, G.** (2001). The p38 mitogen-activated protein kinase pathway plays a critical role in thrombin-induced endothelial chemokine production and leukocyte recruitment. *Blood* **98**, 667-673.

91. **Marlin, S. D. and Springer, T. A.** (1987). Purified intercellular adhesion molecule-1 (ICAM-1) is a ligand for lymphocyte function-associated antigen 1 (LFA-1). *Cell* **51**, 813-819.

92. **McKay, L. I. and Cidlowski, J. A.** (1999). Molecular control of immune/inflammatory responses: interactions between nuclear factor-kappa B and steroid receptor-signaling pathways. *Endocr.Rev.* **20**, 435-459.

93. **Meijerman, I., Blom, W. M., de Bont, H. J., Mulder, G. J., and Nagelkerke, J. F.** (1997). Nuclear accumulation of G-actin in isolated rat hepatocytes by adenine nucleotides. *Biochem.Biophys.Res.Commun.* **240**, 697-700.

94. **Menger, M. D. and Vollmar, B.** (1996). Adhesion molecules as determinants of disease: from molecular biology to surgical research. *Br.J Surg* **83**, 588-601.

95. **Metzler, B., Hu, Y., Sturm, G., Wick, G., and Xu, Q.** (1998). Induction of mitogen-activated protein kinase phosphatase-1 by arachidonic acid in vascular smooth muscle cells. *J Biol.Chem.* **273**, 33320-33326.

96. **Miron, T., Vancompernolle, K., Vandekerckhove, J., Wilchek, M., and Geiger, B.** (1991). A 25-kD inhibitor of actin polymerization is a low molecular mass heat shock protein. *J.Cell Biol.* **114**, 255-261.

97. **Morishita, Y., Sano, T., Ando, K., Saitoh, Y., Kase, H., Yamada, K., and Matsuda, Y.** (1991). Microbial polysaccharide, HS-142-1, competitively and selectively inhibits ANP binding to its guanylyl cyclase-containing receptor. *Biochem.Biophys.Res.Commun.* **176**, 949-957.

98. **Murohara, T., Kugiyama, K., Ota, Y., Doi, H., Ogata, N., Ohgushi, M., and Yasue, H.** (1999). Effects of atrial and brain natriuretic peptides on lysophosphatidylcholine-mediated endothelial dysfunction. *J.Cardiovasc. Pharmacol.* **34**, 870-878.

99. **Nakamura, H., Herzenberg, L. A., Bai, J., Araya, S., Kondo, N., Nishinaka, Y., Herzenberg, L. A., and Yodoi, J.** (2001). Circulating thioredoxin suppresses lipopolysaccharide-induced neutrophil chemotaxis. *Proc.Natl.Acad.Sci.U.S.A* **98**, 15143-15148.

100. **Neish, A. S., Khachigian, L. M., Park, A., Baichwal, V. R., and Collins, T.** (1995a). Sp1 is a component of the cytokine-inducible enhancer in the promoter of vascular cell adhesion molecule-1. *J Biol.Chem.* **270**, 28903-28909.

101. **Neish, A. S., Read, M. A., Thanos, D., Pine, R., Maniatis, T., and Collins, T.** (1995b). Endothelial interferon regulatory factor 1 cooperates with NF-kappa B as a transcriptional activator of vascular cell adhesion molecule 1. *Mol.Cell Biol.* **15**, 2558-2569.

102. **Nelken, N. A., Coughlin, S. R., Gordon, D., and Wilcox, J. N.** (1991). Monocyte chemoattractant protein-1 in human atheromatous plaques. *J Clin.Invest* **88**, 1121-1127.

103. **Nichols, A., Camps, M., Gillieron, C., Chabert, C., Brunet, A., Wilsbacher, J., Cobb, M., Pouyssegur, J., Shaw, J. P., and Arkinstall, S.** (2000). Substrate recognition domains within extracellular signal-regulated kinase mediate binding and catalytic activation of mitogen-activated protein kinase phosphatase-3. *J Biol.Chem.* **275**, 24613-24621.

104. **Obata, T., Brown, G. E., and Yaffe, M. B.** (2000). MAP kinase pathways activated by stress: the p38 MAPK pathway. *Crit Care Med.* **28**, N67-N77.

105. **Okada, M., Matsumori, A., Ono, K., Furukawa, Y., Shioi, T., Iwasaki, A., Matsushima, K., and Sasayama, S.** (1998). Cyclic stretch upregulates production of interleukin-8 and monocyte chemotactic and activating factor/monocyte chemoattractant protein-1 in human endothelial cells. *Arterioscler.Thromb.Vasc.Biol.* **18**, 894-901.

106. **Pedram, A., Razandi, M., and Levin, E. R.** (2001). Natriuretic peptides suppress vascular endothelial cell growth factor signaling to angiogenesis. *Endocrinology* **142**, 1578-1586.

107. **Pilz, R. B., Suhasini, M., Idriss, S., Meinkoth, J. L., and Boss, G. R.** (1995). Nitric oxide and cGMP analogs activate transcription from AP-1- responsive promoters in mammalian cells. *FASEB J.* **9**, 552-558.

108. **Preli RB, Klein KP, Herrington DM**. (2002). Vascular effects of dietary L-arginine supplementation. *Atherosclerosis* **162**:1-15.

108. **Rahman, I. and MacNee, W.** (1998). Role of transcription factors in inflammatory lung diseases. *Thorax* **53**, 601-612.

109. **Raines, E. W. and Ross, R.** (1995). Biology of atherosclerotic plaque formation: possible role of growth factors in lesion development and the potential impact of soy. *J Nutr.* **125**, 624S-630S.

110. **Razandi, M., Pedram, A., and Levin, E. R.** (2000). Estrogen signals to the preservation of endothelial cell form and function. *J Biol.Chem.* **275**, 38540-38546.

111. **Read, M. A., Whitley, M. Z., Williams, A. J., and Collins, T.** (1994). NF-kappa B and I kappa B alpha: an inducible regulatory system in endothelial activation. *J Exp.Med.* **179**, 503-512.

112. **Reape, T. J. and Groot, P. H.** (1999). Chemokines and atherosclerosis. *Atherosclerosis* **147**, 213-225.

113. **Reinhard, M., Giehl, K., Abel, K., Haffner, C., Jarchau, T., Hoppe, V., Jockusch, B. M., and Walter, U.** (1995). The proline-rich focal adhesion and microfilament protein VASP is a ligand for profilins. *EMBO J.* **14**, 1583-1589.

114. **Robinson, E. A., Yoshimura, T., Leonard, E. J., Tanaka, S., Griffin, P. R., Shabanowitz, J., Hunt, D. F., and Appella, E.** (1989). Complete amino acid sequence of a human monocyte chemoattractant, a putative mediator of cellular immune reactions. *Proc.Natl.Acad.Sci.U.S.A* **86**, 1850-1854.

115. **Rosenzweig, A. and Seidman, C. E.** (1991). Atrial natriuretic factor and related peptide hormones. *Annu.Rev.Biochem.* **60**, 229-255.

116. **Salzmann, J., Flitcroft, D., Bunce, C., Gordon, D., Wormald, R., and Migdal, C.** (1998). Brain natriuretic peptide: identification of a second natriuretic peptide in human aqueous humour. *Br.J.Ophthalmol.* **82**, 830-834.

117. **Sanger, J. W., Sanger, J. M., Kreis, T. E., and Jockusch, B. M.** (1980). Reversible translocation of cytoplasmic actin into the nucleus caused by dimethyl sulfoxide. *Proc.Natl.Acad.Sci.U.S.A* **77**, 5268-5272.

118. **Savoie, P., de Champlain, J., and Anand-Srivastava, M. B.** (1995). C-type natriuretic peptide and brain natriuretic peptide inhibit adenylyl cyclase activity: interaction with ANF-R2/ANP-C receptors. *FEBS Lett.* **370**, 6-10.

119. **Saxena, M. and Mustelin, T.** (2000). Extracellular signals and scores of phosphatases: all roads lead to MAP kinase. *Semin.Immunol.* **12**, 387-396.

120. **Schermuly, R. T., Weissmann, N., Enke, B., Ghofrani, H. A., Forssmann, W. G., Grimminger, F., Seeger, W., and Walmrath, D.** (2001). Urodilatin, a natriuretic peptide stimulating particulate guanylate cyclase, and the phosphodiesterase 5 inhibitor dipyridamole attenuate experimental pulmonary hypertension: synergism upon coapplication. *Am.J.Respir.Cell Mol.Biol.* **25**, 219-225.

121. **Schreiber, E., Matthias, P., Muller, M. M., and Schaffner, W.** (1989). Rapid detection of octamer binding proteins with 'mini-extracts', prepared from a small number of cells. *Nucleic Acids Res.* **17**, 6419.

122. **Schulz-Knappe, P., Forssmann, K., Herbst, F., Hock, D., Pipkorn, R., and Forssmann, W. G.** (1988). Isolation and structural analysis of "urodilatin", a new peptide of the cardiodilatin-(ANP)-family, extracted from human urine. *Klin.Wochenschr.* **66**, 752-759.

123. **Sen, R. and Baltimore, D.** (1986). Multiple nuclear factors interact with the immunoglobulin enhancer sequences. *Cell* **46**, 705-716.

124. **Sharma, R., Lovell, H. B., Wiegmann, T. B., and Savin, V. J.** (1992). Vasoactive substances induce cytoskeletal changes in cultured rat glomerular epithelial cells. *J Am.Soc.Nephrol.* **3**, 1131-1138.

125. **Shyy, Y. J., Li, Y. S., and Kolattukudy, P. E.** (1993). Activation of MCP-1 gene expression is mediated through multiple signaling pathways. *Biochem.Biophys.Res.Commun.* **192**, 693-699.

126. **Spiecker, M., Darius, H., Kaboth, K., Hubner, F., and Liao, J. K.** (1998). Differential regulation of endothelial cell adhesion molecule expression by nitric oxide donors and antioxidants. *J Leukoc.Biol.* **63**, 732-739.

127. **Spiecker, M., Darius, H., and Liao, J. K.** (2000). A functional role of I kappa B-epsilon in endothelial cell activation. *J Immunol.* **164**, 3316-3322.

128. **Springer, T. A.** (1994). Traffic signals for lymphocyte recirculation and leukocyte emigration: the multistep paradigm. *Cell* **76**, 301-314.

129. **Stingo, A. J., Clavell, A. L., Aarhus, L. L., and Burnett, J. C., Jr.** (1992a). Cardiovascular and renal actions of C-type natriuretic peptide. *Am.J.Physiol* **262**, H308-H312.

130. **Stingo, A. J., Clavell, A. L., Heublein, D. M., Wei, C. M., Pittelkow, M. R., and Burnett, J. C., Jr.** (1992b). Presence of C-type natriuretic peptide in cultured human endothelial cells and plasma. *Am.J.Physiol* **263**, H1318-H1321.

131. **Sudoh, T., Kangawa, K., Minamino, N., and Matsuo, H.** (1988). A new natriuretic peptide in porcine brain. *Nature* **332**, 78-81.

132. **Sudoh, T., Minamino, N., Kangawa, K., and Matsuo, H.** (1990). C-type natriuretic peptide (CNP): a new member of natriuretic peptide family identified in porcine brain. *Biochem.Biophys.Res.Commun.* **168**, 863-870.

133. **Suga, S., Nakao, K., Hosoda, K., Mukoyama, M., Ogawa, Y., Shirakami, G., Arai, H., Saito, Y., Kambayashi, Y., Inouye, K., and .** (1992). Receptor selectivity of natriuretic peptide family, atrial natriuretic peptide, brain natriuretic peptide, and C-type natriuretic peptide. *Endocrinology* **130**, 229-239.

134. **Sugimoto, T., Haneda, M., Togawa, M., Isono, M., Shikano, T., Araki, S., Nakagawa, T., Kashiwagi, A., Guan, K. L., and Kikkawa, R.** (1996). Atrial natriuretic peptide induces the expression of MKP-1, a mitogen- activated protein kinase phosphatase, in glomerular mesangial cells. *J Biol.Chem.* **271**, 544-547.

135. **Sun, H., Charles, C. H., Lau, L. F., and Tonks, N. K.** (1993). MKP-1 (3CH134), an immediate early gene product, is a dual specificity phosphatase that dephosphorylates MAP kinase in vivo. *Cell* **75**, 487-493.

136. **Takahashi, M., Ikeda, U., Masuyama, J., Funayama, H., Kano, S., and Shimada, K.** (1996). Nitric oxide attenuates adhesion molecule expression in human endothelial cells. *Cytokine* **8**, 817-821.

137. **Tedder, T. F., Steeber, D. A., Chen, A., and Engel, P.** (1995). The selectins: vascular adhesion molecules. *FASEB J.* **9**, 866-873.

138. **Tissieres, A., Mitchell, H. K., and Tracy, U. M.** (1974). Protein synthesis in salivary glands of Drosophila melanogaster: Relation to chromosome puffs. *J.Mol.Biol.* **85**, 389-398.

139. **Tobacman, L. S. and Korn, E. D.** (1983). The kinetics of actin nucleation and polymerization. *J.Biol.Chem.* **258**, 3207-3214.

140. **Tsukagoshi, H., Shimizu, Y., Kawata, T., Hisada, T., Shimizu, Y., Iwamae, S., Ishizuka, T., Iizuka, K., Dobashi, K., and Mori, M.** (2001). Atrial natriuretic peptide inhibits tumor necrosis factor-alpha production by interferon-gamma-activated macrophages via suppression of p38 mitogen-activated protein kinase and nuclear factor-kappa B activation. *Regul.Pept.* **99**, 21-29.

141. **Vachino, G., Chang, X. J., Veldman, G. M., Kumar, R., Sako, D., Fouser, L. A., Berndt, M. C., and Cumming, D. A.** (1995). P-selectin glycoprotein ligand-1 is the major counter-receptor for P- selectin on stimulated T cells and is widely distributed in non- functional form on many lymphocytic cells. *J.Biol.Chem.* **270**, 21966-21974.

142. **van Hinsbergh, W. M.** (1997). Endothelial permeability for macromolecules. Mechanistic aspects of pathophysiological modulation. *Arterioscler.Thromb. Vasc.Biol.* **17**, 1018-1023.

143. **Venugopal, J.** (2001). Cardiac natriuretic peptides--hope or hype? *J Clin.Pharm.Ther.* **26**, 15-31.

144. **Volin, M. V., Joseph, L., Shockley, M. S., and Davies, P. F.** (1998). Chemokine receptor CXCR4 expression in endothelium. *Biochem.Biophys. Res.Commun.* **242**, 46-53.

145. **Vollmar, A. M.** (1997). Influence of atrial natriuretic peptide on thymocyte development in fetal thymic organ culture. *J Neuroimmunol.* **78** , 90-96.

146. **Vollmar, A. M., Schmidt, K. N., and Schulz, R.** (1996). Natriuretic peptide receptors on rat thymocytes: inhibition of proliferation by atrial natriuretic peptide. *Endocrinology* **137**, 1706-1713.

147. **Vollmar, A. M. and Schulz, R.** (1990a). Atrial natriuretic peptide in lymphoid organs of various species. *Comp Biochem.Physiol A* **96**, 459-463.

148. **Vollmar, A. M. and Schulz, R.** (1990b). Atrial natriuretic peptide is synthesized in the human thymus. *Endocrinology* **126**, 2277-2280.

149. **Vollmar, A. M. and Schulz, R.** (1994). Gene expression and secretion of atrial natriuretic peptide by murine macrophages. *J Clin.Invest* **94** , 539-545.

150. **Vollmar, A. M. and Schulz, R.** (1995). Expression and differential regulation of natriuretic peptides in mouse macrophages. *J Clin.Invest* **95**, 2442-2450.

151. **Wang, D. L., Wung, B. S., Shyy, Y. J., Lin, C. F., Chao, Y. J., Usami, S., and Chien, S.** (1995). Mechanical strain induces monocyte chemotactic protein-1 gene expression in endothelial cells. Effects of mechanical strain on monocyte adhesion to endothelial cells. *Circ.Res.* **77**, 294-302.

152. **Wang, J. M., Su, S., Gong, W., and Oppenheim, J. J.** (1998). Chemokines, receptors, and their role in cardiovascular pathology. *Int.J.Clin.Lab Res.* **28**, 83-90.

153. **Ward, Y., Gupta, S., Jensen, P., Wartmann, M., Davis, R. J., and Kelly, K.** (1994). Control of MAP kinase activation by the mitogen-induced threonine/tyrosine phosphatase PAC1. *Nature* **367**, 651-654.

154. **Wen, J. K. and Han, M.** (2000). Comparative study of induction of iNOS mRNA expression in vascular cells of different species. *Biochemistry (Mosc.)* **65**, 1376-1379.

155. **Wojciak-Stothard, B., Entwistle, A., Garg, R., and Ridley, A. J.** (1998). Regulation of TNF-alpha-induced reorganization of the actin cytoskeleton and cell-cell junctions by Rho, Rac, and Cdc42 in human endothelial cells. *J Cell Physiol* **176**, 150-165.

156. **Wu, J., Lau, L. F., and Sturgill, T. W.** (1994). Rapid deactivation of MAP kinase in PC12 cells occurs independently of induction of phosphatase MKP-1. *FEBS Lett.* **353**, 9-12.

157. **Yamagishi, S. I., Edelstein, D., Du, X. L., Kaneda, Y., Guzman, M., and Brownlee, M.** (2001). Leptin induces mitochondrial superoxide production and monocyte chemoattractant protein-1 expression in aortic endothelial cells by increasing fatty acid oxidation via protein kinase A. *J Biol.Chem.* **276**, 25096-25100.

158. **Yla-Herttuala, S., Lipton, B. A., Rosenfeld, M. E., Sarkioja, T., Yoshimura, T., Leonard, E. J., Witztum, J. L., and Steinberg, D.** (1991). Expression of monocyte chemoattractant protein 1 in macrophage-rich areas of human and rabbit atherosclerotic lesions. *Proc.Natl.Acad.Sci.U.S.A* **88**, 5252-5256.

159. **Yuasa, T., Ohno, S., Kehrl, J. H., and Kyriakis, J. M.** (1998). Tumor necrosis factor signaling to stress-activated protein kinase (SAPK)/Jun NH2-terminal kinase (JNK) and p38. Germinal center kinase couples TRAF2 to mitogen-activated protein kinase/ERK kinase kinase 1 and SAPK while receptor interacting protein associates with a mitogen- activated protein kinase kinase kinase upstream of MKK6 and p38. *J.Biol.Chem.* **273**, 22681-22692.

160. **Zeiher, A. M., Fisslthaler, B., Schray-Utz, B., and Busse, R.** (1995). Nitric oxide modulates the expression of monocyte chemoattractant protein 1 in cultured human endothelial cells. *Circ.Res.* **76**, 980-986.

161. **Zimmerman, R. S., Trippodo, N. C., MacPhee, A. A., Martinez, A. J., and Barbee, R. W.** (1990). High-dose atrial natriuretic factor enhances albumin escape from the systemic but not the pulmonary circulation. *Circ.Res.* **67**, 461-468.

# Acknowledgement

I would like to express my gratitude to Prof. Dr. Angelika M. Vollmar for both inspiring this very interesting work and for continuous motivation during lab research. The stimulating discussions during the course have been very helpful for successful work.

I want to thank Prof. Dr. M Biel for his time and effort to be coreferee of this work.

Another person I would like to thank very much is Dr. Alexandra K. Kiemer for supporting and looking after my work. I want to thank her for sharing her wisdom concerning my work with me in several helpful discussions. Dr. Alexandra K. Kiemer was especially in technical questions an ongoing support during this lab course.

I am also indebted to Dr. Thomas Hartung from the University of Konstanz for kindly measuring the MCP-1 ELISA.

Moreover I would like to gratefully thank the following persons:
The lab team, including: Anke Förnges, Nicole Bildner, Christian Müller, Tobias Gerwig, Brigitte Weiss, and Raima Yasar, with whom I shared the whole time of my lab course, for accompanying me through good times and bad times, for laughing and joking with me, cheering me up, criticizing me, and for all the time I could spend with you. I want to thank Peter Bristot and Robert Fürst for critical reading this manuscript. I want to gratefully thank especially Anke Förnges, Nicole Bildner, and Robert Fürst for so many stimulating “cooking and ratsching” dates and for making me feel at home in Munich. A special thanks also to the technical staff of our research group, including Brigitte Weiss, Rita Socher, Ursula Kollmannsberger, and Raima Yasar for the helping hand in several situations. I want to thank Veronika Rickl, for helping to perform the graphic design of many figures and posters. Furthermore I would like to thank the whole PB II team for so many successful practical courses for the students during the time of the lab course. Of course I want to thank all members of the research group of Prof. Vollmar for contributing the pleasant and relaxing working climate. A special thanks to the staff of the Klinikum Großhadern for always providing umbilical cords for me and other “HUVEC people”. As it is impossible to thank all the people who supported me during my lab course at the LMU-Munich, I would like to thank all those people that I have not mentioned above and especially my sister Sabine for supporting me through the lab course all the time.

Munich, April 2002 Nina Weber

## Curriculum vitae

**Personal data**

| | |
|---|---|
| Name: | Nina Claudia Weber |
| Birthdate and place: | 16.11.1973, Cologne |
| Citizenship: | German |

**Education**

| | |
|---|---|
| 06/1993 | Abitur |
| 1985-1993 | Freiherr-vom-Stein grammar school, Leverkusen |
| 1981-1984 | Elementary school, Leverkusen Schlebusch |
| 1980-1981 | Elementary school, Cologne-Flittard |

**Studies**

| | |
|---|---|
| 10/1999-06/02 | Ph.D. dissertation on "ANP protection of TNF-α-induced endothelial cell damage" in the research group of Prof. Dr. A.M. Vollmar. Department of pharmacy and drug research, Ludwig-Maximilians-Univesity of Munich |
| 06-09/1999 | Work as a pharmacist at the Carl-Duisberg Apotheke, Leverkusen |
| 10/1993-05/1999 | Pharmacy studies at the Rheinische-Friedrich-Wilhelms-University of Bonn |
| 05/1999 | Third state examination pharmacy and certificate as a pharmacist |
| 05-10/1998 | Internship at the Carl-Duisberg Apotheke, Leverkusen |
| 11/1998-04/1999 | Internship at the Bayer Inc., Leverkusen on "structural analysis of the Telomerase gene" in the department of gene research |
| 04/1998 | Second state examination pharmacy |
| 03/1996 | First state examination pharmacy |